Pickering Emulsions as Compartmentalized Reaction Media for Catalysis

Carolien Vis

ISBN: 978-94-6416-174-8
Printed by: Ridderprint, The Netherlands

Pickering Emulsions as Compartmentalized Reaction Media for Catalysis

Pickering Emulsies als Gecompartimentaliseerde Reactiemedia voor Katalyse

(met een samenvatting in het Nederlands)

Proefschrift

ter verkrijging van de graad van doctor aan de
Universiteit Utrecht
op gezag van de
rector magnificus, prof.dr. H.R.B.M. Kummeling,
ingevolge het besluit van het college voor promoties
in het openbaar te verdedigen op

woensdag 28 oktober 2020 des middags te 4.15 uur

door

Carolien Mariëlle Vis

geboren op 12 oktober 1991
te Breukelen

Promotor: Prof. dr. P.C.A. Bruijnincx

Dit proefschrift werd (mede) mogelijk gemaakt met financiële steun van de Nederlandse Organisatie voor Wetenschappelijk Onderzoek (NWO VIDI project 723.013.001)

Table of contents

Chapter 1

General Introduction

Based on: F.C. Chang*, C.M. Vis*, W. Ciptonugroho*, P.C.A. Bruijnincx, Recent Developments in Pickering Emulsions for Catalysis, In preparation

** These authors contributed equally*

The research described in this PhD Thesis concerns the separation of incompatible reagents and catalysts in different compartments of a reaction medium. This compartmentalization strategy is a tool often used by nature, e.g. a living cell contains all kind of compartments in which all kinds of parallel and consecutive reactions can take place without interference.[1] We want to mimic this strategy by using Pickering emulsions (PEs) as reaction media. In this introduction Chapter the reader will be familiarized with the concept of PEs (1.1), the materials that can be used to stabilize them (1.2), the recent advances made in performing catalytic reactions in PEs (1.3) and the recent advances made in reactor engineering using PEs (1.4), followed by the scope of this PhD Thesis (1.5).

1.1 Pickering emulsions

Emulsions are dispersions of two immiscible liquid phases (e.g. water and oil), which can be stabilized by surfactants, as is the case in classical emulsions, or by solid micro- or nanosized particles. The latter type of emulsion is a so-called Pickering emulsion (PE), named after S.U. Pickering who was second to describe them in 1907[2], a few years after Ramsden.[3] Generally, two types of emulsions can be readily distinguished, water-in-oil (w/o) or oil-in-water (o/w) as shown in Figure 1.1.[4] Which type of PE is formed is determined by the type of particles used and the corresponding contact angle these particles exhibit with, e.g., the water-oil interface. Hydrophobic particles, such as carbon nanotubes or silylated silica, are more easily wetted by the oil phase than by the aqueous phase, showing contact angles of > 90°, resulting in the formation of w/o PEs. Hydrophilic particles, such as bare silica and metal oxides, are easily wetted by the aqueous phase, resulting in contact angles < 90° and the formation of o/w PEs. Other types of emulsions, such as water-in-water (w/w)[5], gas-in-liquid (g/w or g/o)[6] or multiple emulsions, water-in-oil-in-water (w/o/w) and oil-in-water-in-oil (o/w/o)[7], have been studied as well.

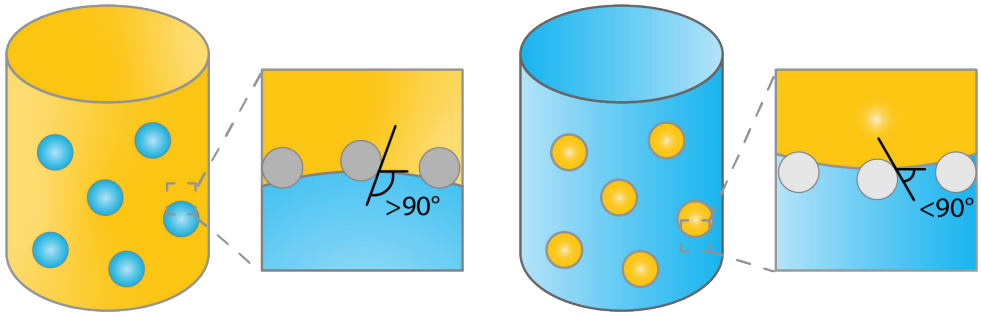

Figure 1.1: Schematic representation of PE types with corresponding contact angles measured through the aqueous phase, yellow: oil, blue: water. Left: Water-in-oil (w/o) PE, stabilized by hydrophobic particles with contact angle > 90°. Right: Oil-in-water (o/w) PE, stabilized by hydrophilic particles with contact angle < 90°.

PEs have received much attention for the application in multiple disciplines, e.g. the food, pharmaceutical and biomedical industries, and more recently, catalysis. In the food industry edible micro- and nanoparticles, such as particles derived from starch and lipids, are used to make, for example reconstituted milk and margarine or foams likes whipped cream.[8] In pharmaceutical and biomedical industries PEs are mainly used for the targeted delivery of drugs through the skin.[9,10]

In the past few years PEs have been shown to be very applicable to use in the field of catalysis, as they can be utilized as improved forms of biphasic reaction media. Biphasic reaction media can be used for several reasons, e.g. performing reactions between immiscible reagents and catalysts, to extract products from the reaction phase to the second liquid phase or to separate a homogeneous chemo- or biocatalyst from reagents and products to improve recyclability.[11–13] Despite the aforementioned advantages of using biphasic systems (BS), there are also some improvements to be made. In conventional BS the interfacial area of the two immiscible phases is rather low, precluding high reaction and extraction efficiencies. Here, emulsification of the BS, i.e. creating a stable dispersion, is a promising strategy to address this challenge and improve the performance of a chemical reaction.

PEs are often chosen over classical emulsions[14,15] because of their higher resistance against destabilization phenomena, such as droplet coalescence and Ostwald ripening. Once the particles are adsorbed at the liquid-liquid interface, the energy required to desorb them is much higher than the thermal energy, making them highly stable. Emulsion stability is often monitored as function of the height of the emulsion phase with respect to the total liquid height as function of time. Any destabilization can then be described in the form of creaming, i.e. a clear liquid phase forms under the emulsion phase, or by sedimentation, i.e. the clear liquid phase forms on top of the emulsion. Which form of destabilized PE occurs depends on the relative densities of the two liquid phases.

In this PhD Thesis, the use of PEs as reaction media for catalytic reactions will be investigated. This nascent field was first reviewed by Nardello-Rataj *et al.* in 2015.[16] They defined two types of PE catalysis, Pickering Assisted Catalysis (PAC) and Pickering Interfacial Catalysis (PIC). In PAC, non-catalytic particles are used to stabilize the PE, in combination with homogeneous catalysts confined in either the aqueous or the organic phase as is schematically shown in Figure 1.2a. With PIC, catalytically active particles are used as stabilizing particles (Figure 1.2b). In the past five years multiple reviews have been published about the formation of PEs[17,18] and their application in the pharmacological industry,[19,20] but none has focused on the advances made in use of PEs as reaction media for catalysis. In this PhD Thesis Chapter, we will address the state of the art in PE catalysis

using the mini-review from Nardello-Rataj *et al.* as reference point. We will address the use of different stabilizing materials, the various catalytic approaches and the use of PEs as continuous flow reactors.

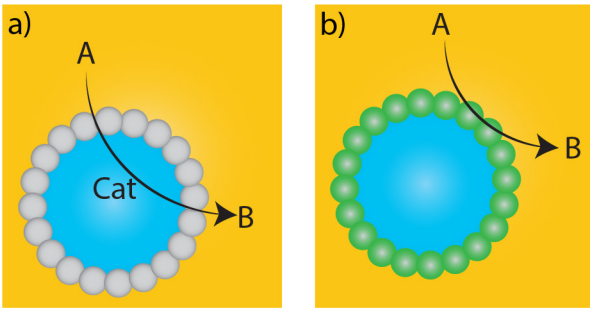

Figure 1.2: Schematic representations of a) Pickering Assisted Catalysis (PAC) and b) Pickering Interfacial Catalysis (PIC) in w/o PEs as defined by Nardello-Rataj *et al.*[16] Yellow: oil phase, blue: aqueous phase, grey: non-catalytic particles, green: catalytic particles.

1.2 Materials

Various kinds of solid particles with moderate wettability have been investigated as solid surfactants for the preparation of PEs, including silica, carbon and polymeric materials as notable examples. Recently, rapid developments in material science has increased the variety of available particles and endowed particles with additional functionality. For example, using functional colloids, PE have been prepared with reversible properties by tuning the surface chemistry of the emulsifiers via light[21], gas[22], chemical auxiliaries[23,24] or temperature variation[25]. Moreover, particles with well-designed anisotropy[26–28] provide superior stability compared to traditional emulsions. These advanced materials also offer many opportunities for application in either a PAC or PIC strategy. Here, we discuss some of the salient properties of (functional) emulsifiers with respect to PE use.

1.2.1 Wettability of particles

The studies of PE stabilization of oil-water emulsions are numerous and include systems containing hydrophobized inorganic materials such as silica[29] and carbon particles[30], synthesized polymers such as crosslinked polystyrene,[31,32] as well as more elaborate Janus (i.e. chemically anisotropic/two-sided) particles[26,33]. To understand how the physicochemical characteristics of a solid emulsifier affect PE stability, we need to know what the orientation and spatial arrangement of these materials is at the liquid-liquid interface. The configuration of the particles adsorbed at the interface depends on the

chemical composition, surface morphology and geometry of the particles. Among these parameters, hydrophobicity of the particles is clearly crucial in dictating the type (oil-in-water or water-in-oil) and coalescence stability of the emulsions. Figure 1.3 summarizes schematically some of the most common material configurations at oil-water interfaces. For hydrophobic materials most of the particle will be located in the oil phase, resulting in contact angles > 90°, (Figure 1.3a), leading to water-in-oil (w/o) type PEs, while hydrophilic particles lead to inverse o/w emulsions, i.e. showing contact angles < 90° (Figure 1.3b). For example, stable oil-in-water (o/w) droplets can be easily prepared using hydrophilic goethite particles, while in comparison, (w/o) droplets can be prepared by hydrophobic polystyrene particles.[34] Notably, while numerous examples report the use of hydrophobic silica for the generation of highly stable PEs, hydrophilic silica spheres have not been able to stabilize PEs without additional surfactants.[29,35] Hydrophobization of silica is often used to allow PE catalysis and the same concept has been utilized to tune the contact angle of other types of materials, including the catalytically active material. For example, hydrophilic zeolites are unable to stabilize oil-water Pickering emulsion whereas hydrophobized zeolites, i.e. silylated, were very efficient as solid emulsifier for same PE system.[36]

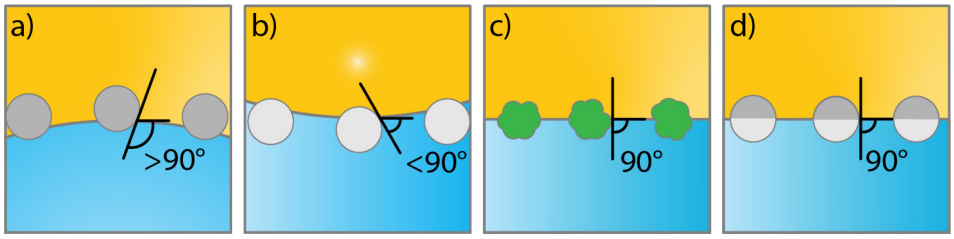

Figure 1.3: Configuration of a) hydrophobic spheres, b) hydrophilic spheres, c) rough spheres and d) amphiphilic Janus spheres at the interface with corresponding contact angles measured through the aqueous phase.

On the other hand, the strength of the adsorption of the particle at the liquid–liquid interface is governed by both the interfacial tensions and the surface morphology of the particles[37]. By increasing the roughness of the surface, solid particles can adsorb very strongly at the interface (Figure 1.3c). Increased surface roughness of the particle not only dramatically improves PE stability, but also offer the opportunity to produce stable o/w and w/o emulsions by dispersing the same type of particle initially into either the aqueous or oil phase.[38] Isa *et al.*[39] prepared non-catalytic silica microparticles with tunable surface roughness and demonstrated that surface roughness caused pinning of the contact line around the adsorbed particles, consequently trapping the particle via strong adsorption and thus dramatically promoting emulsion stability.

1.2.2 Particle geometry

In early work, most of the particles investigated in PE were homogeneous spheres. However, similar to spheres with surface roughness, pinned contact lines can also be achieved using Janus spheres,[40] as the roughness at the Janus boundary is more dense than at homogeneously covered particles (Figure 1.3d). In 2001, Binks and Fletcher explored a theoretical comparison between spheres of uniform wettability and Janus particles with two surface regions of different wettability.[33] By varying the relative surfaces areas or the different wettability of the two surface regions on the Janus particles, they demonstrated that unlike homogeneous particles, Janus particles retain their strong adsorption regardless of the wettability on different regions. Therefore, they predicted that Janus particles with either low or high average contact angles will prove to be efficient emulsion stabilizers. Indeed, inspired by the work by Binks, chemically anisotropic particles like amphiphilic Janus particles (hydrophobic on one side, hydrophilic on the other) were synthesized and proven able to stabilize emulsions and maintain their stability for an extended period of time, more effectively than homogeneous particles. Both Janus spheres[41] and Janus dumbbells[27] were used as stabilizers in PIC systems. Resasco *et al.*, for example, prepared amphiphilic Pd/Janus silica catalyst to catalytic hydrogenation of glutaraldehyde and benzaldehyde.[42] When the catalyst contained Pd on both sides of the Janus particles, high conversion levels were obtained for both reactants (i.e., glutaraldehyde in the water phase and benzaldehyde in the oil phase). However, when the catalyst had Pd selectively deposited on one side (the hydrophobic patch) of the silica spheres, the conversion of benzaldehyde was the same, while the conversion of glutaraldehyde decreased dramatically, demonstrating the high phase selectivity of the system.

With the development of new synthesis techniques, various non-spherical particles could be produced and were tested as colloidal surfactants, including particles shaped like one-dimensional fibers[43,44], ellipsoids[34], rods[45–48], two-dimensional nanosheets[28,49] or plates[5]. In a study of the effect of particle shape on emulsion stability, Vermant *et al.* prepared a series of polystyrene particles of different ellipticity via physical stretching.[34] They found that an increase of aspect ratio of the particles, keeping all other parameters constant, led to more stable PEs. The resulting emulsions were found to be highly stable for over 10 months when the aspect ratio (AR = long axis / short axis) exceeded 4.6. Similarly, Huang *et al.* demonstrated that emulsions stabilized with silica spheres (AR=1) phase separated after 1 day, while higher aspect ratio silica particles gave stable solid-stabilized emulsions if the AR of the particles was ≥ 3.[46] Compared to spherical polystyrene spheres, cylindrically[50] shaped particles also exhibit outstanding stability as stabilizers for PE (Figure 1.4a-d).[34] Erné *et al.* and Capron *et al.* proved respectively that ultrathin plate-like colloidal particles

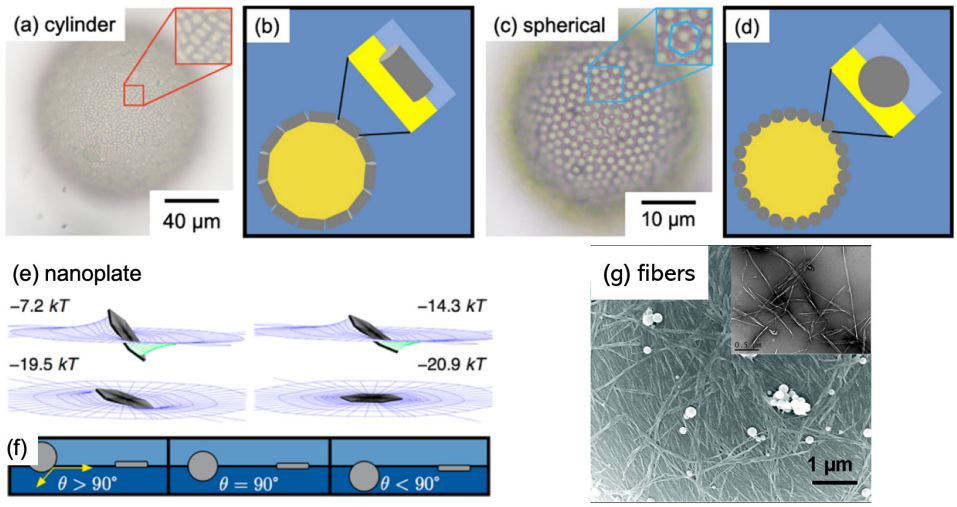

Figure 1.4: Optical micrographs of different arrangements of (a) cylindrical and (c) spherical particles on a droplet of o/w PE. Panels (b) and (d) show schematic image for the optical micrographs in panels (a) and (c), respectively. Adapted from Capron *et al.*[47] (e) Numerical calculations of the adsorption energy of nanoplates with an effective diameter of 167 nm at the water–water interface, interfacial tension is 4 µN/m. Strengthening of the adsorption as a nanoplate reorients itself to lie flat in the liquid–liquid interface (θ = 90°). (f) Schematic representation of the limited effect on blocked area of liquid–liquid interface in the case of a platelet, compared to a sphere at different contact angles. Adapted from Erné *et al.*[5] (g) Scanning electron micrographs (SEM) of polymerized styrene PEs stabilized by bacterial cellulose nanocrystal fibers. Inset, transmission election micrographs (TEM) of bacterial cellulose nanocrystals. Adapted from Capron *et al.*[43]

and nanorods (Figure 1.4e and f) are even effective in stabilizing water-water emulsions, systems that feature ultralow interfacial tension.[5,47] The adsorption of such nanoplates was found to be stronger than for spheres with the same maximal cross section. Capron *et al.* prepared monodisperse oil in water droplets with bacterial cellulose nanocrystal fibers, with the PE remaining stable for several months (Figure 1.4g).[43]

The evident advantage of anisotropic particles with high aspect ratios in stabilizing PEs is that particles tend to lie flat at the interface; hence, little weight is needed to cover a large surface area in contrast to spherical particles.[51] Moreover, the adsorption of particles with high-aspect ratio is much less sensitive to the three-phase contact angle than spheres. Lastly, since the configuration of the particles with high-aspect ratio is relatively independent from the three-phase contact angle (Figure 1.4e and f), by tuning the

fraction between two immiscible liquids, both stable o/w and w/o can be achieved using same type of particles, which is an obvious advantage compared with spherical emulsifier particles that need to be modified to a suitable hydrophobicity.[28,52,53] Anisotropic particles thus offer many opportunities for PIC or PAC strategies. Taking advantage of materials with a high aspect ratio in preparing stable PEs, Resasco *et al.* reported the use of single-walled carbon nanotubes (SWCNT)-silica nanohybrids for the preparation of o/w emulsions with high catalytic activity toward biphasic hydrodeoxygenation and condensation reaction in a water-in-oil emulsion.[54] Similarly, Qiu *et al.* demonstrated that the CNT composite particles showed excellent activity, selectivity and stability in the selective oxidation of benzyl alcohol in a water/toluene system.[55]

1.2.3 Stimuli-responsive materials

Stimuli-responsive materials respond sharply to small changes in physical or chemical conditions with relatively large phase or property changes. These materials are playing an increasingly important role in a diverse range of applications, such as drug delivery, optical devices and coatings.[56] Stimuli-response materials also have great potential in the application of PE systems for catalysis. There is a strong desire to design PEs with tunable states. For example, to facilitate mass transport processes, careful control over wettability and interfacial tensions is needed. Or, to obtain reversible PEs for catalysis and allow easy catalyst recycling, both the formation and destabilization of a PE should be controllably accessible. Indeed, environment-responsive materials have recently attracted considerable interest as they provide not only the ability to stabilize emulsions, but also a tool to reconstruct the emulsion by responding to environmental changes, for example, changes in pH[57] (Figure 1.5a), temperature[58], external fields[59] (Figure 1.5b-d) or even a combination of those[60] (Figure 1.5e-i). Fine control over geometry of the emulsions and easy making and breaking of the emulsions make stimuli-responsive materials promising in reducing surfactant usage, waste generation and process remediation costs.

When the particles are field-responsive, for example magnetic-responsive, the position of the PE stabilized with such particles can be easily changed or the PE itself can be destabilized by applying a magnetic field to easily recycle the emulsifier particles, the reactants and products.[59,61,62] (Figure 1.5b-d). Song *et al.* prepared Fe_3O_4 NPs/$PW_{12}O_40_3$-based ionic liquid composite nanosheets as magnetic-responsive catalysts for the esterification of oleic acid and methanol[61]. The amphipathic and ultrathin magnetic-responsive Janus nanosheets not only served as superior solid surfactants to stabilize PEs, but also showed good catalytic performance (78% esterification yield after recycling four times) and good recyclability. Dong *et al.* reported using Pd NPs-loaded and pH-switchable polymer-grafted UiO-66-type NMOF (nanoscale metal–organic frameworks). The UiO-66

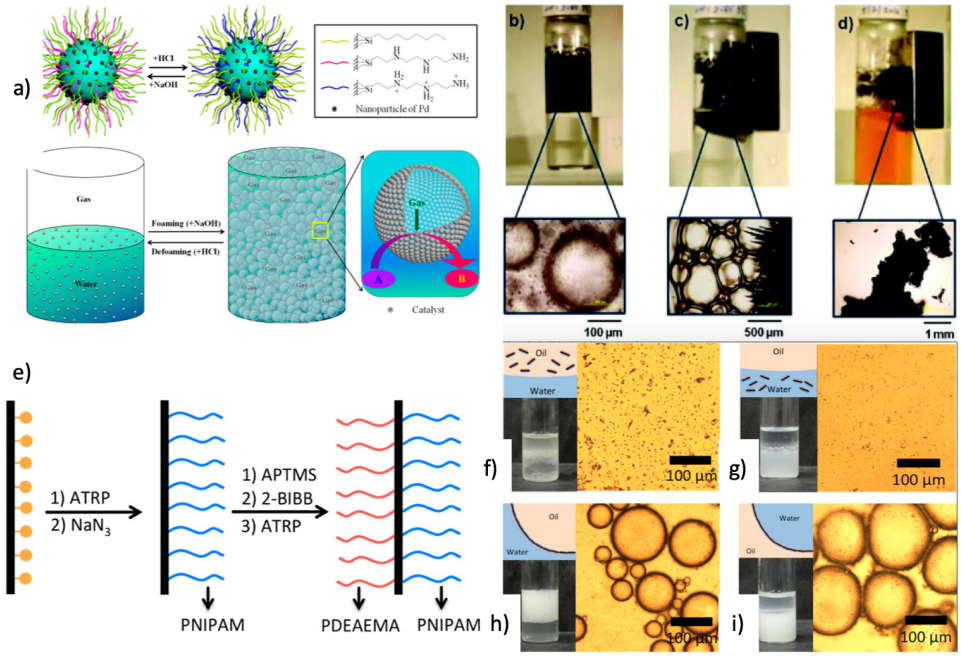

Figure 1.5: Environment-responsive materials to stabilize PEs: a) to control the transforming a gas–water–solid Using pH-responsive, partially hydrophobic nanoparticle catalyst via protonation and deprotonation with acid or base. Adapted from Yang *et al.*[57] b) Wet foam prior to exposure to a magnetic field. c) Collection and d) breakdown of foam responded to the field. Adapted from Velev *et al.*[59] e) Illustrative synthesis of the dually responsive Janus composite nanosheets with poly(N-isopropylacrylamide) and poly(2-(dimethylamino)ethyl methacrylate) as thermal and pH sensitive materials. f) Optical microscopy image of the mixture (inset) at pH = 10 and T =50 °C, no emulsification occurs, the hydrophobic nanosheets dispersed in toluene; g) At pH = 2 and T = 25 °C, no emulsification occurs, the hydrophilic nanosheets dispersed in water; h) A toluene-in-water emulsion forms at pH = 2 and T =50 °C; (i) A water-in-toluene emulsion forms at pH = 10 and T =25 °C. Adapted from Yang *et al.*[60]

NMOF surface-decorated with poly[(2-diethylamino)ethyl methacrylate)] (PDEAEMA) is pH-responsive, and the resulting Pd@MOF-3 could easily transform a traditional BS to an o/w PE.[63] By alternative protonation-deprotonation of the amino groups on PDEAEMA, the system displayed pH-induced (de)emulsification behavior. The solid catalysts were shown to promote a one-pot, biphasic Knoevenagel condensation–hydrogenation cascade reaction under ambient conditions.

1.2.4 Mono-catalytic emulsifying particles

In the previous material sections, we mainly focused on the impact of functionality of the materials on PE formation. In addition, the solid particles can serve not only as emulsifier, but can also act as catalyst themselves, in which case the particles work as emulsifier/catalysts hybrid materials. The immobilization of the catalysts in/on the solid materials can be processed via nanoparticle deposition. For example, Yang *et al.* synthesized Pd/SiO_2 emulsifiers by depositing Pd nanoparticles on mesoporous silica.[64] These materials acted as interfacial active nanoparticle catalysts in a w/o PE and showed significantly enhanced catalytic efficiency in olefin hydrogenation compared to conventional BS. Another method to obtain catalytically active particles is by surface modification, as in the study of Zhang *et al.*[65] Amphiphilic, acidic silica nanoparticles were obtained by grafting silica NPs with inert alkyl chains (C_3, C_8 and C_{18}) and active propylsulfonic acids. After optimizing the ratio between the inert and the active surface functional groups (C_n : SO_3H molar ratio = 54 : 46), stable methanol/triglyceride oil PEs could be obtained. The acid groups were introduced via silane thiol grafting, followed by oxidation to give the sulfonic acids, a strategy that has been often used for monophasic solid acid catalysis. The solid catalysts did not only provide stable MeOH/oil PEs but proved to be highly efficient in the transesterification between methanol and the vegetable oil. Furthermore, the catalyst/emulsifier can also be combined with other functionalities, for example with environment or field responsible properties. Yang *et al.* reported solid catalysts made by combining Pd with amphiphilic silica spheres that can be easily in-situ separated and recycled based on pH-triggered PE inversion. The resulting PIC system was shown to have a much higher catalytic efficiency for olefin hydrogenation (99% conversion) and could be recycled more easily compared to the conventional BS.

1.2.5 Dual-catalytic particles

Endowing the particles with two different catalysts offers potential for more versatile PE catalysis. Dong *et al.* reported that Pd nanoparticles loaded Lewis acidic metal-organic frameworks (MOFs) could be employed for PIC, demonstrating their activity in a one-pot biphasic Knoevenagel condensation–hydrogenation reaction.[63] In such tandem reactions, the intermediate product produced in the first step, can be directly used as the substrate for the next reaction, eliminating the need for separation, purification, and transfer, thereby saving energy. It also helps to reduce byproducts and waste generated in separate single-step reactions. For catalysts that are compatible with each other, traditional catalysts loading strategies for mono-catalyst particles are sufficient, as in the case for the MOFs as host for noble metal nanoparticles.[66] For catalysts that are incompatible, such as acid and base catalysts, spatial separation of the catalysts is necessary.

A classical strategy to spatially separate (antagonistic) catalysts is to use stacked-shell structures like core-shell, yolk-shell or multi-shelled hollow structures (Figure 1.6). For example, Qin *et al.* integrated two distinct metal-oxide interfaces based on a tube-in-tube nanostructure using template-assisted atomic layer deposition[69], in which Ni nanoparticles are supported on the outer surface of the inner Al_2O_3 nanotube and Pt nanoparticles are attached to the inner surface of the outer TiO_2 nanotube. The confined space favored the instant transfer of intermediates between the two metal-oxide interfaces. This tandem catalyst showed remarkably high catalytic efficiency in nitrobenzene hydrogenation with hydrogen formed by in-situ decomposition of $N_2H_4{\cdot}H_2O$. Gu *et al.* in turn prepared hyper cross-linked polystyrene hollow nanospheres having both acidic (sulfonic acid) and basic (amine) in the microporous organic structure.[68] Because of the spherical structure of hyper cross-linked polymers, most of the sulfonic acid groups were located on the external shell of the sphere, while the amine precursors were located preferentially on the inside of the microsphere. The resulting acid-base catalyst was utilized in the one-pot tandem catalytic hydrolysis-Henry and hydrolysis-Knoevenagel condensation reactions using 2-(2-bromophenyl)-1,3-dioxolane as substrate. Similarly, Weck *et al.* developed core-shell cross-linked micelles to immobilize Co-porphyrin and $HNTf_2$ in the core, and Rh-TsDPEN and HCOONa in the shell in site-isolated microenvironments.[71] The high efficiency of the dual catalyst particles for enantioselective tandem reaction (Co-catalyzed hydration and Rh-catalyzed asymmetric transfer hydrogenation) can be ascribed to fast intraparticle diffusion of the intermediates.

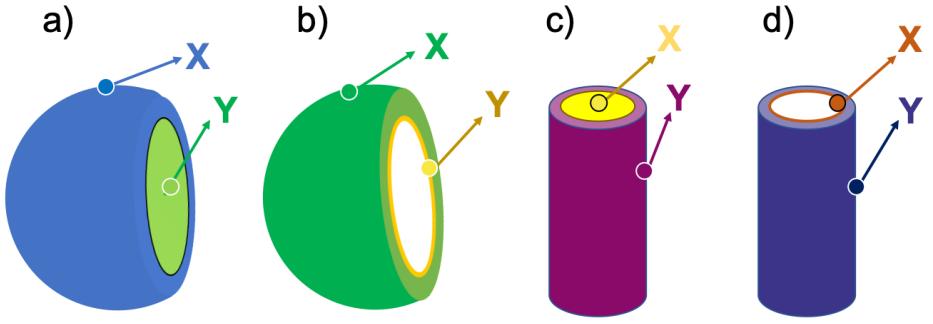

Figure 1.6: Schematic representation of various possible configurations of stacked-shell structure: For convenience, a general spherical and rod-like morphology is adopted in all cases. X and Y represent different catalysts that are incorporated at different compartments. a) core-shell sphere[67], b) double-shelled hollow sphere[68], c) core-shell rod[69,] d) double-layered tube[70].

The second strategy to make particles with multiple functionalities is to use patchy particles like bifunctional Janus spheres and Janus sheets (Figure 1.7). If the distinct faces of the Janus particles can (both) separately be decorated with catalytic functionalities, this would allow compartmentalization of the catalysts in either one of the PE solvents. Alternatively, a catalyst and a functional trigger could be combined on one and the same particle. Zhang *et al.* reported that Janus nanosheets were utilized to achieve ionic liquid (IL) in oil PEs with excellent emulsion stability.[74] Moreover, [BMIM]Cl-based Janus nanosheets showed excellent catalytic performance for desulfurization of dibenzothiophene and proved to be reusable. However, this particle has only one catalytically active site, while the other side is catalytically inert. In general, the Janus spheres and dumbbells that have been reported recently carry at least one patch that is catalytically "inert" (mono-catalyst) and, hence, cannot work as dual-catalyst for tandem reactions.[27,75,76] Therefore, the practical challenges of Janus particles as solid catalysts is to synthesize bifunctional particles, that can be modified with various catalysts. However, bifunctional particles with non-catalytic chemically orthogonal patches have been successfully developed. For example, Weck *et al.* developed bi-functional anisotropic particles featuring chlorine-functionalized patches and carboxylated domains.[77] Kegel *et al.* prepared Janus spheres that carry chemical handles facilitating independent and orthogonal surface modification using Atom Transfer Radical Polymerization (ATRP) and thiol–yne click chemistry, respectively.[72] We expect that these particles will serve as a versatile starting points for the synthesis of dual-catalyst particles for tandem catalysis. In a more general sense, offering PE stabilization by pinning and orthogonally addressable patches, Janus particles offer much potential and their application in PE catalysis is are expected to emerge as class of materials in the near future.

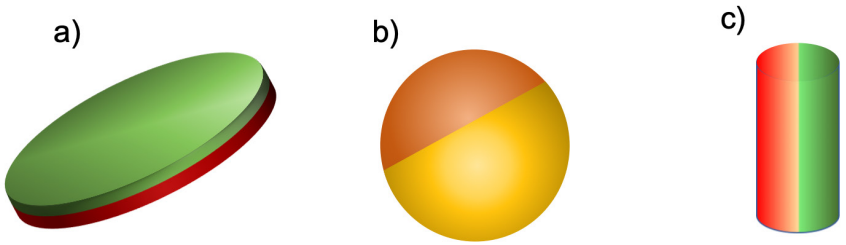

Figure 1.7: Schematic representation of various possible configurations of Janus materials: a) Janus plate or sheets[28], b) Janus sphere[72], c) Janus rod[73].

1.3 Catalytic reactions in PEs

Having established the different possible PE stabilizing materials and their most important properties, in this section we will highlight the advances made and strategies adopted for performing catalysis in PEs as already delineated by Nardello-Rataj *et al.* Figure 1.8 schematically shows the different possible strategies for PAC and PIC in w/o PEs. PAC strategies include the use of homogeneous chemo or biocatalysts, confined in either the dispersed or the continuous phase of the PE (Figure 1.8a and b), depending on the nature of the liquid phases and the solubility of the catalyst. Another possibility is the combination of both catalysts confined in the aqueous and organic phase (Figure 1.8c), which can be used for tandem or cascade reactions, as also illustrated in Chapter 2 of this PhD Thesis. PIC strategies in turn comprise all catalytic reactions in PEs that use catalytically active stabilizing particles. These could be catalytic particles immobilized on or functional groups grafted on a catalytically inert support material (Figure 1.8d). For this approach a single type of particle could be used or a physical mixture of particles with different catalytic functionalities (Figure 1.8e). Another option is to use non-supported catalyst particles as PE stabilizer (Figure 1.8f).

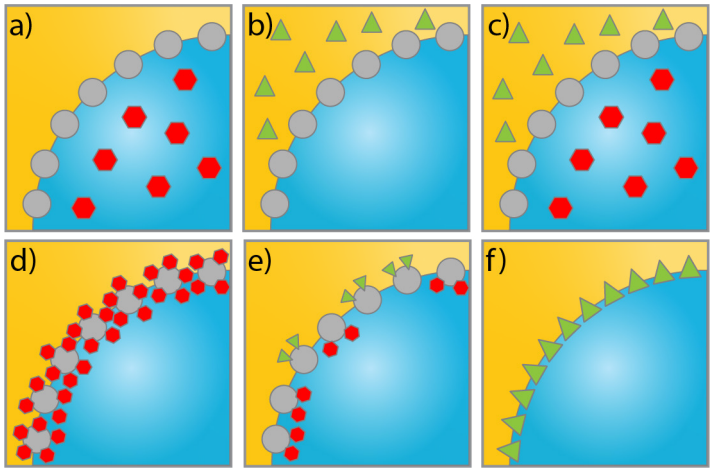

Figure 1.8: Schematic representation of PAC and PIC in w/o PEs. Yellow: organic phase, blue: aqueous phase. a-c) PAC approach with a) catalyst confined in aqueous phase, b) catalyst confined in organic phase and c) catalysts confined in both the aqueous and organic phase. d-f) PIC approach with c) one catalyst supported on inert material used as Pickering stabilizer and e) physical mixture of particles with two distinct catalysts on inert material used as Pickering stabilizer and f) catalyst particles used as Pickering stabilizing particles.

1.3.1 Advances in PAC

One of the reasons to use PEs is the high interfacial area that is beneficial for the rate of reactions taking place at the liquid-liquid interface[16], but also for reactions that require extraction of products from one phase to the other. One such an example was given by Zhang *et al.*, who employed PEs as a reaction medium for the acid-catalyzed dehydration of fructose to 5-(hydroxymethyl)furfural (5-HMF).[78] This reaction is known to be very susceptible for side-product formation as the 5-HMF easily reacts with the acid catalyst to form small organic acids or polymers. Therefore, quite some studies have been performed on the extraction of 5-HMF during reaction in order to prevent this side-product formation, in which methyl isobutyl ketone (MIBK) was identified as suitable extracting solvent.[79]

However, this reaction was only performed in normal BS and not in PEs. First attempts of Zhang *et al.* to prepare MIBK formulated PEs stabilized with polystyrene resins failed, as the particles used were too large. W/o PE preparation was successful, however, when hydrophobic silica particles were used. Fructose dehydration in a PE made with acidic water saturated with NaCl as aqueous phase and methyl isobutyl ketone (MIBK) as organic phase, resulted in suppression of side product formation and, consequently, an increase in yield and selectivity (Figure 1.9). The reactions were performed under conditions that

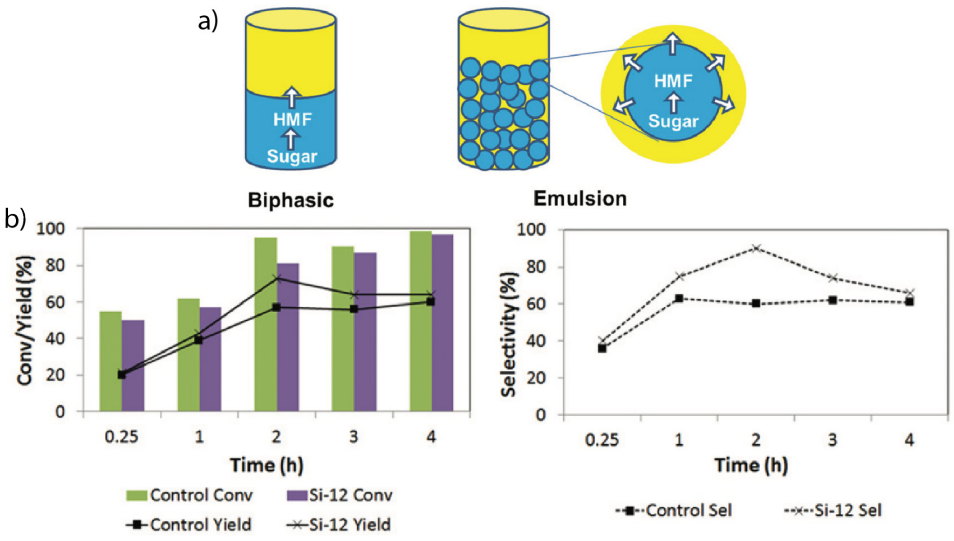

Figure 1.9: a) Biphasic and PE approach for the acid catalyzed dehydration of fructose and subsequent 5-HMF extraction by Zhang *et al.* b) Fructose conversion and 5-HMF yield and selectivity in the biphasic and the PE reaction. Adapted from Zhang *et al.* [78].

are rather demanding for a PE, i.e. at 100 °C for 2 h. Due to the low concentration of solid particles (0.33 wt% with respect to MIBK) no full emulsion phase was created and stirring was required to keep the high interfacial area. However, the addition of particles did enhance the yield and selectivity from 57% to 73% and from 60% to 90%, respectively.

Whereas most PAC examples use liquid-liquid-solid PE systems to increase the interfacial area to enhance the mass transport between the two immiscible phases, this approach can be extended to reactions that require gasses, such as hydroformylation or hydrogenation reactions. Addition of gasses make the systems even more complex as the mass transfer of the gas should also be taken into account. For o/w emulsions, the mass transfer coefficient of the gas is similar to that in the pure aqueous phase.[80] Therefore, the PE system should principally not affect the reaction efficiency other than the effect of the increased interfacial area when compared to the usual biphasic reaction. For w/o emulsions, the volume fraction of oil is proportionately related to the mass transfer coefficient. Therefore, the mass transfer coefficient can be calculated as the mean of the coefficients in the pure components weighted by the respective volume fractions. The group of von Klitzing

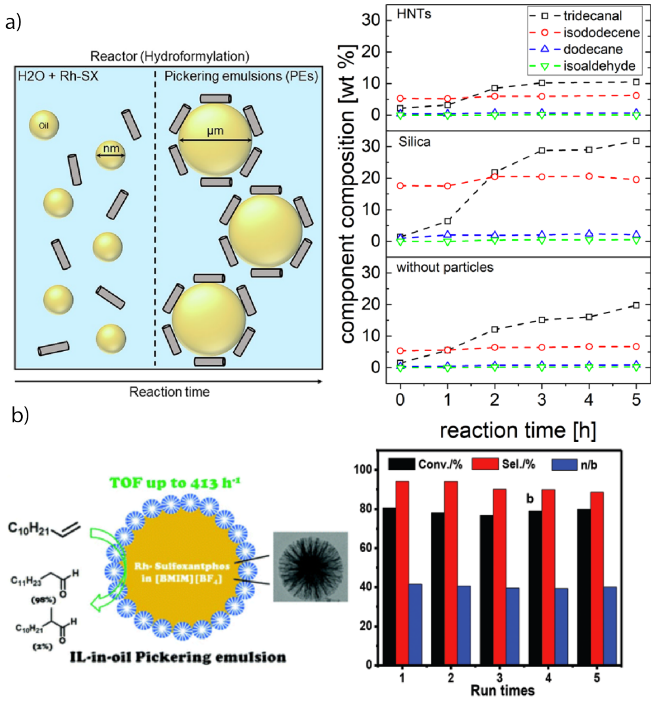

Figure 1.10: a) Approach and catalytic results for hydroformylation of 1-dodecene in BS and silica and HNT stabilized PEs as described by von Klitzing *et al.* Adapted from [81]. b) Approach and catalytic recycling results for hydroformylation of 1-octene in IL/o PEs as published by Yang *et al.* Adapted from [82].

et al. studied hydroformylation of 1-dodecene in o/w PEs.[81] Hydroformylation reactions are commonly catalyzed by a homogeneous rhodium (Rh) catalyst, in the presence of syngas (CO/H_2 mixture). One of the major issues for the hydroformylation of longer hydrocarbons is the mismatch in solubility between the catalyst (water soluble) and the substrates, something that could be addressed by using a PE as alternative reaction medium. They compared the performance of an o/w PE formed with only the catalyst, the catalyst in combination with silica or the catalyst in combination with Halloysite nanotubes (HNTs) (Figure 1.10a) at 100 °C, and 15 bar of syngas. One of the most interesting results was that the activity of the most stable PE, the one stabilized by HNTs, was low (TOF of 18 h^{-1}), however, an aldehyde selectivity of 86% was obtained. The PEs formulated without any particles were, not surprisingly, the least stable, but gave a higher TOF of 26 h^{-1} and an aldehyde selectivity of 84%. The PEs stabilized by silica particles, had the highest activity, a TOF of 55 h^{-1} was measured, but with the lowest aldehyde selectivity (77%). The use of PEs was not intrinsically beneficial for the performance of the catalytic reaction, as the highest TOF was obtained by BS with similar aldehyde selectivity as the HNT-stabilized PE. This could be due to the fact that the reaction mixtures were stirred at 1200 rpm, enhancing the interfacial area of the non-stabilized system as well.

The group of Yang *et al.* used a different type of PE for the hydroformylation of 1-dodecene, namely an IL/o PE stabilized by C18-functionalized mesoporous silica (Figure 1.10b).[82] The solubility of olefins is higher in ILs than in water and ILs also have a higher boiling point than water. They performed the hydroformylation reactions at 110 °C and with 20 bars of syngas, stirring the system at 1000 rpm. With their PE system, a much higher selectivity was obtained than in the normal w/o PE, 94% vs 69% at similar conversions. Also, an excellent TOF of 413 h^{-1} was obtained with this system. The superb performance was ascribed to the higher solubility of substrate and of CO in the IL. The particles could be recycled for 5 runs without significant loss of reactivity.

1.3.2 Advances in PIC

In the past five years, considerable advances have been made in the field of PIC. One example being the heterogenization of biocatalysts, in which enzymes were immobilized on or in the stabilizing materials.[83–85] A regularly used heterogeneous biocatalyst is the lipase from Candida rugosa (CRL) in combination with the metal-organic framework (MOF) ZIF-8, forming an o/w PE with an aqueous buffer phase and heptane. Two different examples of incorporating the enzyme in the MOF were reported, one being the immobilization of CRL on the outer surface of ZIF-8 crystals after synthesis (Figure 1.11a)[83] and the other being encapsulation of CRL inside the ZIF-8 crystals by addition during MOF synthesis (Figure 1.11b).[84] These catalysts were both tested for the hydrolysis of oil-soluble

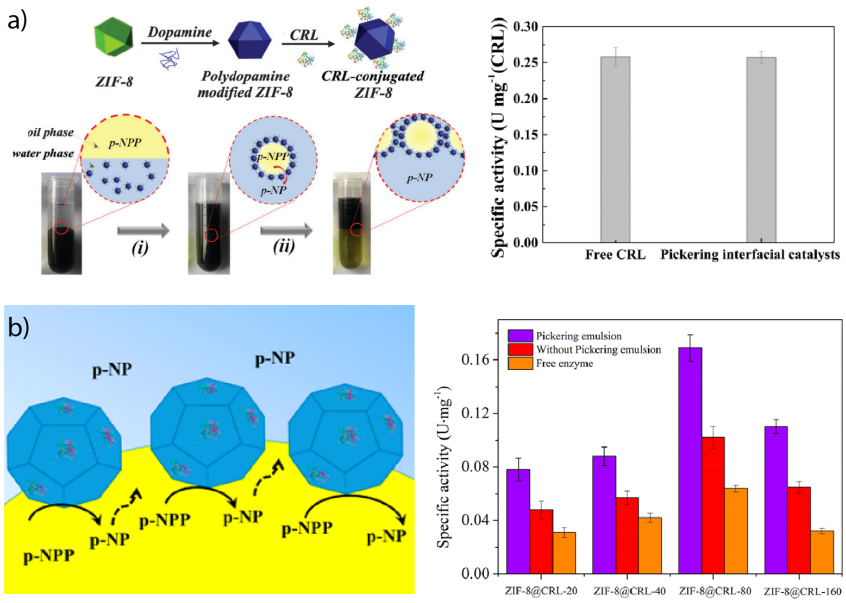

Figure 1.11: a) Approach and specific activity of the hydrolysis of *p*-NPP to *p*-NP catalyzed by CRL immobilized on the surface of ZIF-8 crystals. Adapted from Jiang *et al.*[83]. b) Approach and specific activity of the hydrolysis of *p*-NPP to *p*-NP catalyzed by CRL immobilized inside ZIF-8 crystals. Adapted from Lu *et al.*[84].

p-nitrophenyl palmitate (*p*-NPP) to form and extract water-soluble p-nitrophenol (*p*-NP) at 25 °C. As the pores of the MOF are large enough for these molecules, no mass transfer limitations were expected. The catalyst with the CRL immobilized on the outside of the ZIF-8 crystals was the most active with a specific activity of 0.25 μmol·min^{-1}·mg^{-1} against 0.16 μmol·min^{-1}·mg^{-1} for the catalyst with the enzymes incorporated inside the ZIF-8 crystals. The specific activity of the immobilized enzyme catalyst was similar to that of the free enzyme, but the storage stability of the free enzyme was much lower (85% for the heterogeneous catalyst vs. 60% for the free enzyme). Immobilization of the CRL on the crystal also led to higher retention of the activity during recycling, after 13 recycling runs 83% of the specific activity was observed, while the encapsulation of the enzyme lead to a complete loss of activity after 4 runs.

The same enzyme was successfully adsorbed on carbonaceous microspheres (CMs) in the work of Yang *et al.* and used for the hydrolysis of olive oil in a o/w PE.[85] This reaction was studied as function of interfacial area and interfacial enzyme concentration. An increase of the interfacial area usually leads to an increase in reaction rate due to shortening the distance between substrate and enzyme. However, at a constant enzyme concentration an increase of interfacial area also results in a decrease of interfacial enzyme concentration,

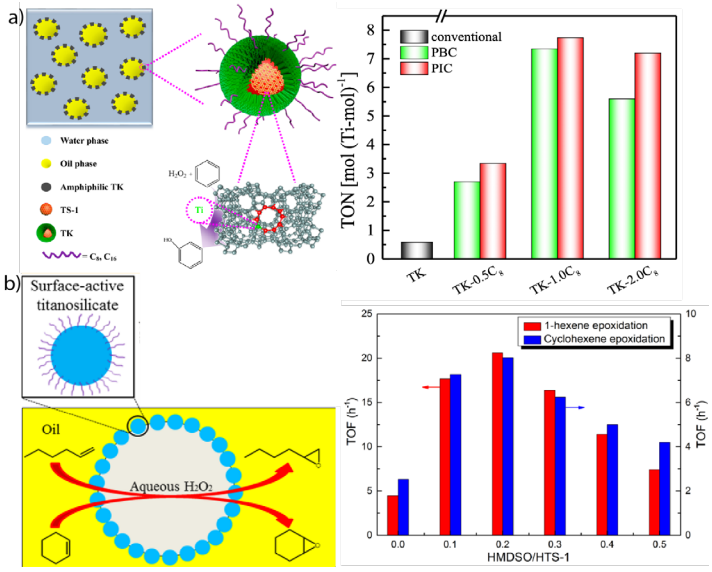

Figure 1.12: a) Approach and catalytic results of 1-hexene epoxidation in TS-1 stabilized PEs. Adapted from Wu *et al.*[86] b) Approach and catalytic results of 1-hexene epoxidation of HTS-1 stabilized PEs. Adapted from Binks *et al.*[87]

leading to a reduced reaction rate. As a result of these two competing effects, no significant influence of the change in interfacial area on the reaction rate was observed.

Another advancement was made by using new catalytic stabilizing materials. For example, titanium containing silicates (TS-1), like the MOFS and carbonaceous microspheres porous catalyst materials, for liquid-phase oxidation and epoxidation were utilized by two different research groups. In 2015, the group of Wu *et al.* published the preparation of a TS-1/mesoporous silica composite material and the use for epoxidation of 1-hexene to 1,2-epoxyhexane (Figure 1.12a).[86] The formation of the composite material was necessary to stabilize PEs as the TS-1 itself is not amphiphilic enough. The catalytic reaction was performed at 60 °C for 1 h, wherein a TON of 7.74 mol·(mol Ti)$^{-1}$ was obtained in the PE, where in the non-PE system a TON of only 0.58 mol·(mol Ti)$^{-1}$ was achieved, a difference attributed to the increased interfacial area in the PE system. However, the activity decreased drastically upon recycling with only 50% of the activity remaining after four runs.

An improved way of using TS-1 as catalyst for 1-hexene epoxidation was shown by Binks *et al.*, where hollow TS-1 (HTS-1) particles were synthesized by treating the TS-1 with tetrapropylammonium hydroxide (TPAOH) (Figure 1.12b).[87] The HTS-1 particles were then post treated with an hydrophobizing agent to make the particles amphiphilic. The

epoxidation experiments were performed under the same conditions as reported by Wu *et al.* resulting in a TOF of 20.6 h^{-1}. This almost threefold improvement was attributed to improved mass transfer. The catalyst particles also proved more resilient towards recycling, resulting in 95% of the starting activity after 5 runs.

Another interesting application of PIC is in the preparation of bio-based surfactants, as reported by Clacens *et al.*[88] by acid catalyzed etherification of glycerol and dodecanol, two immiscible reactants. Glycerol was mixed with dodecanol to form a decanol-in-glycerol-in-decanol PE (d/g/d) stabilized by polystyrene-grafted silica particles functionalized with sulfuric acid groups utilized as PIC. After reaction for 24 h at 150 °C, a dodecanol conversion of 43% and a dodecyl glyceryl ether (DGE) yield of 34% was obtained, while the PE showed slight destabilization, while synergistic stabilization between particles and surfactants is expected.[89] The solid catalyst outperformed benchmark acid catalysts such as p-toluenesulfonic acid (PTSA) and dodecylbenzenesulfonic acid (DBSA) which were not able to form a stable PE at all, showing the benefit of using PEs as reaction media for reactions using immiscible substrates.

Just as in the PAC examples quite some advantages have been made in heterogeneously catalyzed gas-liquid phase reactions. Several different approaches for hydrogenation in PEs have been published by the group of Yang *et al.*[90–92] They created two pH switchable systems stabilized by Pd/SiO_2 particles, one being a w/o PE[90], the other one being a g/w PE[57]. By increasing the pH to ~7 a stable emulsion was created, while lowering the pH by addition of HCl led to destabilization and therefore easy recovery of the catalysts. The g/w PE was shown to be stable at room temperature, however, no stability data during reaction was given. The w/o and g/w PE were utilized for the hydrogenation of oil-soluble and water-soluble substrates, respectively, at relatively low temperatures (≤40 °C) and pressures (max. 3.5 bar). Full conversion could be reached within 2 hours with TOF of around 1400 h^{-1}, with the PE system thus outperforming conventional BS (Figure 1.13). Catalyst stability in the liquid phase was high as after 15 runs a yield of 90% was obtained. In the g/w system the stability was lower, already in the second run longer reaction times were needed to obtain full conversion due to aggregation of Pd particles.

Ru-catalyzed selective hydrogenation of benzene was performed in a o/w and w/o PE stabilized by Ru/TiO_2 nanoparticles, varying the type of PEs by altering the hydrophilicity of the TiO_2 particles.[92] The o/w PE outperformed both the conventional BS and the w/o PE, due to the low solubility of H_2 in water. The selectivity towards cyclohexene was 51% at 84% conversion while, at the same conversion level, only 44 and 46% was reached in the biphasic and the w/o PE, respectively. Recycling of the particles resulted in a gradually drop in activity which the authors claim to be a result of loss of material due to multiple

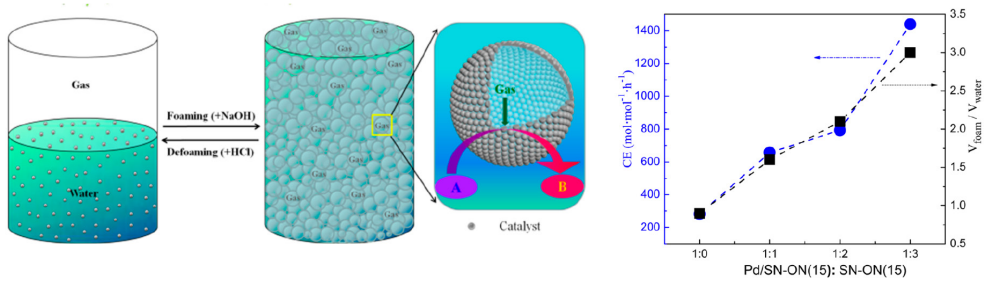

Figure 1.13: Schematic representation of the hydrogenation of p-NP in a pH-switchable g/w PE and the catalytic results as obtained by Yang *et al*. Adapted from [57].

transferring and separation. These results show that the type of PE (w/o or o/w) should be carefully chosen dependent on the targeted reaction and the reactants involved. The examples highlighted above show the versatility of using PEs as reaction media for catalysis., They can, for example, be used to compartmentalize homogeneous chemo- or biocatalysts to improve reactivity between immiscible substrates and catalysts (PAC). Separation between the liquid phase containing catalyst and the liquid phase containing reagents and products also improves the recyclability of the catalysts. The main advantage of the use of PAC is the ability to use catalysts that do not require any complicated syntheses. On the other hand, heterogeneous catalysts, which often do require complex syntheses, can be placed at the liquid-liquid interface to perform PIC. The activity of these catalytic systems is generally higher than the PAC systems. However, the recyclability of the catalytic particles is usually negatively affected by the instability of the particles under reaction conditions. The window of operation of PEs as reaction media has been expanded in the past 5 years by performing reactions requiring elevated temperatures, using enzymes immobilized on and in support materials and the use of pH switchable PEs. One of the main deficiencies in the published work on PE catalysis is the lack of PE stability data. During reaction, stability of PEs is not always easy to investigate, especially when working with closed vessels such as autoclaves. However, without being sure that PEs are stable during reaction, it is impossible to draw hard conclusions about the influence of PE on catalytic results.

1.4 Advances in PE reactor engineering

All previous examples make use of PE as reaction media in batch reactions. The ability of PE to encapsulate the water or oil phase in a stable droplet offers an opportunity to immobilize molecular catalyst in a flow reactor. The combination of flow system and catalyst immobilization provides facile product separation together with catalyst recovery

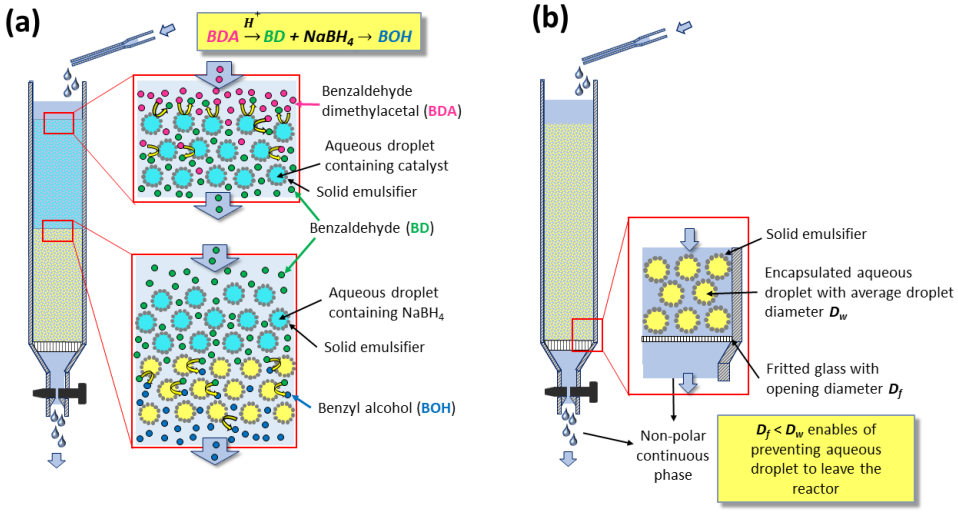

Figure 1.14: a) Illustration of the lamination technique to compartmentalize incompatible substances inside the dispered phase of a Pickering emulsion b) realization of flow Pickering emulsion.

resembling heterogeneous catalysts. Furthermore, performing reaction in flow is also favorable to increase the selectivity due to the shortened contact between product and catalyst preventing the formation of side products. Recently, the implementation of such a flow system was reported by Yang *et al.*[93] In their seminal contribution, they were the first to demonstrate that a cascade reaction involving two incompatible catalysts could be run by isolating those substances in PEs.

The reaction was carried out by continuously feeding benzaldehyde dimethyl acetal dissolved in non-polar solvent to a glass column reactor hosting two layers of w/o emulsion beds (Figure 1.14a). On a first layer of PE containing the acid catalyst, compartmentalized inside the water droplets, the second layer was stacked carrying $NaBH_4$ inside its water droplets. Having the reagents immobilized in the aqueous droplets, neutralization of the catalysts could thus be prevented by the PE. The non-polar benzaldehyde dimethyl acetal, dissolved in the continuous organic phase, could pass the interfacial barrier and be converted to benzaldehyde by the acid catalyst. Further transport of benzaldehyde via the continuous phase to the sodium borohydride containing aqueous droplets in the second layer resulted in reduction to benzyl alcohol. This system shows the ability of PEs to enable the diffusion of non-polar molecules in the continuous phase passing static catalyst droplets packed along a reaction volume, thus resembling a classical continuous plug flow reactor (PFR). This result consequently motivated a number of investigations to

understand and implement flow PEs (FPEs) in a continuous reaction system.

Molecular transport in FPE was first studied by Yang *et al.* in 2016.[94] To realize a continuous operation, n-octane was constantly fed to a column filled with w/o PE with different solid emulsifier concentrations (Figure 1.14b). A steady flow rate was achieved for 360 h suggesting that the PE was stable against gravity and flow shear force. PEs possessing different water droplet diameters (D_W) were successfully prepared by altering the amphiphilic silica concentrations. Higher solid emulsifier concentrations produced smaller D_W which contributes to a low flow rate because of the low permeability in the bed, which contributes to longer residence time. Additionally, a smaller D_W enlarged the ratio between interfacial area and reaction volume (*a/V*) potentially facilitating an enhancement in catalytic efficiency (CE). Contrarily, at lower silica concentrations, high flow rates were observed due to the formation of larger D_W resulting in higher permeability. This behavior suggests that water droplets in the PE resemble the solid particles in a catalyst bed in a packed column used for classical liquid or gas phase catalytic flow reactions. A theoretical understanding of the effect of D_W on the flow rate in PE was sought by applying Darcy's law for laminar fluid permeation through densely packed porous media, as expressed in Eq. 1.1.

$$Q = \frac{kA}{\mu}\frac{\Delta P}{L} \tag{1.1}$$

Where

$$k = \frac{\varepsilon^3}{180\,(1-\varepsilon)^2}\,{D_w}^2 \tag{1.2}$$

For a given cross sectional area (*A*), fluid viscosity (μ), total pressure drop (ΔP) and thickness of the bed (*L*), the discharge volumetric rate (*Q*) is proportional to the permeability (*k*) which is a function of porosity (ε) and D_W in PE (showed in Eq. 1.2). Darcy's law fitted fairly well at smaller D_W (30 – 70) µm, as is shown in Figure 1.15a. However, a large difference is observed between the calculated and the measured flow rate as the droplets grow larger than 70 µm, probably caused by the broad distribution of D_W. Moreover, a residence time distribution (RTD) plot was determined to assess the resemblance of FPE to the plug flow model. A plot of the RTD as function of time (Figure 1.15b) showed a narrow sharp distribution curve implying that the permeation of n-octane is close to ideal plug-flow with negligible dead zone and channeling. Furthermore, a theoretical description has been developed for the stability of PEs under flow condition. This was realized by calculating the adsorption force (F_a) holding particles at w/o interface and the drag force of the running fluid (F_d) attempting to detach the particles from the interface. According to the calculation, F_a is considerably larger than F_d, 5.2×10^{-9} N and 7.47×10^{-17} N respectively,

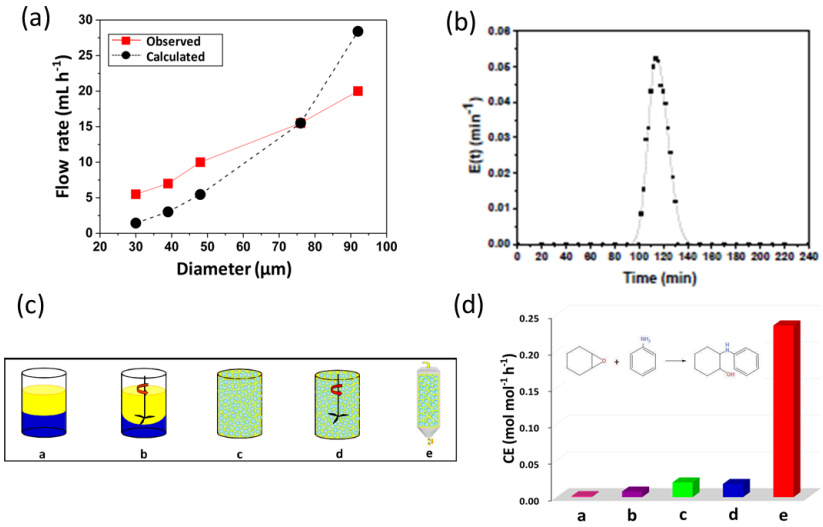

Figure 1.15: a) Correlation flow rate of n-octane and average water droplet size in FPE, b) Residence time distribution curve versus time, c) Five different types of bi-phasic reaction operation, d) catalytic activity of the reaction systems consisting of bi-phasic batch (with and no agitation), batch PE (with and without agitation) and FPE. Adapted from Yang *et al.*[94]

suggesting that the stress caused by the flowing fluid has a negligible effect on breaking PEs.

FPE were furthermore implemented to accommodate catalytic additions of 3,4-dihydro-2H-pyran as well as ring opening of epoxides with aromatic amines. The reactions were performed by feeding non-polar substrate in toluene through a w/o emulsion encapsulating the homogeneous H_2SO_4 catalyst. Firstly, the reaction was carried out in batch systems for sake of comparison, as displayed in Figure 1.15c. Catalytic efficiencies (CE) for the respective systems are exhibited in Figure 1.15d, highlighting the better performance of PE compared to a standard BS. It is also notable that strong agitation did not affect the tested batch systems much. Changing the PE system from batch to continuous substantially enhanced the CE, demonstrating the great advantage of doing catalysis in FPE. Variation of the emulsifier concentration influenced D_W as well, with higher concentrations generating smaller droplets, ultimately leading to a further increase in CE. This is the result of better contact between catalyst and substrates and of the longer residence time as a result of the larger pressure drop over the bed that accompanies a smaller D_W However, it is important to note that excessive emulsifier concentrations negatively affected CE due to the formation of multilayer particles. These layers create

a diffusion barrier for the substrate to reach the active w/o interface buried underneath, resulting in reaction deacceleration. Furthermore, Yang *et al.* were the first to demonstrate that FPE can also be used to increase stereoselectivity in the cyclization of citronellal over $H_3PW_{12}O_{40}$ catalyst to form isopulegol.[95] Citronellal, which is slightly water miscible, enables catalysis to occur both on the interface and in aqueous droplets. However, since FPE offers substantially large w/o interface, interfacial catalysis is dominant resulting in a higher selectivity to isopulegol.

The two examples above the benefits of FPE in promoting interfacial catalysis. Despite being very active, only catalyst molecules occupying the w-o interface contribute to the reaction while most of the catalyst is present inside the droplet. In order to maximize the participation of catalyst, utilizing the droplets instead as a microreactor can be a solution (Figure 1.16a). Thus, Yang *et al.* demonstrated that enantiomeric transesterification of alcohols with chiral esters can be successfully performed in ([BMIM]PF6) IL/octane system catalyzed by CLAB lipase.[96] IL were chosen as dispersed phase rather than water, as they are also immiscible with the organic continuous phase, but do dissolve a wider range of organic substrates than water. In this FPE, the substrate diffused into an IL droplet in which the molecular catalyst is confined. Furthermore, a theoretical study based on Fick's 2nd law to solve the mass balance of limiting reactant and product gave the concentration profiles of reactant and product inside the droplets. The profiles suggest that the transport of reactant and product molecules is driven by the diffusion of these compounds and that the reaction takes place in the droplet only a very short distance away from the shell. As a result, there is an optimum in IL droplet diameter (D_{IL}) providing the highest CE for the reaction (Figure 1.16b) Principally, when D_{IL} is too large, the contribution of catalyst located far inside the shell will be small leading to a lower CE. On the other hand, if the D_{IL} is too small, most reactant molecules will reside too shortly in the droplet responsible for a decrease of CE. This approach was also applied in continuous cyanosilylation of ketones over [bmim]Cl IL catalyst encapsulated in [bmim]BF_4 IL droplet with n-octane as continuous phase. After performing the reaction in FPE for even up to 250 h, no signs of deactivation were observed.[97]

Despite these first successful examples, PEs stabilized by amphiphilic silica nanoparticles are still prone to coalescence, especially at higher substrate concentrations, temperatures and pressures. Those limitations limit the operating window available to do catalysis in FPE. To address this issue, the stability of FPE was improved by fortifying the IL droplet with a silica crust grown by sol-gel condensation of trimethoxysilane (TMS).[98] The silica crust thickness can be adjusted by altering TMS concentration during the synthesis. N_2-physisorption confirmed the mesoporous structure of the resulting material which is advantageous to avoid diffusional resistance of the substrates. w/o PEs with the silica

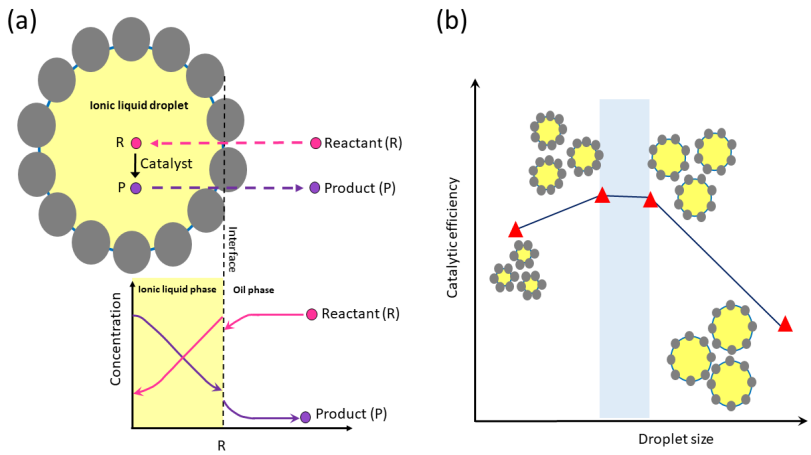

Figure 1.16: a) Illustration of an IL droplet to confine molecular catalyst in PE under flow condition, b) Illustration of the CE in a droplet as a function of droplet size.

crust maintained their stability under continuous flow at 120 °C and 1.0 MPa for 70 h. In the absence of the silica crust the droplets collapsed already after 0.5 h under 0.3 MPa. Moreover, this stable material showed a high CE accompanied with high ee for enantiomeric transesterifications, asymmetric ring opening of epoxides and Tsuji-Trost reactions even after being exposed to an n-octane flow for at least 100 h.

So far, the FPE discussed above were all performed using a glass column hosting a PE bed with continuous addition of the organic continuous phase. A more dynamic operation for FPE was studied by the group of Drews. In their study, Stöber silica was silylated with trimethoxy-octadecyl silane to create amphiphilic particles to compartmentalize water droplets under a flow of organic phase in a continuous stirred tank reactor. Owing to the increased viscosity of the emulsion, N_2 pressure and elevated temperature were applied simultaneously to readily squeeze the organic phase out of a membrane mounted at the bottom of the vessel.[99] Interestingly, the applied pressure positively affected the flux of organic phase leaving the vessel. Optical micrographs confirmed that the increased flux along with the pressure was caused by the coalescence of small droplets to form larger ones. This FPE system was tested in the transesterification of vinyl-butyrate with phenyl ethanol catalyzed by lipase Ca1A.[100] Flow behavior in the presence and absence of lipase Ca1A were firstly studied in an unreactive system before advancing to the continuous reaction. Noteworthy, the addition of lipase Ca1A, which is a surface-active enzyme, to FPE system appreciably altered the composition of solid emulsifier on the interface because of competitive adsorption of solid emulsifier and lipase. The competitive adsorption lead to particle detachment from the w/o interface (Figure 1.17a). These unbound particles got

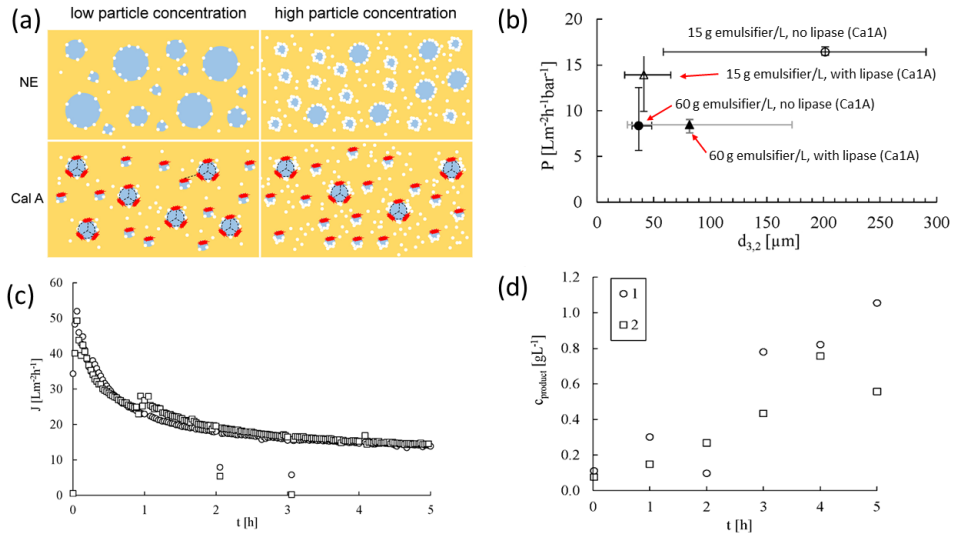

Figure 1.17: a) Schematic illustration of lipase (Ca1A) addition in PE with different solid emulsifier concentrations, as a note: high and low particle concentration stand for 15 and 60 g emulsifier·L^{-1} dispersed phase, respectively. b) Influence of Sauter mean diameter particles on the flux of organic phase, Sauter diameter is defined as the diameter of particle (water droplets) having the same ratio of volume to surface area. c) Flux of organic effluent leaving the reactor over time in a continuous transesterification. d) Time on stream for the ester product concentration. Adapted from Drews *et al.*[100]

dispersed in the organic phase, ultimately leading to a build-up of a cake layer covering the membrane surface responsible to the reduced permeability (Figure 1.17b). Figure 1.17c presents the flux of organic phase over time for continuous transesterification. The rate of the organic liquid leaving the vessel declines with time due to the progressive increase of pressure drop accompanying the formation of dense droplet packing on the membrane by emulsifier particles. The decrease of flow rate however led to enhanced product yield owing to a longer residence time (Figure 1.17d). Amphiphilic colloidal silica could prevent membrane blockage as it created a solid network dispersed in continuous phase leading to improved flux and reproducibility.[101]

Apart from its promising first applications, there are several limitations that have to be overcome for FPE systems. Due to the soft characteristics of the droplets, tight packing of tiny droplets is required to achieve good emulsion stability compensated by high viscosity. Practically, charging a column having large height to diameter ratio with thick emulsion is not trivial, potentially leading to local heterogeneities. Heterogeneous

packing may contribute to less reproducible results, e.g. as a result of channeling and dead zones along the bed. As in packed bed reactors filled with solid catalysts, the filling technique should be carefully considered. In packed bed reactors with solid catalysts, shaping of fine powder in heterogeneous catalyst is crucial to reduce the pressure drop built along the catalyst bed without significantly reducing the effectiveness factor of the catalyst. Solid catalyst also offers high flexibility to change the flow rate to conveniently control the fluid residence time inside the reactor. This is hard to replicate with the soft droplets. Instead, the pressure drop in the emulsion bed can be reduced by using lower emulsifier concentration resulting in bigger droplets. However, larger droplets tend to be unstable. Enlarging the droplets also shortens the residence time and decreases the surface to volume ratio resulting in lower conversion. Another option is to apply additional pressure to the system. However, the applied pressure could promote coalescence of the droplets, affecting FPE performance. Moreover, strong attention must be given to the fact that there is a tendency of particles detachment out of the interface. These unbound particles could deposit on the filter grid creating a cake that can potentially impose additional pressure build up in the system. Therefore, the development and application of amphiphilic materials with a hollow structure, larger size and rigid shell-crust would be an interesting approach to address this problem. Thus, it would give more flexibility to control the process and more reproducible results.

1.5 Scope and Outline of this Thesis

In this PhD thesis we explore the possibilities of using PEs as reaction media for catalysis. We have used the continuous and dispersed phases of the PEs to compartmentalize homogeneous catalysts to perform (tandem) catalytic reactions and compare the performance of these PE systems with conventional BS. Additionally, we investigated the use of catalytically active particles as Pickering stabilizers for the tandem catalytic conversion of biomass. Finally, we have used a droplet microfluidic approach to study catalytic reactions in PEs in flow, including the use of in-situ Raman spectroscopy for online monitoring.

In **Chapter 2** the antagonistic deacetalization-Knoevenagel condensation reaction of benzaldehyde dimethyl acetal is studied in water-in-toluene PEs. This acid-base probe reaction can be performed at room temperature and the performance was examined using various acid and base concentrations.

In **Chapter 3** the stability of alkylphenol formulated w/o PEs is investigated under conditions relevant for catalytic biomass conversion. The stability of PEs using three different alkylphenols is theoretically assessed based on physicochemical properties

as contact angle, interfacial tension and viscosity. The stability of the PEs is studied as a function of solid stabilizing concentration, salinity, pH and temperature. Additionally, the 5-(hydroxymethyl)furfural (5-HMF) extraction efficiency of high and low interfacial systems is shown.

The alkylphenol formulated PEs are subsequently tested as reaction media for catalytic biomass conversion using homogeneous catalysts in **Chapter 4.** Firstly, the acid-catalyzed fructose dehydration reaction to 5-HMF is studied in PEs and BS. Second, fructose dehydration is coupled to a Knoevenagel condensation step to give a tandem catalytic reaction.

In **Chapter 5** heterogeneous catalytic particles are employed for the tandem catalytic conversion of fructose. Monocatalytic particles, acidic and basic, are synthesized as well as, for the first time, bifunctional acid-base Janus particles. The particles were characterized by TEM, FT-IR, and ICP-OES and used as stabilizing particles for PEs showing catalytic activity in the deacetalization-Knoevenagel condensation of fructose.

Finally, a droplet microfluidic approach for the formation of PEs and the execution of antagonistic tandem catalysis in FPE is described in **Chapter 6.** A tube-in-tube co-flow setup is used to form equally spaced droplets inside the tubing allowing the acquisition of kinetic traces of the deacetalization reaction of benzaldehyde dimethyl acetal by in-situ Raman spectroscopy.

A summary of the research described in this PhD Thesis and an outlook are given in **Chapter 7**.

References

1 S. B. P. E. Timmermans and J. C. M. van Hest, *Curr. Opin. Colloid Interface Sci.*, **2018**, *35*, 26.

2 S. U. Pickering, *J. Chem. Soc. Trans.*, **1907**, *91*, 2001.

3 W. Ramsden, *Proc. R. Soc. London*, **1903**, *72*, 156.

4 Y. Chevalier and M. A. Bolzinger, *Colloids Surfaces A Physicochem. Eng. Asp.*, **2013**, *439*, 23.

5 M. Vis, J. Opdam, I. S. J. Van 't Oor, G. Soligno, R. Van Roij, R. H. Tromp and B. H. Erné, *ACS Macro Lett.*, **2015**, *4*, 965.

6 D. G. Shchukin, K. Köhler, H. Möhwald and G. B. Sukhorukov, *Angew. Chem.- Int. Ed.*, **2005**, *44*, 3310.

7 R. Pal, *Curr. Opin. Colloid Interface Sci.*, **2011**, *16*, 41.

8 E. Dickinson, *Curr. Opin. Colloid Interface Sci.*, **2010**, *15*, 40.

9 J. Frelichowska, M. A. Bolzinger, J. P. Valour, H. Mouaziz, J. Pelletier and Y. Chevalier, *Int. J. Pharm.*, **2009**, *368*, 7.

10 J. Marto, A. Ascenso, S. Simoes, A. J. Almeida and H. M. Ribeiro, *Expert Opin. Drug Deliv.*, **2016**, *13*, 1093.

11 H. Hugl and M. Nobis, *Top Organomet Chem*, **2008**, *23*, 1.

12 L. Wu, J. Liu, B. Ma and Q. H. Fan, *Bridg. Heterog. Homog. Catal. Concepts, Strateg. Appl.*, **2014**, 111.

13 L. Gonsalvi, *Catalysts*, **2018**, *8*, 1.

14 S. M. Kelly and B. H. Lipshutz, *Org. Lett.*, **2014**, *16*, 98.

15 M. Cortes-Clerget, N. Akporji, J. Zhou, F. Gao, P. Guo, M. Parmentier, F. Gallou, J. Y. Berthon and B. H. Lipshutz, *Nat. Commun.*, **2019**, *10*, 1.

16 M. Pera-Titus, L. Leclercq, J. M. Clacens, F. De Campo and V. Nardello-Rataj, *Angew. Chem.- Int. Ed.*, **2015**, *54*, 2006.

17 J. Wu and G. H. Ma, *Small*, **2016**, *12*, 4633.

18 W. Fei, Y. Gu and K. J. M. Bishop, *Curr. Opin. Colloid Interface Sci.*, **2017**, *32*, 57.

19 Y. Yang, Z. Fang, X. Chen, W. Zhang, Y. Xie, Y. Chen, Z. Liu and W. Yuan, *Front. Pharmacol.*, **2017**, *8*, 1.

20 C. Albert, M. Beladjine, N. Tsapis, E. Fattal, F. Agnely and N. Huang, *J. Control. Release*, **2019**, *309*, 302.

21 Z. Chen, L. Zhou, W. Bing, Z. Zhang, Z. Li, J. Ren and X. Qu, *J. Am. Chem. Soc.*, **2014**, *136*, 7498.

22 J. Jiang, Y. Zhu, Z. Cui and B. P. Binks, *Angew. Chem.- Int. Ed.*, **2013**, *52*, 12373.

23 Y. Zhu, J. Jiang, K. Liu, Z. Cui and B. P. Binks, *Langmuir*, **2015**, *31*, 3301.

24 F. Tu and D. Lee, *J. Am. Chem. Soc.*, **2014**, *136*, 9999.

25 F. Chen, C. Dong, C. Chen, W. D. Yin, W. Zhai, X. Y. Ma and B. Wei, *Ultrason. Sonochem.*, **2019**, *58*, 104705.

26 T. Tanaka, M. Okayama, H. Minami and M. Okubo, *Langmuir*, **2010**, *26*, 11732.

27 T. Yang, L. Wei, L. Jing, J. Liang, X. Zhang, M. Tang, M. J. Monteiro, Y. I. Chen, Y. Wang, S. Gu, D. Zhao, H. Yang, J. Liu and G. Q. M. Lu, *Angew. Chem.- Int. Ed.*, **2017**, *56*, 8459.

28 F. Liang, K. Shen, X. Qu, C. Zhang, Q. Wang, J. Li, J. Liu and Z. Yang, *Angew. Chem.- Int. Ed.*, **2011**, *50*, 2379.

29 B. P. Binks and S. O. Lumsdon, *Langmuir*, **2000**, *16*, 2539.

30 P. Venkataraman, B. Sunkara, J. E. St. Dennis, J. He, V. T. John and A. Bose, *Langmuir*, **2012**, *28*, 1058.

31 A. D. Dinsmore, M. F. Hsu, M. G. Nikolaides, M. Marquez, A. R. Bausch and D. A. Weitz, *Science*, **2002**, *298*, 1006.

32 O. D. Velev, K. Furusawa and K. Nagayama, *Langmuir*, **1996**, *12*, 2374.

33 B. P. Binks and P. D. I. Fletcher, *Langmuir*, **2001**, *17*, 4708.
34 B. Madivala, S. Vandebril, J. Fransaer and J. Vermant, *Soft Matter*, **2009**, *5*, 1717.
35 B. P. Binks and C. P. Whitby, *Colloids Surfaces A Physicochem. Eng. Asp.*, **2005**, *253*, 105.
36 P. A. Zapata, J. Faria, M. P. Ruiz, R. E. Jentoft and D. E. Resasco, *J. Am. Chem. Soc.*, **2012**, *134*, 8570.
37 Y. Nonomura, S. Komura and K. Tsujii, *J. Phys. Chem. B*, **2006**, *110*, 13124.
38 A. San-Miguel and S. H. Behrens, *Langmuir*, **2012**, *28*, 12038.
39 M. Zanini, C. Marschelke, S. E. Anachkov, E. Marini, A. Synytska and L. Isa, *Nat. Commun.*, **2017**, *8*, 1.
40 B. P. Binks and P. D. I. Fletcher, *Langmuir*, **2001**, *17*, 4708.
41 L. C. Bradley, K. J. Stebe and D. Lee, *J. Am. Chem. Soc.*, **2016**, *138*, 11437.
42 J. Faria, M. P. Ruiz and D. E. Resasco, *Adv. Synth. Catal.*, **2010**, *352*, 2359.
43 I. Kalashnikova, H. Bizot, B. Cathala and I. Capron, *Langmuir*, **2011**, *27*, 7471.
44 Z. Hu, S. Ballinger, R. Pelton and E. D. Cranston, *J. Colloid Interface Sci.*, **2015**, *439*, 139.
45 I. Capron and B. Cathala, *Biomacromolecules*, **2013**, *14*, 291.
46 F. Lou, L. Ye, M. Kong, Q. Yang, G. Li and Y. Huang, *RSC Adv.*, **2016**, *6*, 24195.
47 K. R. Peddireddy, T. Nicolai, L. Benyahia and I. Capron, *ACS Macro Lett.*, **2016**, *5*, 283.
48 S. V. Daware and M. G. Basavaraj, *Langmuir*, **2015**, *31*, 6649.
49 Q. B. Meng, P. Yang, T. Feng, X. Ji, Q. Zhang, D. Liu, S. Wu, F. Liang, Z. Zheng and X.-M. Song, *J. Colloid Interface Sci.*, **2017**, *507*, 74.
50 W. Li, T. Suzuki and H. Minami, *J. Colloid Interface Sci.*, **2019**, *552*, 230.
51 J. S. Guevara, A. F. Mejia, M. Shuai, Y.-W. Chang, M. S. Mannan and Z. Cheng, *Soft Matter*, **2013**, *9*, 1327.
52 C. Yu, L. Fan, J. Yang, Y. Shan and J. Qiu, *Chem. - A Eur. J.*, **2013**, *19*, 16192.
53 Y. Nonomura and N. Kobayashi, *J. Colloid Interface Sci.*, **2009**, *330*, 463.
54 S. Crossley, J. Faria, M. Shen and D. E. Resasco, *Science*, **2010**, *327*, 68.
55 X. Yang, X. Wang and J. Qiu, *Appl. Catal. A Gen.*, **2010**, *382*, 131.
56 M. A. C. Stuart, W. T. S. Huck, J. Genzer, M. Müller, C. Ober, M. Stamm, G. B. Sukhorukov, I. Szleifer, V. V. Tsukruk, M. Urban, F. Winnik, S. Zauscher, I. Luzinov and S. Minko, *Nat. Mater.*, **2010**, *9*, 101.
57 J. Huang, F. Cheng, B. P. Binks and H. Yang, *J. Am. Chem. Soc.*, **2015**, *137*, 15015.
58 B. P. Binks, R. Murakami, S. P. Armes and S. Fujii, *Angew. Chem.- Int. Ed.*, **2005**, *44*, 4795.
59 S. Lam, E. Blanco, S. K. Smoukov, K. P. Velikov and O. D. Velev, *J. Am. Chem. Soc.*, **2011**, *133*, 13856.
60 Z. Zhao, F. Liang, G. Zhang, X. Ji, Q. Wang, X. Qu, X. Song and Z. Yang,

Macromolecules, **2015**, *48*, 3598.
61 D. Xue, Q. B. Meng and X.-M. Song, *ACS Appl. Mater. Interfaces*, **2019**, *11*, 10967.
62 H. Kim, J. Cho, J. Cho, B. J. Park and J. W. Kim, *ACS Appl. Mater. Interfaces*, **2018**, *10*, 1408.
63 W.-L. Jiang, Q.-J. Fu, B.-J. Yao, L.-G. Ding, C.-X. Liu and Y.-B. Dong, *ACS Appl. Mater. Interfaces*, **2017**, *9*, 36438.
64 L. Fu, S. Li, Z. Han, H. Liu and H. Yang, *Chem. Commun.*, **2014**, *50*, 10045.
65 H. Yang, T. Zhou and W. Zhang, *Angew. Chem.- Int. Ed.*, **2013**, *52*, 7455.
66 S. Luo, Z. Zeng, G. Zeng, Z. Liu, R. Xiao, M. Chen, L. Tang, W. Tang, C. Lai, M. Cheng, B. Shao, Q. Liang, H. Wang and D. Jiang, *ACS Appl. Mater. Interfaces*, **2019**, *11*, 32579.
67 G. Yang, C. Xing, W. Hirohama, Y. Jin, C. Zeng, Y. Suehiro, T. Wang, Y. Yoneyama and N. Tsubaki, *Catal. Today*, **2013**, *215*, 29.
68 Z. Jia, K. Wang, B. Tan and Y. Gu, *ACS Catal.*, **2017**, *7*, 3693.
69 H. Ge, B. Zhang, X. Gu, H. Liang, H. Yang, Z. Gao, J. Wang and Y. Qin, *Angew. Chem.- Int. Ed.*, **2016**, *55*, 7081.
70 J. Zhang, Z. Yu, Z. Gao, H. Ge, S. Zhao, C. Chen, S. Chen, X. Tong, M. Wang, Z. Zheng and Y. Qin, *Angew. Chem.- Int. Ed.*, **2017**, *56*, 816.
71 J. Lu, J. Dimroth and M. Weck, *J. Am. Chem. Soc.*, **2015**, *137*, 12984.
72 F. Chang, B. G. P. van Ravensteijn, K. S. Lacina and W. K. Kegel, *ACS Macro Lett.*, **2019**, *8*, 714.
73 J. Yan, K. Chaudhary, S. Chul Bae, J. a Lewis and S. Granick, *Nat. Commun.*, **2013**, *4*, 1516.
74 L. Xia, H. Zhang, Z. Wei, Y. Jiang, L. Zhang, J. Zhao, J. Zhang, L. Dong, E. Li, L. Ruhlmann and Q. Zhang, *Chem. - A Eur. J.*, **2017**, *23*, 1920.
75 W. Cao, R. Huang, W. Qi, R. Su and Z. He, ACS *Appl. Mater. Interfaces*, **2015**, *7*, 465.
76 Y. Liu, J. Hu, X. Yu, X. Xu, Y. Gao, H. Li and F. Liang, *J. Colloid Interface Sci.*, **2017**, *490*, 357.
77 X. Zheng, Y. Wang, Y. Wang, D. J. Pine and M. Weck, *Chem. Mater.*, **2016**, *28*, 3984.
78 S. P. Teong, G. Yi, H. Zeng and Y. Zhang, *Green Chem.*, **2015**, *17*, 3751.
79 J. N. Chheda, Y. Roman-Leshkov and J. A. Dumesic, *Green Chem.*, **2007**, *9*, 342.
80 V. Linek and P. Beneš, Chem. Eng. Sci., 1976, 31, 1037.
81 D. Stehl, N. Milojević, S. Stock, R. Schomäcker and R. Von Klitzing, I*nd. Eng. Chem. Res.*, **2019**, *58*, 2524.
82 L. Tao, M. Zhong, J. Chen, S. Jayakumar, L. Liu, H. Li and Q. Yang, *Green Chem.*, **2018**, *20*, 188.
83 J. Shi, X. Wang, S. Zhang, L. Tang and Z. Jiang, *J. Mater. Chem. B*, **2016**, *4*, 2654.
84 L. Qi, Z. Luo and X. Lu, *ACS Sustain. Chem. Eng.*, **2019**, *7*, 7127.
85 L. Liu, L. Jiang, X. Xie and S. Yang, *Chempluschem*, **2016**, *81*, 629.

86 Y. Yang, W. J. Zhou, A. Liebens, J. M. Clacens, M. Pera-Titus and P. Wu, J. *Phys. Chem. C*, **2015**, *119*, 25377.
87 G. Lv, F. Wang, X. Zhang and B. P. Binks, *Langmuir*, **2018**, *34*, 302.
88 H. Shi, Z. Fan, V. Ponsinet, R. Sellier, H. Liu, M. Pera-Titus and J. M. Clacens, *ChemCatChem*, **2015**, *7*, 3229.
89 B. P. Binks and J. A. Rodrigues, *Langmuir*, **2007**, *23*, 3626.
90 J. Huang and H. Yang, *Chem. Commun.*, **2015**, *51*, 7333.
91 J. Huang, F. Cheng, B. P. Binks and H. Yang, *J. Am. Chem. Soc.*, **2015**, *137*, 15015.
92 Y. Zhang, M. Zhang and H. Yang, *ChemCatChem*, **2018**, *10*, 5224.
93 H. Yang, L. Fu, L. Wei, J. Liang and B. P. Binks, *J. Am. Chem. Soc.*, **2015**, *137*, 1362.
94 M. Zhang, L. Wei, H. Chen, Z. Du, B. P. Binks and H. Yang, *J. Am. Chem. Soc.*, **2016**, *138*, 10173.
95 H. Chen, H. Zou, Y. Hao and H. Yang, *ChemSusChem*, **2017**, *10*, 1989.
96 M. Zhang, R. Ettelaie, T. Yan, S. Zhang, F. Cheng, B. P. Binks and H. Yang, *J. Am. Chem. Soc.*, **2017**, *139*, 17387.
97 Z. Meng, M. Zhang and H. Yang, *Green Chem.*, **2019**, *21*, 627.
98 X. Zhang, Y. Hou, R. Ettelaie, R. Guan, M. Zhang, Y. Zhang and H. Yang, *J. Am. Chem. Soc.*, **2019**, *141*, 5220.
99 T. Skale, D. Stehl, L. Hohl, M. Kraume, R. von Klitzing and A. Drews, *Chemie Ing. Tech.*, **2016**, *88*, 1827.
100 A. Heyse, C. Plikat, M. Grün, S. Delaval, M. Ansorge-Schumacher and A. Drews, *Process Biochem.*, **2018**, *72*, 86.
101 A. Heyse, C. Plikat, M. Ansorge-Schumacher and A. Drews, *Catal. Today*, **2019**, *331*, 60.

Chapter 2

Tandem Catalysis with Antagonistic Catalysts Compartmentalized in the Dispersed and Continuous Phases of a Pickering Emulsion

Tandem catalysis combines multiple conversion steps, catalysts, and reagents in one reaction medium, offering the potential to reduce waste and time. In this study, Pickering emulsions — emulsions stabilized by solid particles — are used as easy-to prepare and bioinspired, compartmentalized reaction media for tandem catalysis. Making use of simple and inexpensive acid and base catalysts, the strategy of compartmentalization of two noncompatible catalysts in both phases of the emulsion is demonstrated by using the deacetalization–Knoevenagel condensation reaction of benzaldehyde dimethyl acetal as a probe reaction. In contrast to simple biphasic systems, which do not allow for tandem catalysis and show instantaneous quenching of the acid and base catalysts, the Pickering emulsions show efficient antagonistic tandem catalysis and give the desired product in high yield, as a result of an increased interfacial area and suppressed mutual destruction of the acid and base catalysts.

Based on: C.M. Vis, L.C.J. Smulders, P.C.A. Bruijnincx, Tandem Catalysis with Antagonistic Catalysts Compartmentalized in the Dispersed and Continuous Phases of a Pickering Emulsion *ChemSusChem* **2019**, *12*, 2176.

2.1 Introduction

Biomimicry, that is, science inspired by biological entities and processes, has served catalysis well, for instance by mimicking enzyme active sites for the development of new atom-efficient conversions and the design of new biomimetic catalysts.[1] However, less attention has been given to bio-inspired reactor and process design, emulating the efficiency with which living cells are capable of performing multiple sequential and parallel reactions simultaneously.[2]

In this Chapter, we aim to emulate nature's strategy of compartmentalization to efficiently perform coupled, one-pot reactions and, in particular, to allow antagonistic orthogonal tandem catalytic reactions.[3,4] Orthogonal tandem catalysis has been defined by Lohr *et al.* as a one-pot reaction in which sequential catalytic processes occur through two or more functionally distinct, and preferably non-interfering catalytic cycles.[4] The major challenge of operating tandem reactions for non-interfering catalysts is that the optimal process parameters and kinetic regimes for each are typically quite different. Furthermore, noninterference cannot always be avoided and catalyst non-compatibility in fact offers another main challenge for efficient tandem catalysis, for example when combining antagonistic catalysts such as an acid and a base. In that case, the two catalysts need to be kept physically separate, but still be accessible for the substrates. Various approaches have been taken towards the design of bifunctional acid–base catalysts, often relying on the spatial separation of the reactive entities on polymeric or oxidic support materials[5,6,] for example, in the form of yolk–shell materials[7], metal–organic frameworks (MOFs)[8–11], shell cross-linked micelles[12,13], or star polymers[14]. An alternative strategy is to use bio-inspired reaction media and process options in which compartmentalization can be reversibly induced to physically separate soluble antagonistic catalysts. Herein, we report on such a compartmentalization approach in the form of a Pickering emulsion (PE), an emulsion stabilized by solid particles.[15] PEs can be obtained as either water-in-oil (w/o), or oil-in-water (o/w) systems, based on the hydrophobic/hydrophilic nature of the particles used.[16] These PEs then constitute a special case of a biphasic system, offering the advantage of a higher interfacial area, which is anticipated to result in higher reaction efficiencies even when compared to stirred biphasic systems.[17] The PEs also offer wider stability windows than traditional emulsions and are therefore highly interesting media for catalysis.

Although PEs were invented in the early 1900s, their use as reaction media for catalysis is a topic that has only much more recently been explored.[18–22] For example, Resasco and coworkers reported on phase-selective catalysis using carbon nanotube–silica nanohybrids stabilized PEs in catalytic hydrogenation reactions[23,24] and the catalytic upgrading of biofuels by using hydrophobic zeolites acting as PE stabilizers.[25] Recently,

Yang *et al.* were the first to use PE compartmentalization to perform various tandem catalytic reactions by using laminated w/o PEs.[26] PEs containing either Brønsted acidic or Brønsted basic water droplets, dispersed in toluene as the continuous phase, were combined in a layered fashion, thus having both incompatible catalyst components compartmentalized in the water phase of the laminated PE. This strategy allowed several tandem catalytic reactions to be performed successfully. Long reaction times in small volumes were required, indicating that mass transfer may be limiting.

In this chapter, we show a new, alternative way of compartmentalizing two antagonistic catalysts in a PE, that is, by confining the acid and base catalyst to the dispersed and continuous phase of the w/o PE, respectively. This would allow the additional flexibility of being able to use both phases of the emulsion and minimize transport-related issues. The deacetalization–Knoevenagel reaction, a common probe reaction for bifunctional acid–base catalysis,[26–29] was selected to study this general strategy for antagonistic tandem catalysis. To this extent, a water/toluene (w/o) PE stabilized by hydrophobic silica (HDK® H20 silica) was prepared, consisting of a dispersed aqueous phase containing an inorganic acid (HCl) to catalyze the deacetalization of benzaldehyde dimethyl acetal (**1**) to form the intermediate benzaldehyde (**2**). The oil phase of the PE contains an organic base, piperidine, and malononitrile for the subsequent catalytic Knoevenagel reaction to form

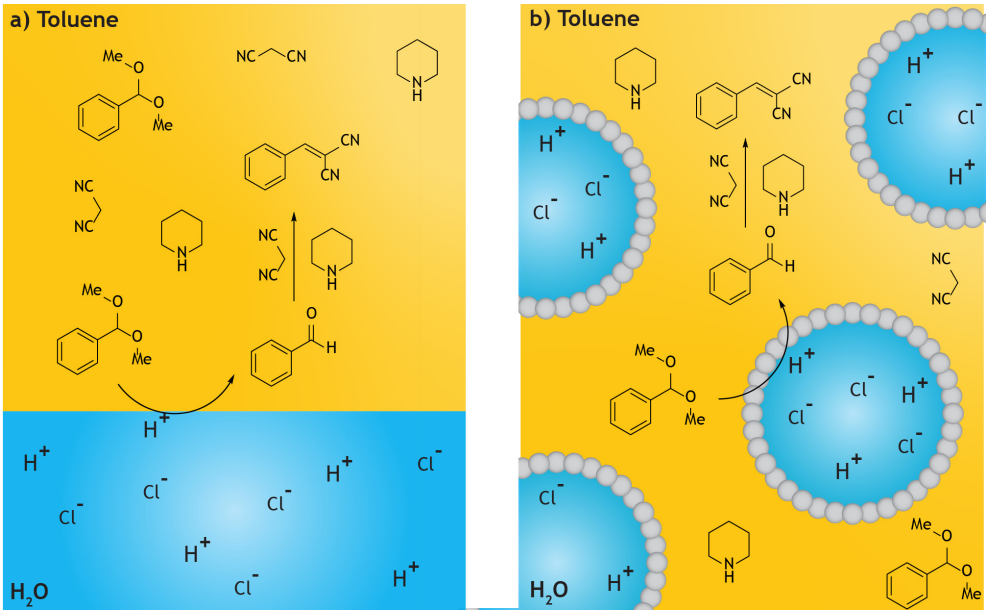

Figure 2.1: Schematic representations of an orthogonal tandem reaction with compartmentalized, antagonistic catalysts, exemplified by a deacetalization-Knoevenagel tandem probe reaction in a) a biphasic system and b) a Pickering emulsion (PE).

benzylidene malononitrile (**3**; Figure 2.1). The performance of the PE as reaction medium for this tandem reaction is compared to a simple biphasic system with the same components.

2.2 Results and Discussion

2.2.1 Pickering emulsion preparation

The PEs used in this work were formulated with toluene and water as continuous and dispersed phase and stabilized by 3 wt% partially hydrophobic silica. After preparation a milky reaction mixture was obtained (Figure 2.2a, left) which was fully resistant against destabilization phenomena such as coalescence, creaming, and sedimentation, also under reaction conditions (Figure 2.2a, right). Optical microscopy images were obtained by using a Zeiss upright microscope (Figure 2.2b). While the large focal depth precludes a reliable droplet size distribution to be obtained from these images, confocal fluorescence microscopy (CFM) images showed a broad droplet size distribution with droplet diameters varying between 5 and 35 mm (Figure 2.2c,d). As the organic phase was stained with Nile red, the CFM images confirmed that the PE is of the w/o type (Figure 2.2c).

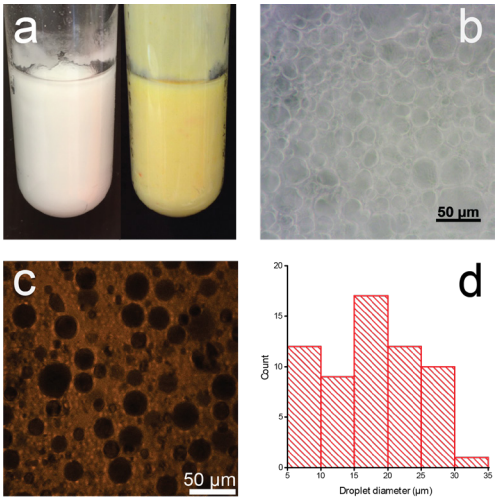

Figure 2.2: a) Physical appearance of the water/toluene PE stabilized with 3 wt% silica immediately after preparation (left) and after reaction (right), b) Optical microscopy image of the PE, c) Confocal fluorescence microscopy (CFM) image of the PE with the oil phase stained with Nile red, d) Droplet size distribution of the PE based on the CFM image.

2.2.2 Kinetic experiments

First, deacetalization of **1** was monitored in a PE (w/o 2:6 v/v) as function of time and compared to stirred and static biphasic systems of the same composition (Figure 2.3a).

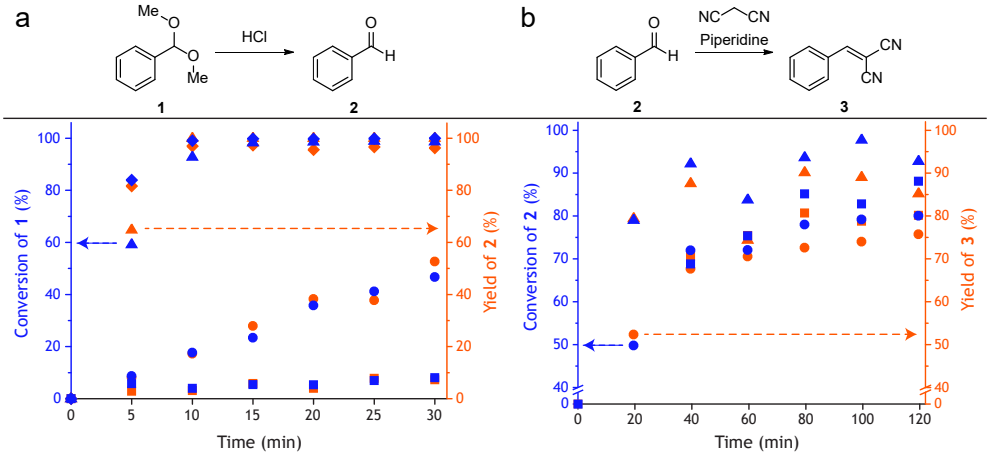

Figure 2.3: a) Conversion of 1 and yield of 2 followed over time in a stirred biphasic system (1250 rpm) (●), static biphasic system (■), static PE with water:toluene 2:6 (▲) and a static PE with water:toluene 3:5 (♦) as function of time. All systems contain 1 (1 mmol) and 10 mol% HCl at t = 0 min, 50 °C. b) Conversion of 2 and yield of 3 followed over time in a stirred biphasic system (●), static biphasic system (■) and static PE with water:toluene 2:6 (▲) during 120 min. All systems contain 2 (1 mmol) and 10 mol% piperidine at t = 0 min, r.t.

Second, the influence of the water/oil ratio in the PE was assessed by comparing the performance of the PE to a 3:5 w/o PE. For these reactions only the substrate (**1**, 1 mmol) and 10 mol% HCl as catalyst were present in the different systems and reactions were executed at 50°C. As **1** is hardly water soluble and deacetalization requires the acid catalyst, the higher interfacial area between the organic and the aqueous phase in the PE was expected to lead to faster conversion. This was truly the case, as the conversion of **1** in the biphasic system without or with stirring reached only 12% or 46%, respectively, after 30 min, while the 2:6 water/toluene PE showed full conversion within 15 min. With a higher water content PE (3:5 w/o) the reaction proceeded even faster, with full conversion being reached in 10 min. This clearly shows the beneficial effect of the use of the PE for biphasic catalysis, as has been shown before for other types of reactions.[17]

The conversion of **2** into **3** was also followed over time at room temperature in a static and stirred biphasic system and in a PE (Figure 2.3b). The Knoevenagel condensation part of the tandem reaction is an all-organic phase reaction, using excess malononitrile as second substrate. The differences in performance between the three systems in this second step is less pronounced than for the first deacetalization reaction, with all reaching about 80–90% conversion of **2** in 2 h. Therefore, only the static biphasic system and a PE were compared in further studies of the influence of catalyst concentration on efficiency, using only base or both acid and base.

2.2.3 Knoevenagel condensation reaction

When only piperidine, and no hydrochloric acid, was present as catalyst in the biphasic system, a conversion of **2** of 49% was reached with 5 mol% of base (Figure 2.4a). Increasing the piperidine concentration to 10 and 20 mol% increased conversion to 84 and 93% respectively. For the PE, higher conversions were observed of 91% with 5 mol% base and full conversion when 10 or 20 mol% base was used. However, the yield of **3** dropped on increasing base concentration, owing to the formation of side products. As piperidine is somewhat water soluble, this results in some alkalinity of the water phase, allowing for benzaldehyde to react in a Cannizzaro reaction to form benzoic acid and benzyl alcohol.[30,31] These products are highly soluble in the aqueous phase and are therefore not detected in the GC analysis of the organic phase.

Using an acidified aqueous phase clearly impacts the conversion of **2** in the organic phase in both the biphasic system and the PE (Figure 2.4b). The decrease in conversion observed when equimolar amounts acid and base or excess acid are used can be contributed to some interface quenching of the antagonistic catalysts. This effect is even more pronounced in PE than in the biphasic system due to the higher interfacial area. The use of an excess of base (10 mol% acid, 20 mol% base), led to a marginal increase in conversion in the biphasic

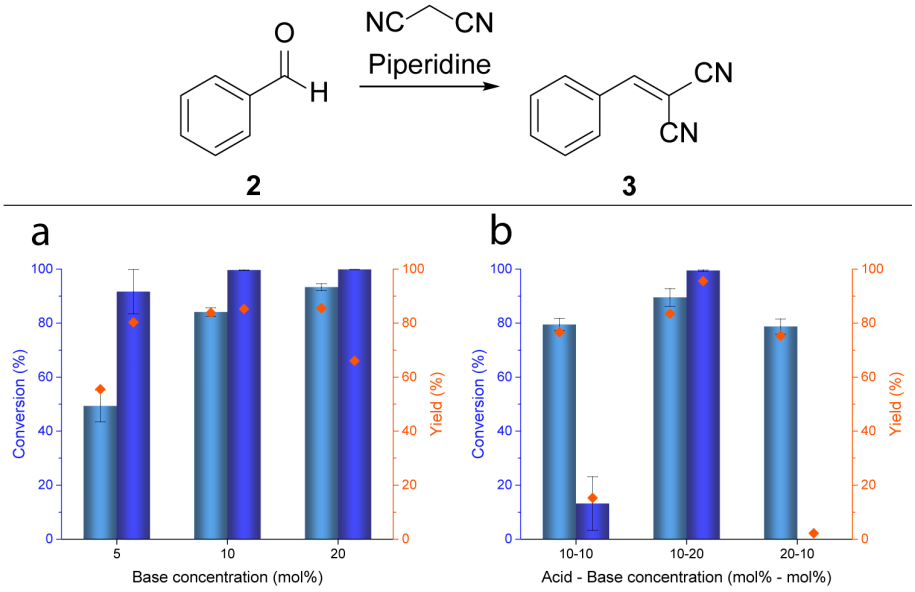

Figure 2.4: Conversion (bars) of benzaldehyde (2) and yield (diamonds) of benzylidene malononitrile (3) in static biphasic system (left bars; light blue) and PE (right bars; dark blue) with a) only base or b) acid and base catalysts present. Reaction conditions: 1 mmol 2, 2.5 eq. malononitrile, r.t., 3 h.

system, but a significant improvement for the PE with conversion shooting up to 99 %. The 10 mol% excess of base present in the system explains the similarity in conversion to the reaction with 10 mol% base only. These results emphasize the balance that needs to be struck to achieve efficient coupling between the two tandem catalytic steps. Indeed, where the larger interfacial area of the PE was advantageous in the first step of the reaction in terms of kinetics, the opposite is seen in the second step if the acid and base are not present in the appropriate ratio, most likely because of more extensive quenching. Even though some recombination of acid and base and consequent salt formation thus may occur, this does not adversely affect the stability of the PE as no sedimentation or creaming was observed during the reaction (Figure 2.2a). The 10–20 mol% acid–base experiments, however, suggested that actual PE tandem catalysis should be possible, provided that the acid–base ratio is properly tuned. It should also be noted that in all experiments with both acid and base catalysts present, the yield of **3** closely matched the conversion of **2**, indicating that the presence of acid prevents the formation of side products.

2.2.4 Tandem catalytic reactions

Having established the subtle (dis)advantageous effects of Pickering emulsification on the individual steps of the tandem reaction, the influence on the overall tandem catalytic conversion of **1** with both acid and base present in the systems was assessed. The tandem reactions were run for 3 h at room temperature in both static biphasic systems and PE. The normalized product distributions are shown in Figure 2.5.

As expected from the results of the deacetalization reaction, independent of the acid–base ratio applied, little to no conversion of **1** was observed for the static biphasic system, precluding any further tandem catalytic conversion. Importantly, when a stirred biphasic system with high acid and base concentrations (20 mol% acid, 20 mol% base) was used, no conversion of **1** was observed either due to rapid quenching. Gratifyingly, the PE reactions did show tandem catalysis, however, with efficiency, as expected, depending greatly on the relative acid and base concentrations. When equimolar amounts of acid and base were used (10 mol% acid, 10 mol% base), the conversion of **1** reached 82% with a yield of **3** of 76 %. Only 6% of the product distribution was attributable to the intermediate **2**, implying that under these conditions deacetalization is rate limiting. With excess base (10 mol% acid, 20 mol% base), the conversion of **1** was rather low, because of partial quenching of the limiting amount of acid. Nevertheless, **3** was still produced in 40% yield. Under these conditions, intermediate **2** was not detected in the final reaction mixture, in line with deacetalization being rate limiting. Using an excess of acid (20 mol% acid, 10 mol% base) led to full conversion of **1** into **2** but limited conversion of **2** into **3**, reflecting the effect of partial quenching of the limiting amount of base, resulting in 35% yield of **3**. Equimolar amounts of acid and base thus gave the best tandem catalytic conversion of **1** into **3** in the

PE. The comparison with the biphasic system shows that the mutual destruction of acid and base, which is to an extent unavoidable, is thus clearly offset by the higher efficiency of the deacetalization reaction. Overall, this results in the complete tandem catalytic reaction performing much better in the PE than in the (stirred or static) biphasic system. When the tandem catalytic activity of our simple, compartmentalized PE is compared to that of the more complex laminated one reported by Yang *et al.*,[26] we show that confining the acid and base catalysts to both phases rather than only the aqueous phase, results in a more rapid reaction, even at lower temperature. Mass transport and the desired partitioning are also expected to benefit from the higher oil/water ratio and lower silica loading, leading to a reduced viscosity, used in the reactions reported in this Chapter.

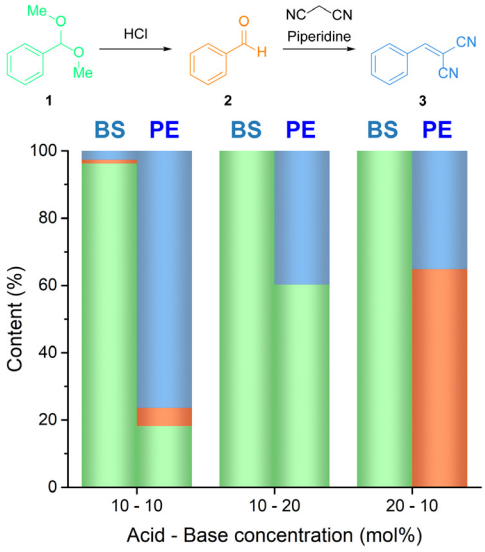

Figure 2.5: Normalized product distributions of the tandem catalytic reactions in static biphasic systems (left bars) and PEs (right bars). Green bars show benzaldehyde dimethyl acetal (1), orange bars benzaldehyde (2) and blue bars benzylidene malononitrile (3) content in the reaction mixture. Reaction conditions: 1 mmol 1, 2.5 eq. malononitrile, r.t., 3 h.

2.3 Conclusions

In conclusion, we have demonstrated a new, alternative method for the compartmentalization of simple acid and base catalysts in the two phases of a PE, a strategy that resulted in efficient tandem catalysis. This compartmentalization strategy thus allowed antagonistic catalysts to be used and accelerated phase transfer of reagents over the interface. Using the deacetalization–Knoevenagel condensation tandem reaction as a probe reaction, the PE system was shown to clearly outperform the simple biphasic one. All tandem reactions were executed at room temperature using

inexpensive, commercially available catalysts in easily obtainable PEs as reaction media. Furthermore, the stability of the PEs was not influenced by the presence of substrate, catalysts, or products formed. The larger interfacial area of the PE, compared to a simple biphasic system, obtained by the stable dispersion of the acidic aqueous phase inside the continuous organic phase, was highly beneficial for the rate of the acid-catalyzed reaction and therefore for the overall tandem catalytic reaction. The scope can be expanded to other substrates that benefit from acid–base tandem catalysis, including the conversion of biomass-derived compounds. Conversion of this type of compounds requires higher reaction temperatures and operates under different reaction mechanisms.

2.4 Experimental procedures

2.4.1 Materials

All chemicals were used as received without any further purification. HDK® H20 silica was obtained from Wacker Chemie. Benzaldehyde (≥99%) was obtained from Fluka Analytical. Anisole (99%), hydrochloric acid (HCl, 37%, analytical grade), malononitrile (99%), piperidine (99%) and toluene (99.8%, analytical grade) were obtained from Acros Organics. Benzaldehyde dimethyl acetal (≥98%), benzylidene malononitrile (98%) and Nile Red (≥98%) were obtained from Sigma-Aldrich.

2.4.2 Pickering emulsion preparation

HDK® H20 silica (3 wt%) was dispersed in toluene using a VCX 130 Vibra-Cell Ultrasonic Processor (Sonics, 20 kHz, 10 W, 2 min). The aqueous phase was added (6/2 v/v toluene/H2O or 5/3 v/v toluene/H2O) and the mixture was vigorously stirred using an UltraTurrax® T 18 digital rotor stator (IKA, 15200 rpm, 2 min). The resulting white, milky, emulsion was used for catalysis.

2.4.3 Pickering emulsion characterization

Droplet size was determined by optical microscopy images, obtained by a Zeiss Axio Zoom V16 microscope equipped with a PlanNeofluar Z 2.3x/o.25 FWD 56 mm lens (magnification 410x). The type of emulsions was determined by staining the organic phase with Nile Red and performing confocal fluorescence microscopy using a Nikon Eclipse 90i upright microscope using a 50x/0.55 NA dry objective. The microscope was equipped with a Nikon-Eclipse A1R scan head. CFM images were recorded using excitation from a Melles Griuot Argon ion 488 nm laser providing 70 mW. A pinhole size of 21.7 µm was used to obtain the images. Nile red was used to stain the toluene phase and visualize this under excitation.

2.4.4 Kinetic experiments

A 15 mL Ace pressure tube was charged with 6 mL toluene and 2 mL HCl or a PE as was described previously. The aqueous phase consisted of a 0.05 M or 0.033 M HCl solution, depending on the oil-to-water ratio, to reach a total of 10 mol% HCl with respect to the substrate. After addition of benzaldehyde dimethyl acetal (1 mmol, 0.16 M), the tube was sealed and placed in a preheated heating mantle at 50 °C. The reaction was stopped by placing the tube in an ice bath after 5, 10, 15, 20, 25 or 30 minutes. Anisole was added as internal standard and 2 mL of the organic phase or PE was taken as a sample for GC analysis. The PEs were filtered over a 13 mm syringe filter (0.45 µm, PFTE) to provide phase separation and the organic phase was analyzed on GC on a Varian GC equipped with a VF-5 ms capillary column and an FID detector. Response factors were determined using commercially available reference materials. The kinetic experiments for the Knoevenagel condensation reactions were executed in a similar way. The reaction mixtures contained benzaldehyde (1 mmol, 0.16 M) and 10 mol% of piperidine and reactions were executed at room temperature. The reactions were stopped after 20, 40, 60, 80, 100 and 120 minutes by placing the tube in an ice bath and samples were measured on GC immediately using the same work-up procedure.

2.4.5 Catalytic experiments

A 15 mL Ace pressure tube was charged with 6 mL toluene and 2 mL HCl (0.05 M in Milli-Q water) or a PE as was described previously. After addition of substrate, benzaldehyde dimethyl acetal or benzaldehyde, (1 mmol, 0.16 M), malononitrile (2.5 mmol, 0.4 M) and piperidine (0.05, 0.1 or 0.2 mmol, 0.008 M, 0.016 M, 0.032 M) the tube was sealed and was left for 3 h at room temperature. Afterwards, anisole was added as internal standard and an aliquot was taken for GC analysis. The PEs were phase separated using a Rotina 38-R Hettich centrifuge (11000 rpm, 4 °C, 10 min) before GC sample preparation. Aliquots of reaction mixtures were analyzed as described previously.

Acknowledgements

Anne-Eva Nieuwelink (Utrecht University) is kindly acknowledged for her help with obtaining the optical and confocal fluorescent microscopy images.

References

1 A. E. Rawlings, J. P. Bramble and S. S. Staniland, *Soft Matter*, **2012**, *8*, 6675.

2 S. B. P. E. Timmermans and J. C. M. van Hest, *Curr. Opin. Colloid Interface Sci.*,

2018, *35*, 26.
3 M. J. Climent, A. Corma, S. Iborra and M. J. Sabater, *ACS Catal.*, **2014**, *4*, 870.
4 T. L. Lohr and T. J. Marks, *Nat. Chem.*, **2015**, *7*, 477.
5 Z. Jia, K. Wang, B. Tan and Y. Gu, *ACS Catal.*, **2017**, *7*, 3693.
6 Z. Weng, T. Yu and F. Zaera, *ACS Catal.*, **2018**, *8*, 2870.
7 Y. Yang, X. Liu, X. Li, J. Zhao, S. Bai, J. Liu and Q. Yang, *Angew. Chem. - Int. Ed.*, **2012**, *51*, 9164.
8 A. Dhakshinamoorthy and H. Garcia, *ChemSusChem*, **2014**, *7*, 2392.
9 M. H. Qi, M. L. Gao, L. Liu and Z. B. Han, *Inorg. Chem.*, **2018**, *57*, 14467.
10 Z. Wang, X. Luo, B. Zheng, L. Huang, C. Hang, Y. Jiao, X. Cao, W. Zeng and R. Yun, Eur. J. *Inorg. Chem.*, **2018**, *57*, 1309.
11 S. Mistry, A. Sarkar and S. Natarajan, *Cryst. Growth Des.*, **2019**, *19*, 747.
12 L. C. Lee, J. Lu, M. Weck and C. W. Jones, *ACS Catal.*, **2016**, *6*, 784.
13 M. Kuepfert, A. E. Cohen, O. Cullen and M. Weck, *Chem. - A Eur. J.*, **2018**, *24*, 18648.
14 B. Helms, S. J. Guillaudeu, Y. Xie, M. McMurdo, C. J. Hawker and J. M. J. Fréchet, *Angew. Chem. - Int. Ed.*, **2005**, *44*, 6384.
15 S. U. Pickering, *J. Chem. Soc. Trans.*, **1907**, *91*, 2001.
16 R. Aveyard, B. P. Binks and J. H. Clint, *Adv. Colloid Interface Sci.*, **2003**, *100–102*, 503.
17 W. Zhang, L. Fu and H. Yang, *ChemSusChem*, **2014**, *7*, 391.
18 M. Pera-Titus, L. Leclercq, J. M. Clacens, F. De Campo and V. Nardello-Rataj, *Angew. Chem. - Int. Ed.*, **2015**, *54*, 2006.
19 J. Cho, J. Cho, H. Kim, M. Lim, H. Jo, H. Kim, S.-J. Min, H. Rhee and J. W. Kim, *Green Chem.*, **2018**, *20*, 2840.
20 M. Zhang, R. Ettelaie, T. Yan, S. Zhang, F. Cheng, B. P. Binks and H. Yang, *J. Am. Chem. Soc.*, **2017**, *139*, 17387.
21 T. Yang, L. Wei, L. Jing, J. Liang, X. Zhang, M. Tang, M. J. Monteiro, Y. I. Chen, Y. Wang, S. Gu, D. Zhao, H. Yang, J. Liu and G. Q. M. Lu, *Angew. Chem. - Int. Ed.*, **2017**, *56*, 8459.
22 F. Xue, Y. Zhang, F. Zhang, X. Ren and H. Yang, *ACS Appl. Mater. Interfaces*, **2017**, *9*, 8403.
23 M. Shen and D. E. Resasco, *Langmuir*, **2009**, *25*, 10843.
24 S. Crossley, J. Faria, M. Shen and D. E. Resasco, *Science*, **2010**, *327*, 68.
25 P. A. Zapata, J. Faria, M. P. Ruiz, R. E. Jentoft and D. E. Resasco, *J. Am. Chem. Soc.*, **2012**, *134*, 8570.
26 H. Yang, L. Fu, L. Wei, J. Liang and B. P. Binks, *J. Am. Chem. Soc.*, **2015**, *137*, 1362.
27 H. Liu, F. G. Xi, W. Sun, N. N. Yang and E. Q. Gao, *Inorg. Chem.*, **2016**, *55*, 5753.
28 J. Park, J.-R. Li, Y.-P. Chen, J. Yu, A. A. Yakovenko, Z. U. Wang, L.-B. Sun, P. B.

Balbuena and H.-C. Zhou, *Chem. Commun.*, **2012**, *48*, 9995.

29 L. Zhong, C. Anand, K. S. Lakhi, G. Lawrence and A. Vinu, Sci. Rep., 2015, 5, 1.

30 T. A. Geissman, in *Organic Reactions*, **1944**, p. 94.

31 C. G. Swain, A. L. Powell, W. A. Sheppard and C. R. Morgan, *J. Am. Chem. Soc.*, **1979**, *101*, 3576.

Chapter 3

Pickering Emulsions Formulated with Alkylphenols: A Stability Study

Pickering emulsions (PEs) can be used as advanced biphasic reaction media, for example for application in catalytic biomass conversion. Such reactions are usually performed at elevated temperatures, pressures and high salt concentrations. Limited studies are available, however, on the stability and performance of PEs under such conditions. Here, we explore this regime using the alkylphenol solvents 2-*iso*propylphenol (IPP), 4-propylguaiacol (PG) and 2-*sec*-butylphenol (SBP), effective extractants for 5-HMF, as oil component of the PE. In this chapter, the stability of silica-stabilized alkylphenol formulated PEs is studied as function of solid emulsifier concentration, salinity, pH, temperature and pressure. The measured physicochemical properties of the alkylphenol solvents, such as three-phase contact angle, viscosity and interfacial tension, suggested that PEs formulated with SBP and PG would be the most and least stable, respectively. However, experimentally these differences were not observed as the differences in the physicochemical properties were rather small. Using 2 wt% of hydrophobic silica for stabilization, PEs could be formulated with an acidified aqueous phase (pH 2) containing 30 wt% NaCl and found to be stable for over a month at room temperature and atmospheric pressure. The PEs formulated with PG and SBP even showed high stability at 100 °C in a N_2-pressurized vessel, maintaining emulsion fractions of 0.69 and 0.78 respectively, after 3 h. The silica particles themselves were found to be stable up to 100 °C; at 150 °C hydrolysis of the hydrophobic trimethylsilyl groups took place, resulting in increased hydrophilicity and collapse of the PEs. The extraction capacity of the alkylphenols was studied in biphasic systems (BS) with high and low interfacial area. IPP showed the highest 5-HMF extraction capacity of the three alkylphenols reaching full extraction within 30 min in a high interfacial area biphasic system. The new PEs thus widen the window of operation for PE catalysis.

3.1 Introduction

Biphasic reaction media have shown to be of great practical value for the efficient and sustainable synthesis of value-added chemicals.[1–3] The Shell Higher Olefins Process (SHOP), a nickel-catalyzed oligomerization process of ethylene, and the Wacker process, the oxidation of ethylene by palladium(II)chloride are prominent examples of this.[4] Biphasic systems could be of similar value in future biorefinery operations, e.g. for the conversion of lignocellulosic biomass into useful platform chemicals.[5–7] Lignocellulosic biomass consists of three main parts, cellulose, hemicellulose and lignin. The most abundant fraction of the biomass, the cellulosic part, is a linear polysaccharide consisting of glucose monomers linked via β-glycosidic bonds.[8] These polymers can be hydrolyzed to obtain the glucose monomers that subsequently can be used to produce useful chemicals and fuels.[9]

The production of biobased platform chemicals, such as furanic compounds and small organic acids, from sugar molecules is currently receiving much attention.[6] Direct dehydration of glucose to form the platform molecule 5-hydroxymethylfurfural (5-HMF) is a process of poor efficiency with a maximum yield of approximately 52%, and a selectivity of 57%.[10] A solution was found by first isomerizing the glucose to fructose, as the dehydration of fructose to 5-HMF is a much more efficient reaction. These dehydration reactions are usually performed by acid catalysts in aqueous media. However, they suffer from selectivity issues: under the applied acidic conditions 5-HMF can react further to form small organic acids such as levulinic acid (LA) and (precursors to) 5-HMF can oligomerize to form large insoluble compounds called humin by-producs.[11] A solution to these issues is to perform the reactions in biphasic reaction media as rapid extraction of 5-HMF from the aqueous phase to an organic phase can reduce side product formation.[7] The partitioning of 5-HMF over the two phases can be enhanced by saturating the aqueous phase with sodium chloride (NaCl) to make use of the so-called salting-out effect. Initially, research focused on the use of n-butanol and methyl *iso*butyl ketone (MIBK) as extracting solvents for 5-HMF.[10] In 2012, Dumesic *et al.* then showed the potential of 4-propylguaiacol (PG) for the extraction of 5-HMF in stirred 1:1 aqueous-organic biphasic reaction media.[12] Following up on these studies, Palkovits *et al.* used thermodynamic modelling to predict the partitioning of 5-HMF in stirred 1:1 aqueous-organic biphasic systems in 110 different organic solvents, identifying alkylphenol solvents as potentially very efficient 5-HMF extracting solvents.[13]

Proper mixing between the two phases of a biphasic system enhances the rate of extraction, which normally requires fast stirring, as a result of an increased interfacial surface area. An alternative approach to increase the interaction between the two liquids is to exploit the advantages brought by emulsification of two immiscible liquids. Emulsion

stabilization can be achieved by surfactant addition or the use of solid particles. The latter biphasic systems are so-called Pickering emulsions (PEs), emulsions stabilized by solid micro- or nanoparticles,[14] which are the topic of study here. Due to their high resistance against destabilization phenomena such as droplet coalescence and aggregation[15], PEs have received much interest in various field of research, for instance in the pharmaceutical and cosmetic industries[16] or as reaction media for catalysis.[17]

The high stability of PEs is due to the strong adsorption of the particles on the liquid-liquid interface.[14,18] This strong adsorption requires partial wetting of the particles by both liquid phases, leading to water-in-oil (w/o) or oil-in-water (o/w) emulsions when more hydrophobic or more hydrophilic particles are used, respectively. The position of the particles at the liquid-liquid interface is determined by the interfacial tensions of the three phases with each other, being the solid-water ($\gamma_{s\text{-}w}$), solid-oil ($\gamma_{s\text{-}o}$) and oil-water ($\gamma_{o\text{-}w}$). The relation between these three interfacial tensions is given by Young's law:

$$\cos\theta = \frac{\gamma_{s-o} - \gamma_{s-w}}{\gamma_{o-w}} \tag{3.1}$$

where θ is the three-phase contact angle. This equation shows that particles that are completely amphiphilic ($\gamma_{s\text{-}o} = \gamma_{s\text{-}w}$) have a contact angle of 90°, whereas particles that are hydrophilic ($\gamma_{s\text{-}o} > \gamma_{s\text{-}w}$) will have a contact angle of < 90°. The opposite is the case for hydrophobic particles.

The strength of adsorption of particles at the oil-water interface is defined as the energy that is required to remove the particle from this interface.[19] Adsorption of particles at the interface results in a gain in energy, and therefore a driving force to do so, due to the reduction of the oil-water interfacial area. This energy depends on the contact angle, interfacial tension of oil and water and the radius of the particle. For a spherical particle, with a radius *r* small enough to neglect gravitational effects, the energy required to desorb the particle from the oil-water interface (E_{des}) can be described as:

$$E_{des} = \pi r^2 \gamma_{o-w} (1 \pm \cos\theta)^2 \tag{3.2}$$

in which the sign within the brackets is positive for particle desorption to the oil phase and negative for removal of the particle into the water phase. Indeed, adsorption at the interface traps the particles in an energy well that makes the adsorption almost irreversible. However, in practice, when the particles are too large or wetting by both phases is not ideal, fast destabilization does occur.

Previous research on PEs has mainly focused on either the intrinsic stability of many kinds of water-oil, oil-oil and water-water combinations with different solid stabilizing particles, as part of fundamental PE studies without demonstration of (or sometimes reference to) a certain application.[19–28] Conversely, when an application was demonstrated for a PE system, e.g. as reaction medium in catalysis, this often with selected, showcase reactions that could be performed under mild reaction conditions. Studies applying PEs as reaction media for more relevant reactions, requiring hasher conditions, such as elevated temperatures or pressures, reported little about the key physical properties or about the stability of the PE under these conditions.[17,33] The operating window that is accessible for PE catalysis therefore largely remains to be established.

Here, we explore the use of PEs as reaction and extraction media in the catalytic conversion of biomass combined with a thorough assessment of the stability of these PEs under actual reaction conditions (Figure 3.1). Those alkylphenols that emerged from the studies by Dumesic and Palkovits as most promising, i.e. 2-*iso*propylphenol (IPP), 4-propylguaiacol (PG) and 2-*sec*-butylphenol (SBP) were used as organic PE components. Hydrophobic fumed silica particles were used to stabilize the PEs and the influence of these solid particles on the physical properties of the alkylphenol solvents was assessed. The stability of the PEs was thoroughly studied as function of silica concentration, NaCl concentration and pH over the course of 1 month. Furthermore, the PEs were found to be stable for 3 h at 100 °C under N_2 pressure. The extraction efficiency of the three alkylphenol solvents was studied in non-stirred and stirred biphasic systems, the latter to model extraction in PE, showing improved extraction in the systems with high interfacial area.

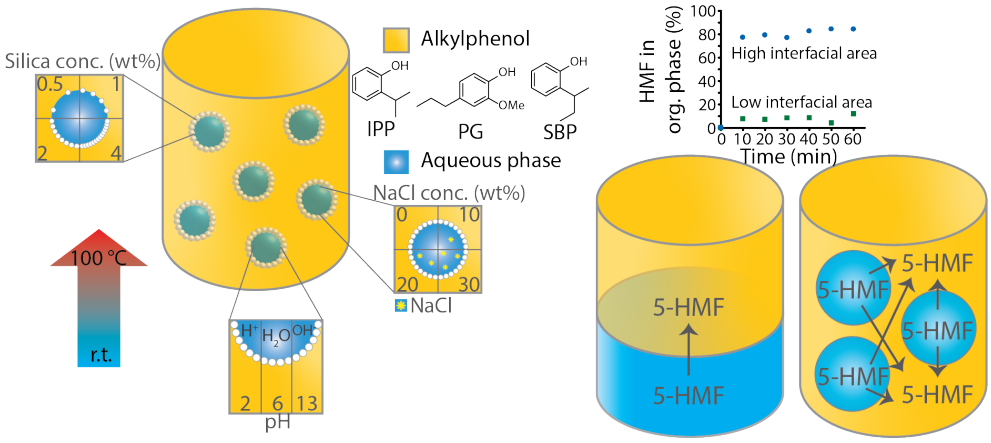

Figure 3.1: Left: Stability of alkylphenol formulated PEs studied as a function of silica concentration, NaCl concentration, pH and temperature. Right: 5-HMF extraction in biphasic systems with low and high interfacial area.

3.2 Results and Discussion

3.2.1 Hydrophobization of silica

To stabilize the targeted alkylphenol formulated w/o PEs in this study, commercially available silica (AEROSIL® 200) was used after hydrophobization by silylation with chloro(trimethyl)silane (TMSCl). While a discrete particle size distribution could not be determined as the fumed silica forms aggregates, the Transmission Electron Microscopy (TEM) images in Figure 3.2 clearly show a similar morphology for the treated and untreated silica. The specific surface area of the material only slightly decreased, from 196 m^2/g to 174 m^2/g, as determined by N_2-physisorption. The grafting of hydrophobic moieties on the surface was successful, as is shown in the Fourier Transform Infrared (FT-IR) spectrum in Figure 3.3. The spectra were taken under vacuum at 400 °C to ensure the complete removal of water. The O-H stretch region, 3800-3500 cm^{-1} (blue area) and the C-H stretch region, 2970-2850 cm^{-1} (yellow area) show the expected change upon silylation of the AEROSIL® 200 sample.

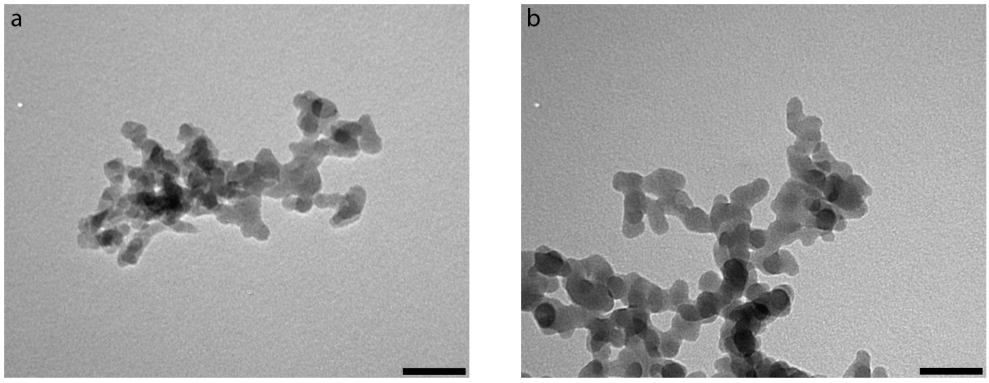

Figure 3.2: Transmission Electron Microscopy (TEM) images of AEROSIL® 200 a) before and b) after silylation. Scale bar = 50 nm.

To assess the amphiphilicity of the silylated silica, three-phase contact angles were measured of which the results are shown in Figure 3.4. Contact angles for the water droplets were determined to be 158.8° in IPP, 153.9° in PG and 146.4° in SBP. These results show that the silica is highly hydrophobic and will be preferentially wetted by the alkylphenol solvent. The differences between the three alkylphenol solvents are small, but significant, with the experimental error for these contact angles measurements being ± 2°. As the contact angle for SBP is the lowest and closest to 90°, this system would be expected to give the most stable PE.

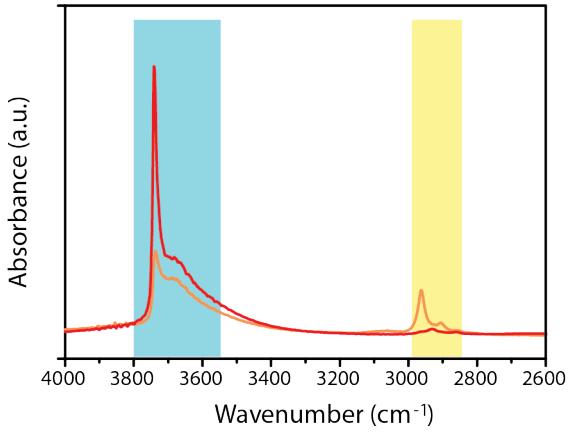

Figure 3.3: Partial FT-IR spectra of AEROSIL® 200 (red) and silylated AEROSIL® 200 (orange). The blue area (3800-3500 cm^{-1}) shows the region in which the O-H stretch vibration is visible. The yellow area (2970-2850 cm^{-1}) shows the region in which the C-H stretch vibration is visible.

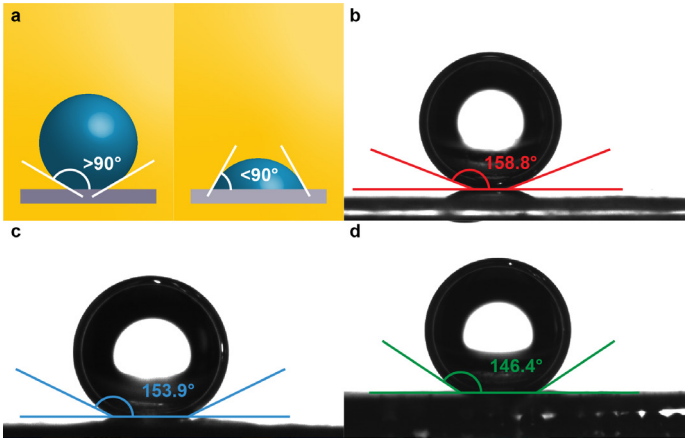

Figure 3.4: a) Schematic representation of the three-phase contact angle of a water droplet on a hydrophobic (left) and hydrophilic (right) solid substrate, b-d) Contact angle of aqueous droplet on a pellet of silylated AEROSIL® 200 in an alkylphenol environment, IPP (b), PG (c), SBP (d).

3.2.2 Physical properties of the alkylphenol solvents

To compare the properties of the different PEs formulated with the three different alkylphenol solvents their physical properties, such as boiling point, density and viscosity must be known. Boiling points and densities can be found in literature, but viscosities of these compounds were not available and needed to be experimentally determined by

rheology measurements, which measures viscosity as function of shear rate (Figure 3.5). The viscosity of the three alkylphenol solvents were all found to be in the same range, 10-20 mPa·s, with SBP being more viscous (17.8 mPa·s) than PG (12.4 mPa·s) and IPP (11.3 mPa·s). The viscosity of all three alkylphenols is stable with increasing shear rate, they can therefore be treated as Newtonian fluids. The viscosities of these solvents are comparable to that of ethylene glycol (16.6 mPa·s) and much higher than common organic solvents used for the formulation of PEs, such as toluene (0.56 mPa·s), methyl *iso*butyl ketone (0.55 mPa·s), n-octane (0.51 mPa·s) and decalin (1.95 mPa·s).[34] As noted by Binks *et al.* a higher viscosity of the organic phase decreases the degree of coalescence of a w/o PE.[35] Therefore, PEs formulated with the alkylphenol solvents will, theoretically, have a higher stability than the PEs reported with the above mentioned solvents. Addition of silica at 2 wt% led to a small increase in the viscosity of the organic solvents, again yielding the highest viscosity for SBP (21.1 mPa·s), followed by PG (14.7 mPa·s) and IPP (12.9 mPa·s). Remarkably, the addition of silica did lead to a difference in behavior of the solvents. Whereas without silica the liquids behaved as Newtonian fluids, the addition of silica led to non-Newtonian behavior. A decrease of viscosity was observed with an increasing shear rate, called shear-thinning, which could have an influence during PE preparation. After preparation the solvents are more viscous than during the fast stirring, increasing the stability of the PEs.

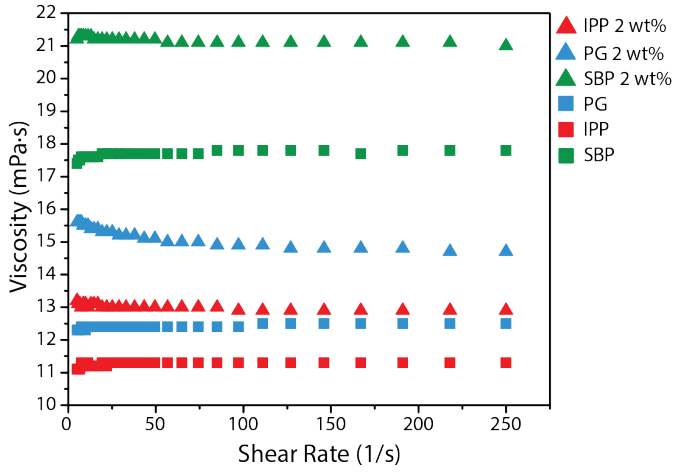

Figure 3.5: Viscosity of alkylphenol solvents with (triangles) and without (squares) silica as a function of shear rate. Red; IPP, Blue; PG, Green; SBP.

The interfacial tension of water with the alkylphenol solvents was determined using the pendant drop method. A water droplet saturated with NaCl of 9.5 µL was formed on the tip of a flat needle, which was placed in a cuvette filled with one of the alkylphenol solvents. The curvature of the droplet was measured, and the interfacial tension was

calculated using the Young-Laplace theory (Figure 3.6). Of our alkylphenols, PG had the lowest interfacial tension with water with a value of 13.3 mN/m. The interfacial tension of IPP with water was slightly higher at 14.1 mN/m and the highest interfacial tension was obtained for SBP; 17.0 mN/m. All interfacial tensions are in the same order of magnitude as reported for liquids with similar molecular structures. These values are much lower than, for example the interfacial tensions of n-octane with water (52.5 mN/m)[36] or toluene with water (35.4 mN/m).[37] The difference in interfacial tension between the alkylphenol solvents and the hydrocarbons is as anticipated and can be attributed to the higher polarity of alkylphenols compared octane and toluene.[18]

Figure 3.6: Interfacial tension of a water droplet in IPP (red), PG (blue) or SBP (green), values given in mN/m.

Interfacial tension can, under specific conditions, be correlated with emulsion stability, as shown by equation 3.2. A higher interfacial tension would theoretically lead to the formation of more stable emulsions.[38] However, this is only true if the three-phase contact angle would be the same for all three alkylphenol solvents, which is shown in Figure 3.4 to be not the case. If a particle would be removed from the alkylphenol-water interface this would happen by desorption to the organic phase as the particles are hydrophobic. The desorption energies, calculated using equation 3.2, were found to be $52.5\pi r^2$ for IPP, $47.9\pi r^2$ for PG and $57.1\pi r^2$ for SBP. As the particles stabilizing the PE are similar in size for each alkylphenol emulsion, theoretically SBP should give the most stable emulsions. In addition, SBP also has the highest viscosity of the three alkylphenols, which would further benefit the stability of the SBP emulsion.

The theory behind equation 3.2 assumes that the particles used are perfectly spherical and homogeneously covered by hydrophobic and hydrophilic groups. However, the silica used in our work is not spherical, and due to its highly porous structure, the distribution of hydrophobic groups may also not be homogeneous. Additionally, when these PEs will be studied for the catalytic conversion of lignocellulosic biomass this involves much more complex emulsion systems, thus requiring experimental validation. Stability of the PEs formulated with the three alkylphenols will be studied as a function of silica concentration,

salinity, and temperature in the next section to investigate whether these PEs are suitable reaction media for biomass conversion.

A summary of key physicochemical properties of the three alkylphenol solvents is given in Table 3.1.

Table 3.1: Key physicochemical properties of the alkylphenol solvents.

Alkylphenol solvent	Boiling point (°C)[a]	Density (g/L)[b]	Viscosity (mPa·s)	Viscosity with 2 wt% silica (mPa·s)	Interfacial tension (mN/m)
IPP	212-213	1.012	11.3	12.9	14.1
PG	246[34]	1.038	12.4	14.7	13.3
SBP	226-228	0.982	17.8	21.1	17.0

[a] Boiling point at 0.1013 MPa derived from MSDS unless stated otherwise.
[b] Density at 25 °C, derived from MSDS.

3.2.3 PE formation and stability

There are two types of emulsion destabilization phenomena: reversible, i.e. sedimentation and creaming, and irreversible destabilization, i.e. Ostwald ripening and coalescence (Figure 3.7). The reversible destabilization events are due to droplet aggregation which can lead to a settled emulsion phase with a liquid phase on top (sedimentation) or a liquid phase with a floating emulsion phase (creaming), depending on the relative densities of the dispersed and continuous phases. While the droplets stay intact with reversible destabilization, irreversible Ostwald ripening and coalescence is caused by merging of droplets and droplet size increases until complete phase separation.

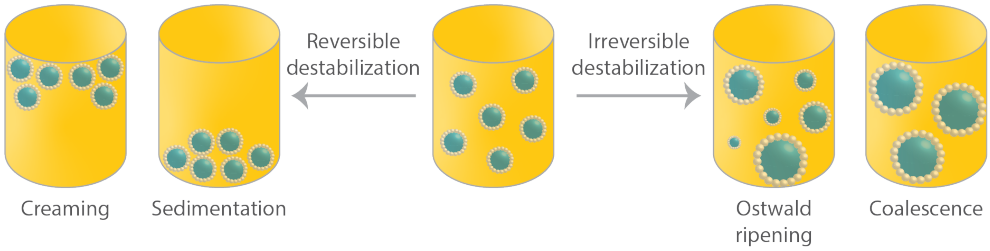

Figure 3.7: Reversible, creaming and sedimentation, and irreversible, Ostwald ripening and coalescence, destabilization phenomena of emulsions.

Silica concentration

Water-in-oil (w/o) emulsions were targeted here, using hydrophobic particles and a volume ratio of the organic to aqueous phase of 3 to 1. To demonstrate that these new

alkylphenol formulated w/o emulsions were indeed formed, the organic and aqueous phase were stained with Nile Red and FITC-dextran dyes, respectively, as is shown in Figure 3.8a-c. The droplet size distributions of the PEs formulated with all three alkylphenols were similar as is demonstrated in Figure 3.8d for PEs stabilized with 1 wt% silica.

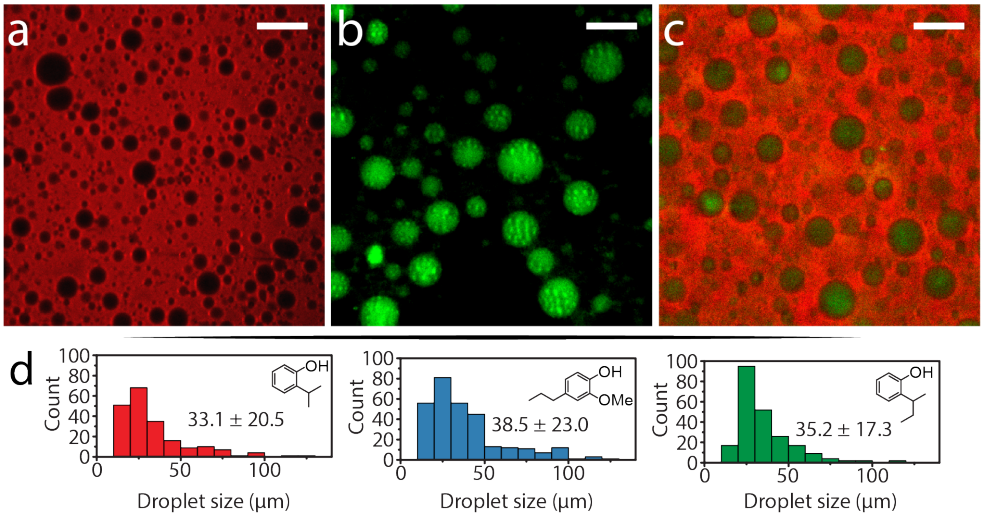

Figure 3.8: a-c) Confocal fluorescence microscopy images of PEs formulated with PG as organic phase, a) organic phase stained with Nile Red (10^{-5} M), b) aqueous phase stained with FITC-dextran (10^{-6} M) c) organic phase stained with Nile Red (10^{-5} M) and aqueous phase stained with FITC-dextran (10^{-6} M), scale bars: 100 µm d) droplet size distributions for PEs formulated with IPP (red), PG (blue) and SBP (green) stabilized by 1 wt% silica directly after preparation.

The stability of the PEs formulated with the three alkylphenol solvents, using different compositions of the organic and aqueous phases, was monitored over the course of 1 month and quantified based on optical images. Figure 3.9 shows the appearance of the PEs formulated with different silica concentrations (0.5 – 4 wt%) for each of the alkylphenol solvents and the emulsion fraction determined after 1 month. Expectedly, the stability of all PEs increased with an increase of the silica concentration. At the lowest silica concentration (0.5 wt%) highly unstable PEs were obtained when using PG and SBP as organic phase, with the emulsion fractions being only 0.20 and 0.49 for these two PEs after one month. The PE formulated with 0.5 wt% silica in IPP did not seem to be as unstable as the other two, still showing 69% emulsification of the total volume.

An increase of the silica concentration to 1 wt% leads to an increase in the stability of the PEs with IPP, PG and SBP, giving emulsion fractions of 0.90, 0.36 and 0.67, respectively. Even though destabilization does occur for all three alkylphenol solvents, the type of destabilization is solvent-dependent. Destabilization in the form of sedimentation was

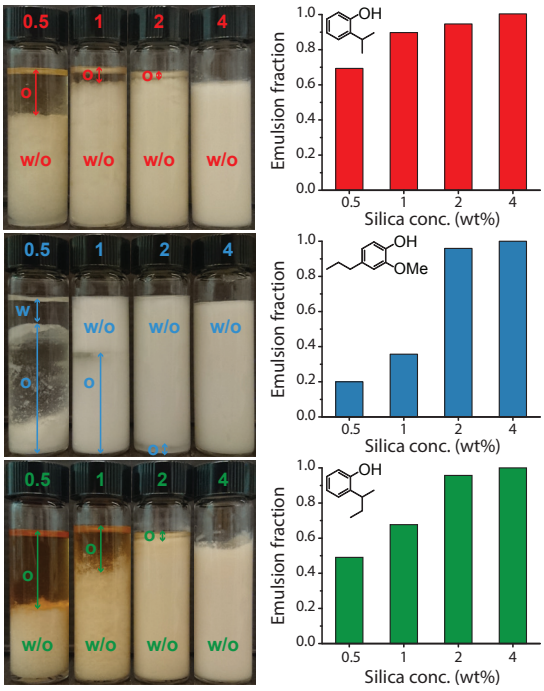

Figure 3.9: Appearance and emulsion fractions of PEs formulated with IPP (Red), PG (Blue), SBP (Green) containing different concentrations hydrophobic silica after 1 month. PE: 6 mL alkylphenol solvent, 2 mL Milli-Q water.

observed for PEs with IPP and SBP, while for the PE with PG creaming occurred. IPP and SBP have lower densities than PG (1.012 g/mL, 0.982 g/mL and 1.038 g/mL respectively), which are very close to or lower than the density of water (0.998 g/mL), leading to sedimentation. As PG is heavier than water, any emerging oil will naturally sink below the emulsion phase.

PEs formulated with 2 wt% of silica in the organic phase are all quite stable with emulsion fractions of 0.95, 0.96 and 0.96 for IPP, PG and SBP, respectively, after 1 month. Although the PEs formulated with 4 wt% of silica seem to be the most stable, with all emulsion fractions being 1, the high concentration of silica also causes them to be highly viscous, making the PEs less suited for use as liquid phase reaction media. Therefore, the PEs containing 2 wt% silica were chosen to be used for further experiments.

Based on the physicochemical properties of the alkylphenols, SBP was expected to produce the most stable PEs and PG the least stable ones. However, with a sufficient silica concentration (2 wt%), all PEs are highly stable over the course of one month. At lower

silica concentrations, the PEs formulated with IPP are most stable, and PEs with PG as organic phase are highly unstable under these conditions.

Salinity

The stability of the PEs was tested as a function of NaCl concentration in the dispersed aqueous phase, ranging from 0 wt% to almost full saturation of the aqueous phase, 30 wt%. The salinity of the aqueous phase is very important for the efficiency of the targeted sugar dehydration chemistry, as high salinity induces the so-called 'salting-out' effect. Previous work from the group of Dumesic, for example, showed an increase of the partitioning coefficient for 5-HMF from 1.7 to 3.1 in a 1-butanol/water biphasic system in which the aqueous phase was saturated with NaCl (35 wt%).[39] Addition of NaCl to the aqueous phase of o/w PEs formulated with heptane was demonstrated to result into lower stability as the ionic species caused particle flocculation.[40,41] However, addition of NaCl was beneficial for the stability of air-in-water foams due to solvation forces induced by the salt.[42] No data seems to have yet been reported for the stability of w/o PEs using different salt concentrations.

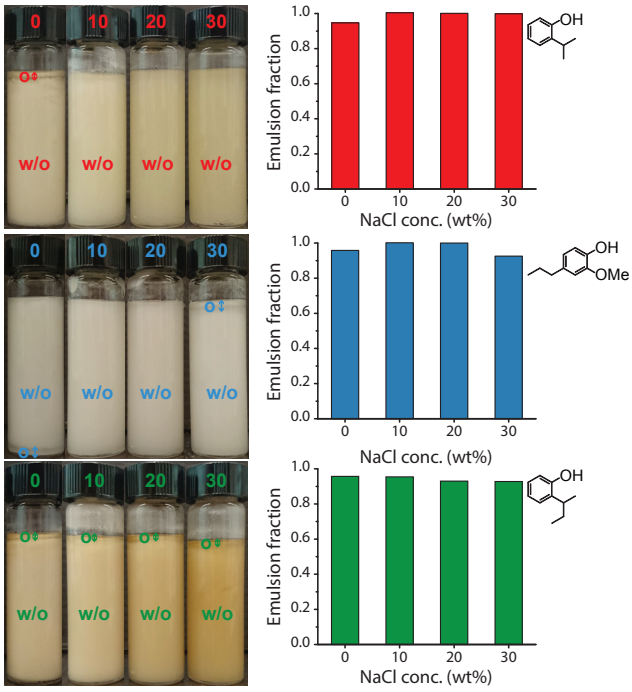

Figure 3.10: Appearance and emulsion fractions of PEs formulated with IPP (Red), PG (Blue), SBP (Green) containing different NaCl concentrations after 1 month. PE: 6 mL alkylphenol solvent, 2 wt% hydrophobic silica, 2 mL Milli-Q water.

Figure 3.10 shows the appearance of the PEs formulated with the three alkylphenol solvents after one month and the emulsion fraction was again determined based on these optical images. All PEs are rather stable over the course of the month with emulsion fractions deviating between 0.93 and 1.0. The addition of NaCl led to an increase of the stability of the PEs formulated with IPP, 10 wt% NaCl is already enough to produce a PE that is stable over the course of one month. The PE prepared with PG also became more stable with addition of NaCl. Nevertheless, addition of 30 wt% led to slight sedimentation of the emulsion phase to give an emulsion fraction of 0.93 after one month. The inversion of the type of destabilization from creaming without NaCl, to sedimentation that occurs with 30 wt% of NaCl is due to the increasing density of the aqueous phase with the addition of NaCl (ρ=1.19). The SBP formulated PEs do not show the same stabilization by the addition of NaCl, the degree of sedimentation is constant with all concentrations NaCl as the emulsion fraction only deviates between 0.93 and 0.96. The high stability of all PEs with high salt concentrations suggest that these systems have potential as reaction media for catalytic sugar dehydration reactions.

pH

Catalytic fructose dehydration reactions are usually performed using an acidic aqueous phase. To investigate the influence of the pH on the stability of the PEs three different aqueous phases were used, one consisting of pure Milli-Q water (pH 6), one with added HCl (pH 2), and one with added NaOH (pH 13), all containing 30 wt% NaCl. The organic phases contained 2 wt% of silica. Ralston has previously already shown that particle hydrophobicity is highest at its point of zero charge (PZC).[43] As the PZC of silica lies around 2, low pH should probably be beneficial for PE stability.

Changing the pH of the dispersed aqueous phase of a PE had a tremendous impact on the stability as is shown in Figure 3.11. Addition of NaOH to the aqueous phase to reach pH 13 causes complete collapse of the PEs and partitioning of the silica particles to the aqueous phase. This is due to deprotonation of the silanol groups, which increases the wettability of the particles by water and destabilizes w/o PEs.[35] Lowering the pH by addition of HCl to the aqueous phase led to slight destabilization of all PEs in the form of sedimentation. This led to a decrease in emulsion fraction from 1 to 0.86, 0.93 to 0.90 and 0.93 to 0.86 for IPP, PG and SBP, respectively. Again, the good stability at low pH could be beneficial for the intended catalytic dehydration reactions as they require acidic conditions.

Temperature

While several examples of PE catalysis at elevated temperatures have been published,[44–47] these studies often lack the assessment of the thermal stability of PEs. The fructose dehydration reaction of interest here, demands temperatures around or over 100 °C,

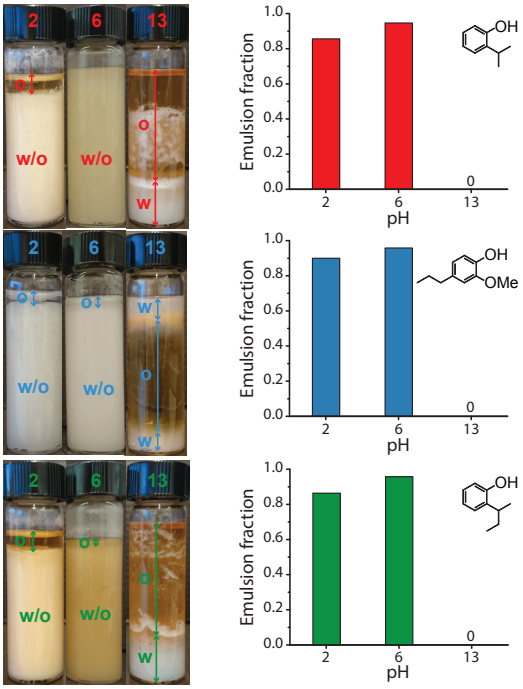

Figure 3.11: Appearance and emulsion fractions of PEs formulated with IPP (Red), PG (Blue), SBP (Green) at different pH values after 1 month. PE: 6 mL alkylphenol solvent, 2 wt% hydrophobic silica, 2 mL Milli-Q water, 30 wt% silica.

the boiling point of our dispersed aqueous phase. The largest effect of increasing the temperature on PE stability would be a decrease in interfacial tension, thus negatively affecting stability, as was already described by Jennings in 1967.[48]

The stability of the alkylphenol formulated PEs was studied using the optimal parameters for the catalytic system, i.e. 2 wt% silica, 30 wt% NaCl and an acidic aqueous phase. The vials with the three different PEs were placed in a small heating mantle at 100 °C under static conditions. The stability was checked after 1 h, 1 day, 1 week and 2 weeks, after which the emulsion fraction was again determined using the optical images (Figure 3.12). Only a slight destabilization was observed after 1 h, giving emulsion fractions of 0.85, 0.95 and 0.92 for IPP, PG and SBP, respectively. This shows that reactions could be performed in these emulsions for 1 h. Exposing the PEs for longer times to this high temperature led to further destabilization. After two weeks a top and a bottom layer of clear liquids are observed with a layer of PE in between. The emulsion fraction that these PE layers represent are 0.63, 0.45 and 0.61 for the IPP, PG and SBP. Boiling the aqueous phase led to rupture of the droplets and eventually to phase separation. This is also evident from the cracks and the big droplets inside of the PE layer.

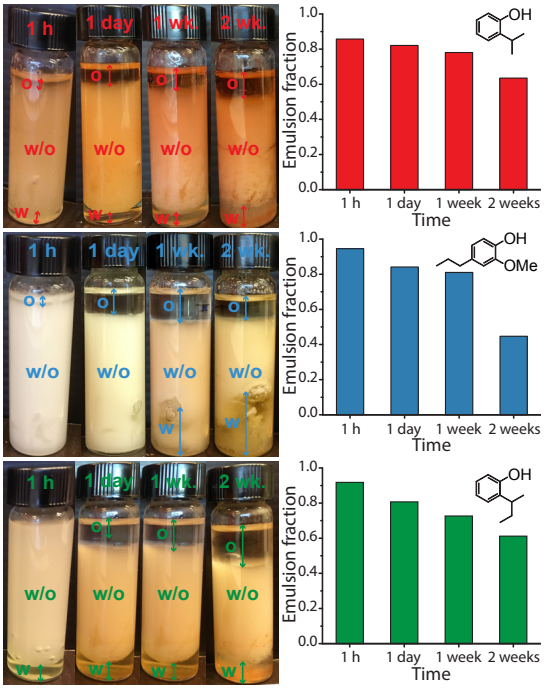

Figure 3.12: Appearance and emulsion fractions of PEs formulated with IPP (Red), PG (Blue), SBP (Green) over time at 100 °C. PE: 6 mL alkylphenol solvent, 2 wt% hydrophobic silica, 2 mL Milli-Q water, 30 wt% NaCl, pH 2.

To suppress the boiling of the aqueous phase, PE stability at elevated temperature was tested under N_2 pressure. For this, we used a high-pressure batch autoclave with optical windows covering the complete height of the vessel, thus allowing us to monitor the stability directly under these conditions. First, the vessel, containing PEs formulated with the alkylphenol solvent and acidic and saline water, was pressurized with 6 bar of nitrogen and heated to 100 °C. The stability was followed over the course of 3 h as is shown in Figure 3.13. The PE formulated with IPP destabilizes very quickly leaving an emulsion fraction of 0.76 after 30 min. The destabilization rate decreased over time and after 2 h a stable emulsion phase of 63 % of the total volume was obtained. The destabilization of the PE formulated with PG is slower and after 3 h an emulsion fraction of 0.69 is left. The PE formulated with SBP shows the same slow destabilization, giving an even higher emulsion fraction of 0.78 after 3 h at 100 °C. The stability in the non-pressurized systems was much higher at this temperature, with emulsion fractions of 0.82, 0.84 and 0.81 for IPP, PG and SBP respectively, after 1 full day. Subsequently, the temperature and pressure were increased to 150 °C and 11 bar, in order to increase the boiling point of water to 200 °C, which required approximately 15 min. As can be deduced from Figure 3.14, the IPP emulsion proved to be unstable, already after 15 min after reaching 150 °C, an emulsion

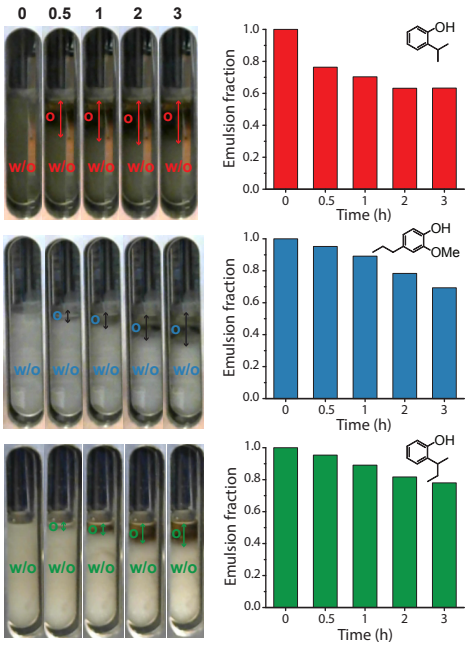

Figure 3.13: Left: Appearance and emulsion fraction of PEs formulated with IPP (red), PG (blue) and SBP (green) over time at 100 °C and 6 bar N_2 pressure. PE: 42 mL alkylphenol solvent, 2 wt% hydrophobic silica, 14 mL Milli-Q water, 30 wt% NaCl, pH 2. Right: Picture and schematic representation of the window autoclave.

fraction of 0.19 was obtained, which did not further change over time. The PG formulated PE was again more stable reaching an emulsion fraction of 0.69 after 1 h. The PE with SBP showed a similar high stability with an emulsion fraction of 0.72 after 1 h.

Leaving the PEs for some more hours at 150 °C led to complete collapse of the PEs with the particles residing on the bottom of the autoclave in the aqueous phase. This indicates a decrease in hydrophobicity of the particles, as confirmed by FT-IR. The recovered particles were thoroughly washed in toluene to remove all the water and organic solvent and dried in air prior to recording the FT-IR spectrum. Comparison to the fresh hydrophobized particles, as is shown in Figure 3.15, shows the relative decrease in intensity of the C-H stretch vibration (2970-2850 cm^{-1}) of the hydrophobic methyl groups with respect to the O-H stretch vibration (3800-3500 cm^{-1}) for the spent particles. This indicates that during heating at 150 °C, in an acidic environment, hydrolysis of the trimethylsilyl groups occurred, as also previously noted for 3-aminopropylsilane-functionalized (APS).[49] The hydrolysis and therefore loss of hydrophobic groups on the silica surface lead to less efficient wetting of the organic phase, causing destabilization of the PE.

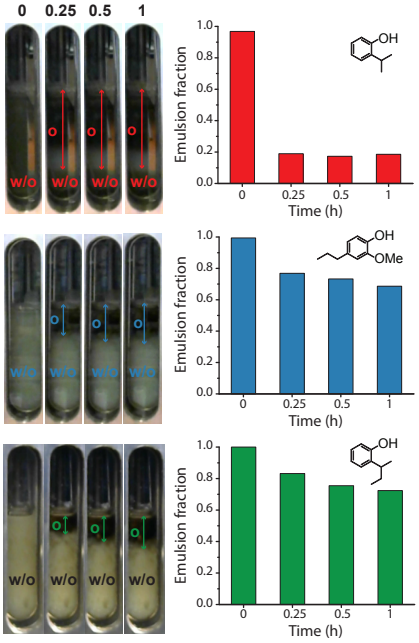

Figure 3.14: Appearance and emulsion fraction of PEs formulated with IPP (red), PG (blue) and SBP (green) over time at 150 °C and 11 bar N_2 pressure. PE: 42 mL alkylphenol solvent, 2 wt% hydrophobic silica, 14 mL Milli-Q water, 30 wt% NaCl, pH 2.

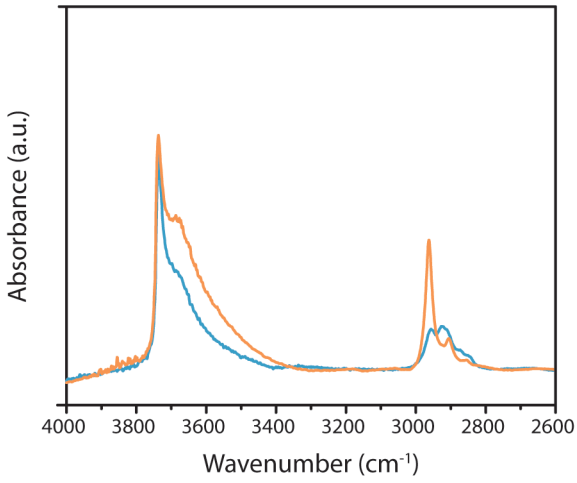

Figure 3.15: Partial FT-IR spectra of hydrophobized silica before (orange) and after (blue) reaction at 150 °C and under 11 bar N_2.

Taken together, this stability study demonstrates that PEs formulated with alkylphenol solvents can be suitable for our catalytic application. The PEs stabilized with 2 wt% silica were stable under high salinity and formulated with acidic aqueous phases, even at elevated temperatures for at least 1 day, which makes them interesting for acid-catalyzed sugar dehydration reactions. However, as is shown in this work, the stability is very much influenced by little changes in the system. Therefore, it is essential to perform thorough stability tests before applying catalytic reactions in PEs, something that is not yet commonly done.

3.2.4 5-HMF extraction

To investigate whether the alkylphenol formulated PEs are not only promising based on their stability but also based on reactivity, the 5-HMF extraction efficiency of the alkylphenol formulated systems was tested using BS with low and high interfacial area and followed over the course of one hour. Ideally, PEs would have been used for the high interfacial area system, but the vigorous stirring that is necessarily part of PE preparation would already induce the extraction of 5-HMF, resulting in unreliable kinetic traces. Therefore, a static BS was used for the low interfacial area system while a stirred BS was used for the high interfacial area system (Figure 3.16), as the results of the latter can be extrapolated to what can be expected from the analogous PE.

The high interfacial area clearly is beneficial for the rate of 5-HMF extraction in BS, as expected. In the stirred BS maximum extractions of 5-HMF of 100% (IPP), 84% (PG) and 91% (SBP) corresponding to partitioning coefficients of ∞ (IPP), 5.4 (PG) and 10.2 (SBP) were reached. In PG and SBP the maximum extraction of 5-HMF was already reached at first sampling after 10 min while in IPP extraction plateaued after 30 min, when full extraction was reached. So, while in the end IPP has the highest 5-HMF extraction capacity, its extraction efficiency is lower than that of PG and SBP. In the non-stirred BS maximum 5-HMF extractions of 25% (IPP), 12% (PG) and 20% (SBP) were observed in 1 h, corresponding to partitioning coefficients of 0.33 (IPP), 0.14 (PG) and 0.24 (SBP). To reach the final partitioning coefficients, ∞ (IPP), 5.4 (PG) and 10.2 (SBP), much longer time is required for these low interfacial systems.[50] Again, the percentage of extracted 5-HMF plateaus immediately for PG and SBP, while for IPP it increases over time. There thus appears to be a kinetic barrier in the non-stirred BS to achieve thermodynamic equilibrium.

The kinetic barrier of the 5-HMF extraction can be estimated using the Stokes-Einstein diffusion coefficient (D),

$$D = \frac{k_B T}{6\pi\eta r} \tag{3.3}$$

with k_B being the Boltzman constant, T temperature, the viscosity of water and r the radius of a 5-HMF molecule. For a rough estimation of the kinetic barrier a 5-HMF molecule can be assumed to be a sphere, of which the radius can be determined from the molar volume (V_m),

$$V_m = \frac{M}{\rho} \tag{3.4}$$

In which M is the molar mass (126 g/mol) and ρ the mass density of 5-HMF (1.29 g/mL), giving a molar volume of 97.67 mL/mol, implying a volume of 0.162 nm^3 per molecule of 5-HMF. The radius of one 5-HMF molecule, as shown in eq. 3.5, equals 0.338 nm.

$$r = \left(\frac{3V_m}{4\pi}\right)^{\frac{1}{3}} \tag{3.5}$$

Using a water viscosity of 0.9 mPa·s and a temperature of 298 K, the Stokes-Einstein coefficient equals $71.6 \cdot 10^{-7}$ m^2/s. The mean squared displacement (MSD) of a molecule in one-dimensional diffusion in the x-direction over t time is given by:

$$< x^2 > = 2Dt \tag{3.6}$$

As the volume of the water phase is 2 mL, assuming the water phase is in a cubic container, the maximum length a 5-HMF molecule should diffuse through the aqueous phase to the interface equals 1.26 cm. The time for a 5-HMF molecule to diffuse to the interface, without kinetic barrier, would then be around 11 s. As is shown in Figure 3.16, the diffusion takes much longer, implying that indeed there is a kinetic barrier. The effective diffusion constant (D_{eff}) over a volume (V) can be described as function of *k*T:

$$D_{eff} \approx D^{-\frac{V}{kT}} \tag{3.7}$$

This shows that already with a low kinetic barrier, e.g. 3 *k*T, the time to diffuse to the interface would increase from 11 s to 3.7 h.

The data in Fig 3.16 shows that such a kinetic barrier must be much less pronounced in the high interfacial systems, highlighting the applicability of the alkylphenols as efficient 5-HMF extracting solvents when used in a high interfacial area system. This makes them highly interesting for the catalytic conversion of lignocellulosic biomass.

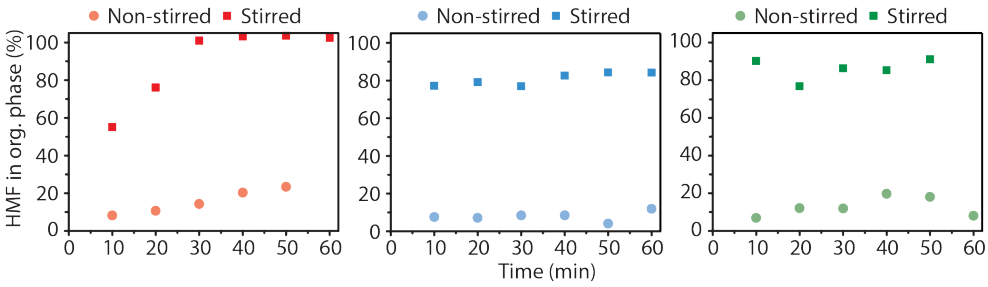

Figure 3.16: Kinetic traces of 5-HMF extraction from the aqueous to the organic phase using IPP (red), PG (blue) and SBP (green) as organic solvents. Reaction conditions: 2 mL Milli-Q water with 30 wt% NaCl and 0.2 M 5-HMF, 6 mL alkylphenol solvent, RT, stirring 750 rpm.

3.3 Conclusions

The stability of PEs formulated with alkylphenol solvents and partially hydrophobic fumed silica was studied under reaction conditions relevant for catalysis. Silica addition to the alkylphenol solvents led to a slight increase of the viscosity for all the solvents and resulted in a switch from Newtonian to slightly non-Newtonian behavior. The differences in viscosity of the three alkylphenol solvents (IPP, PG and SBP) were very small and therefore not expected to play a big role in the differences in stability of the formed PEs. As SBP showed the smallest contact angle (146.4°) and the highest interfacial tension (17.0 mN/m), PEs formulated with this alkylphenol were expected to be the most stable. However due to the overall small differences between the three alkylphenols, this was not evidently presented in the experimental results.

The stability of the PEs was studied over the course of one month while varying the silica concentration, the NaCl concentration and the pH. Stable PEs were obtained using 2 wt% silica, 30 wt% NaCl and an acidic aqueous phase (pH 2), conditions relevant for catalytic biomass conversion. No large differences were observed between the stability of the PEs formulated with the three alkylphenols. The temperature stability window was limited to the boiling point of water under ambient pressures but could be extended to higher temperatures (100-150 °C) if the PE was pressurized. Heating to 150 °C under acidic conditions lead to destabilization of the PE due to hydrolysis of the trimethylsilyl groups on the silica surface. At 100 °C, the PEs were moderately stable for at least 3 h making them useful for our catalytic application. However, slight changes in PE components can have a great impact on the stability, making this thorough stability assessment crucial when applying PEs as reaction media for catalytic reactions.

The 5-HMF extraction efficiency of the three alkylphenols was studied using BS with high and low interfacial area. The use of high interfacial area BS resulted in high partitioning of 5-HMF from the aqueous to the organic phase with the lowest extraction efficiency for PG (84%) and the highest for IPP (100%). The stability and extraction efficiency of the alkylphenol formulated PEs and BS thus hold considerable promise for the catalytic conversion of lignocellulosic biomass.

3.4 Experimental procedures

3.4.1 Materials

All chemicals were used as received without any further purification. AEROSIL® 200 silica powder was purchased from Evonik Industries. Toluene was purchased from Interchema. Hydrochloric acid (HCl, 37%, analytical grade), chloro(trimethyl)silane (TMSCl, ≥ 98%), 2-*iso*propylphenol (IPP, 98%), 4-propylguaiacol (PG, ≥ 99%, food grade), 2-*sec*-butylphenol (SBP, 98%) and Nile red (≥ 98%) were purchased from Sigma-Aldrich. Sodium hydroxide (NaOH, pellets pure) and sodium chloride (NaCl) were obtained from Merck.

3.4.2 Hydrophobization of silica

Silylated silica was prepared using a procedure adapted from literature.[51] A solution of TMSCl in toluene (10 wt%; V_T = 10 mL) was added to 1 g of silica powder AEROSIL® 200. The mixture was stirred for 2 h under reflux. The resulting silylated silica particles were filtered, washed twice with toluene and dried in air overnight.

3.4.3 Characterization of silica

The silylated silica was analyzed by Fourier-Transform Infrared (FT-IR) Spectroscopy, for which self-supported wafers of ~20 mg were mounted in an FT-IR cell connected to an oven. The wafer was dried by heating the sample to 400 °C with a heating rate of 5 °C/min under vacuum. A Perkin-Elmer System 2000 instrument was used to record the FT-IR spectra in transmission mode in the spectral range of 4000 to 1000 cm^{-1}. For each spectrum 32 scans were collected with a spectral resolution of 4 cm^{-1}.

N_2-physisorption isotherms for all support materials were measured at -196 °C on a Micromeritics TriStar 3000 apparatus. The specific surface area of the support was calculated by fitting experimental data with the BET equation ($0.05 < p/p° < 0.25$).

Transmission Electron Microscopy (TEM) images were recorded with a FEI tecnai 12 Icor TEM operating at 120 kV to analyze any differences in morphology and particles size of the silica before and after silylation.

Contact angle measurements were performed using a Dataphysics OCA 15 optical contact angle measuring setup equipped with a single direct dosing module (SD-DM). Silica was pressed to form a pellet which was placed inside a cuvette filled with alkylphenol solvent. A 2 µL droplet of water (30% NaCl) was dispensed at a rate of 1 µL/min and placed gently on top of the wafer. After 5 min of equilibration the three-phase contact angle between the wafer, alkylphenol solvent and water was determined using SCA 20 software.

3.4.4 Physical properties of the alkylphenol solvents

The viscosity of the alkylphenol solvents with and without silica present was determined with a Physica MCR 300 rheometer (Anton Paar) equipped with a cone-plate geometry (CP50-2, 50 mm, 2°, Anton Paar). The temperature was kept constant at 20 °C. The interfacial tension between the alkylphenol solvent and water containing 30 wt% NaCl was determined using a Dataphysics OCA 15 setup equipped with a single direct dosing module (SD-DM). A cuvette was filled with alkylphenol solvent after which a droplet of 9.5 µL of aqueous phase was dosed with a rate of 1 µL/min. The interfacial tension was determined using the Young-Laplace equation (3.3) with the SCA 20 software.[52]

$$\Delta P = P_{int} - P_{ext} = \gamma\left(\frac{1}{R_1} + \frac{1}{R_2}\right) \tag{3.8}$$

In this equation, ΔP is the pressure difference between the inside (P_{int}) and outside (P_{ext}) the droplet, γ the interfacial tension and R_1 and R_2 the principle radii of the curve (Figure 3.17). Gravity pulling on the droplet causes a pressure gradient over the length axis (z) of the droplet. Therefore, the pressure over this vertical axis can be described as:

$$\Delta P(z) = P_0 \pm \Delta\rho g z \tag{3.9}$$

With P_0 being a reference pressure at z = 0, Δρ the density difference of the drop phase and the continuous phase and g the gravitational acceleration. For pendant droplets, the principal radii at the bottom, apex, of the droplet are $R_1 = R_2 = R$, at every point above this, $R_2 = x/\sin\Phi$. Combining these equations gives:

$$\frac{1}{R_1} + \frac{sin\Phi}{x} = \frac{2}{R} \pm \frac{\Delta\rho g z}{\gamma} \tag{3.10}$$

This equation can be translated into three dimensionless differential equations in terms of the arc length s of the droplet shape:

$$\frac{d\Phi}{ds} = 2 - Bo\ z - \frac{\sin\Phi}{x} \tag{3.11}$$

$$\frac{dx}{ds} = \cos \Phi \tag{3.12}$$

$$\frac{dz}{ds} = \sin \Phi \tag{3.13}$$

With Bo being the dimensionless Bond number defined as $(\Delta\rho g R^2)/\gamma$. These differential equations are only valid under the conditions, x = 0, z = 0 and Φ = 0 at s = 0. By determining the Bond number, the interfacial tension can be calculated.

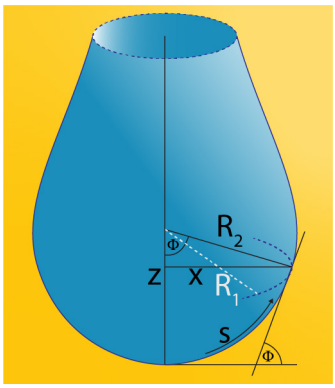

Figure 3.17: Graphic representation of a droplet in oil and all parameters used for interfacial tension measurements, figure adapted from Dataphysics, Germany.

3.4.5 Pickering emulsion preparation

All PEs were prepared by first dispersing a known mass of silylated silica particles into 6 mL of alkylphenol solvent (IPP, PG or SBP) using a VCX 130 Vibra-Cell Ultrasonic Processor equipped with a 3 mm diameter tip (Sonics, 20 kHz, 10 W, 2 min). During sonication, it was necessary to cool the vessel in an ice-bath. After the addition of 2 mL of the aqueous phase with appropriate NaCl concentration and required pH to the alkylphenol phase, the resulting mixture was emulsified using a UltraTurrax T25 homogenizer with a S25N-10G dispersing tool (IKA, 15200 rpm, 2 min).

3.4.6 Pickering emulsion characterization

The type of emulsion was determined by staining the organic phase with Nile Red (10^{-5} M) or the aqueous phase with FITC-dextran (10^{-6} M) and performing confocal fluorescence microscopy using a Nikon ECLIPS 90i upright confocal laser scanning fluorescence microscope with a 10x 0.3 NA dry objective lens. Fluorescence microphotographs were collected using 561 nm laser light. The emission was detected at 575-635 nm using an A1R

scanning head equipped with a spectral detection unit consisting of a diffraction grating and a 32-photomultiplier tube array. The stability of the Pickering emulsions under high temperatures and pressures were studied using a custom-made Parr window autoclave (Figure 3.18). After loading the vessel with the PE, the vessel was pressurized with 40 bars of N_2 after which the PE was heated to the temperature set while stirring for optimal heat transfer. Upon reaching the desired temperature, stirring was stopped and the PE was left static under these conditions while taking pictures using a Logitech webcam with a constant time interval. Emulsion fractions were determined using the optical photographs and ImageJ (Fiji).

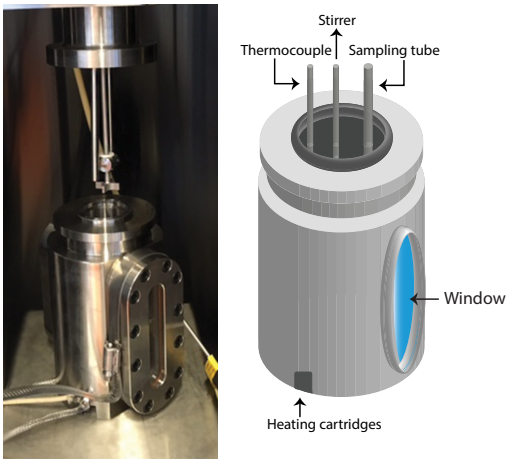

Figure 3.18: Picture and schematic representation of the window autoclave.

3.4.7 5-HMF extraction

15 mL Ace pressure tubes were loaded with 6 mL alkylphenol solvent and 2 mL of Milli-Q water saturated with NaCl containing 0.2 M 5-HMF. The tubes were left at room temperature for 10, 20, 30, 40, 50 or 60 minutes with or without stirring (750 rpm), and an aliquot of the organic phase was taken for GC analysis on a Varian GC equipped with a VF-5 ms capillary column and an FID detector using anisole as internal standard to determine the amount of 5-HMF that was extracted.

Acknowledgements

Prof. dr. Albert Philipse (Physical and Colloid Chemistry, PCC, Utrecht University) is acknowledged for the discussion on the kinetic experiments. Dr. Pasi Paalanen (Inorganic Chemistry and Catalysis, UU) is acknowledged for the N_2-physisoprtion measurements. Lars van der Wal (ICC, UU) is acknowledged for the TEM measurements. Dr. Dominique Thies-Weesie and Bonny Kuipers (PCC, UU) are acknowledged for their help with the experiments to determine the physical chemical properties of the alkylphenol solvents,

such as the contact angle, rheology and interfacial tension measurements and for fruitful discussions.

References

1 R. A. Sheldon, *Green Chem.*, **2005**, *7*, 267.
2 W. C. Lee and B. J. Frost, *Green Chem.*, **2012**, *14*, 62.
3 L. C. Matsinha, S. F. Mapolie and G. S. Smith, *Dalt. Trans.*, **2014**, *44*, 1240.
4 A. Behr and P. Neubert, *Applied Homogeneous Catalysis*, WILEY-VCH Verlag GmbH & Co. KGaA, 2012.
5 S. G. Wettstein, D. M. Alonso, Y. Chong and J. A. Dumesic, *Energy Environ. Sci.*, **2012**, *5*, 8199.
6 J. E. Romo, N. V. Bollar, C. J. Zimmermann and S. G. Wettstein, *ChemCatChem*, **2018**, *10*, 4819.
7 J. N. Chheda, Y. Roman-Leshkov and J. A. Dumesic, *Green Chem.*, **2007**, *9*, 342.
8 D. M. Alonso, J. Q. Bond and J. A. Dumesic, *Green Chem.*, **2010**, *12*, 1493.
9 Y. B. Huang and Y. Fu, *Green Chem.*, **2013**, *15*, 1095.
10 R. Van Putten, J. C. Van Der Waal, E. De Jong, C. B. Rasrendra, H. J. Heeres and J. G. De Vries, *Chem. Rev.*, **2013**, *113*, 1499.
11 I. van Zandvoort, Y. Wang, C. B. Rasrendra, E. R. H. van Eck, P. C. A. Bruijnincx, H. J. Heeres and B. M. Weckhuysen, *ChemSusChem*, **2013**, *6*, 1745.
12 P. Azadi, R. Carrasquillo-Flores, Y. J. Pagán-Torres, E. I. Gürbüz, R. Farnood and J. A. Dumesic, *Green Chem.*, **2012**, *14*, 1573.
13 L. C. Blumenthal, C. M. Jens, J. Ulbrich, F. Schwering, V. Langrehr, T. Turek, U. Kunz, K. Leonhard and R. Palkovits, *ACS Sustain. Chem. Eng.*, **2016**, *4*, 228.
14 Y. Chevalier and M. A. Bolzinger, *Colloids Surfaces A Physicochem. Eng. Asp.*, **2013**, *439*, 23.
15 L. L. Schramm, *Emulsions, Foams, and Suspensions: Fundamentals and Applications*, WILEY-VCH Verlag GmbH & Co. KGaA, 2005.
16 J. Marto, A. Ascenso, S. Simoes, A. J. Almeida and H. M. Ribeiro, *Expert Opin. Drug Deliv.*, **2016**, *13*, 1093.
17 M. Pera-Titus, L. Leclercq, J. M. Clacens, F. De Campo and V. Nardello-Rataj, *Angew. Chem.- Int. Ed.*, **2015**, *54*, 2006.
18 B. P. Binks, *Curr. Opin. Colloid Interface Sci.*, **2002**, *7*, 21.
19 B. P. Binks and S. O. Lumsdon, *Langmuir*, **2000**, *16*, 8622.
20 B. R. Midmore, *Colloids Surfaces A Physicochem. Eng. Asp.*, **1998**, *132*, 257.
21 B. P. Binks and S. O. Lumsdon, *Langmuir*, **2000**, *16*, 2539.
22 R. Aveyard, B. P. Binks and J. H. Clint, *Adv. Colloid Interface Sci.*, **2003**, *100–102*, 503.

23 B. P. Binks, J. Philip and J. A. Rodrigues, *Langmuir*, **2005**, *21*, 3296.

24 B. P. Binks, A. Desforges and D. G. Duff, *Langmuir*, **2007**, *23*, 1098.

25 S. Sacanna, W. K. Kegel and A. P. Philipse, *Phys. Rev. Lett.*, **2007**, *98*, 158301.

26 Z. G. Cui, K. Z. Shi, Y. Z. Cui and B. P. Binks, *Colloids Surfaces A Physicochem. Eng. Asp.*, **2008**, *329*, 67.

27 J. Frelichowska, M. A. Bolzinger and Y. Chevalier, *Colloids Surfaces A Physicochem. Eng. Asp.*, **2009**, *343*, 70.

28 C. Monteux, C. Marliére, P. Paris, N. Pantoustier, N. Sanson and P. Perrin, *Langmuir*, **2010**, *26*, 13839.

29 H. Fan and A. Striolo, *Soft Matter*, **2012**, *8*, 9533.

30 M. Vis, J. Opdam, I. S. J. Van 't Oor, G. Soligno, R. Van Roij, R. H. Tromp and B. H. Erné, *ACS Macro Lett.*, **2015**, *4*, 965.

31 N. M. Briggs, J. S. Weston, B. Li, D. Venkataramani, C. P. Aichele, J. H. Harwell and S. P. Crossley, *Langmuir*, **2015**, *31*, 13077.

32 J. Shi, X. Wang, W. Zhang, Z. Jiang, Y. Liang, Y. Zhu and C. Zhang, *Adv. Funct. Mater.*, **2013**, *23*, 1450.

33 R. von Klitzing, D. Stehl, T. Pogrzeba, R. Schomäcker, R. Minullina, A. Panchal, S. Konnova, R. Fakhrullin, J. Koetz, H. Möhwald and Y. Lvov, *Adv. Mater. Interfaces*, **2017**, *4*, 1.

34 D. R. Lide, in *CRC Handbook of Chemistry and Physics*, Internet Version, 2005.

35 B. P. Binks and S. O. Lumsdon, *Phys. Chem. Chem. Phys.*, **2000**, *2*, 2959.

36 K. Thakkar, B. Bharatiya, D. Ray, V. K. Aswal and P. Bahadur, *Langmuir*, **1997**, *13*, 369.

37 M. Z. Shahid, M. R. Usman, M. S. Akram, S. Y. Khawaja and W. Afzal, *J. Chem. Eng. Data*, **2017**, *62*, 1198.

38 R. Pal, *Fluids*, **2017**, *3*, 2.

39 Y. Román-Leshkov and J. A. Dumesic, *Top. Catal.*, **2009**, *52*, 297.

40 B. P. Binks and C. P. Whitby, *Colloids Surfaces A Physicochem. Eng. Asp.*, **2005**, *253*, 105.

41 È. Tsabet and L. Fradette, *Chem. Eng. Res. Des.*, **2015**, *97*, 9.

42 E. Dickinson, R. Ettelaie, T. Kostakis and B. S. Murray, *Langmuir*, **2004**, *20*, 8517.

43 L. G. J. Fokkink and J. Ralston, *Colloids and Surfaces*, **1989**, *36*, 69.

44 S. Crossley, J. Faria, M. Shen and D. E. Resasco, *Science*, **2010**, *327*, 68.

45 P. A. Zapata, J. Faria, M. P. Ruiz, R. E. Jentoft and D. E. Resasco, *J. Am. Chem. Soc.*, **2012**, *134*, 8570.

46 J. Faria, M. Pilar Ruiz and D. E. Resasco, *ACS Catal.*, **2015**, *5*, 4761.

47 Y. Zhang, M. Zhang and H. Yang, *ChemCatChem*, **2018**, *10*, 5224.

48 H. Y. Jennings, *J. Colloid Interface Sci.*, **1967**, *24*, 323.

49 P. Van Der Voort and E. F. Vansant, *J. Liq. Chromatogr. Relat. Technol.*, **1996**, *19*,

2723.

50 A. T. Fisk, B. Rosenberg, C. D. Cymbalisty, G. A. Stern and D. C. G. Muir, *Chemosphere*, **1999**, *39*, 2549.

51 M. C. Capel-Sanchez, L. Barrio, J. M. Campos-Martin and J. L. G. Fierro, *J. Colloid Interface Sci.*, **2004**, *277*, 146.

52 J. D. Berry, M. J. Neeson, R. R. Dagastine, D. Y. C. Chan and R. F. Tabor, *J. Colloid Interface Sci.*, **2015**, *454*, 226.

Chapter 4

Catalytic Conversion of Fructose to 5-HMF and 5-HMF-derivatives in Alkylphenol-based Pickering Emulsions

In Chapter 3, Pickering emulsions (PEs) formulated with the alkylphenols 2-*iso*propylphenol (IPP), 4-propylguaiacol (PG) and 2-*sec*-butylphenol (SBP), were shown to be sufficiently stable under reaction conditions relevant for acid-catalyzed sugar dehydration chemistry. The alkylphenols showed a high and rapid extraction of 5-(hydroxymethyl)furfural (5-HMF), potentially increasing product yields and selectivities by reducing side product formation, such as small organic acids and humins. Here, the effect of emulsification on the efficiency of fructose dehydration was studied and the alkylphenol-based PEs were compared to normal biphasic systems (BS). PEs outperformed the BS in terms of fructose conversion and 5-HMF extraction, with IPP showing the highest 5-HMF selectivity of the three alkylphenols: ~90% at 48% 5-HMF yield. The excellent performance of these reaction media in the fructose dehydration reaction prompted the study of these systems for tandem (catalytic) reactions for further functionalization of the 5-HMF platform molecule. Coupling acid-catalyzed dehydration to a base-catalyzed Knoevenagel condensation with diethyl malonate, proved possible in PE, but not in BS. The mutual destruction of acid and base catalysts seen in BS, was (partially) prevented in the PE system as a result of compartmentalization. Optimization studies showed that product yields could be enhanced if 5-HMF was allowed to accumulate in the organic phase. This was achieved by postponing base and diethyl malonate addition, resulting in product yields of 24% after 32 h.

4.1 Introduction

Given the unsustainability of fossil resource use, chemists started looking for other, more sustainable, feedstocks for the generation of fuels and chemicals. One of these alternatives is lignocellulosic biomass, which consists of three main parts, cellulose, hemicellulose and lignin, of which cellulose is the most abundant part, accounting for 40-50% of the dry weight of the material.[1] Cellulose is a polymer of glucose, in which monomers are linked via β-glycosidic bonds. By enzymatic hydrolysis of these bonds, the glucose monomers can be retrieved in high yields (>90%) and subsequently used in the synthesis of fuels and chemical building blocks.[2]

Conversion of sugar molecules into valuable renewables-based products often proceeds via the furanic intermediate platform molecule 5-(hydroxymethyl)furfural (5-HMF).[3] However, direct dehydration of glucose to form 5-HMF is a poorly efficient process, with a maximum overall yield of approximately 12%, and a selectivity of 40% using a homogeneous catalyst[4], and 29% yield and 67% selectivity with a heterogeneous catalyst.[5] A solution to this issue was found in the isomerization of glucose to fructose, of which the acid-catalyzed dehydration to 5-HMF is much more efficient. For example, the best results shown in a homogeneous catalyzed process was reported by Liu *et al.* yielding 58% 5-HMF with a selectivity of 64%[6], and in a heterogeneous catalyzed process reported by Yoshida *et al.* 49% of 5-HMF was obtained with 61% selectivity.[7] The selectivity issues in the dehydration of glucose and fructose are caused by parallel and consecutive reactions of (precursors to) 5-HMF with the acid catalyst, resulting in the formation of small organic acids and large polymeric compounds, called humin by-products.[8,9]

To improve efficiency and cope with the major challenge of side product formation, much research has been done on performing fructose dehydration reactions in liquid-liquid biphasic reaction media.[10] By adding a second, organic liquid to the acidic aqueous reaction mixture, the 5-HMF product can be extracted to this second liquid phase and away from the acid catalyst, reducing side product formation. This extraction can be enhanced by saturating the aqueous phase, e.g. with sodium chloride (NaCl), to make use of the so-called 'salting-out effect'. Dumesic *et al.* first showed the benefit of using biphasic catalysis for sugar dehydration reactions using various aliphatic alcohols, aliphatic ketones and cyclic ethers such as tetrahydrofuran (THF) and 2,5-dimethylfuran (DMF)[11,12] for extraction, followed by biomass-derived solvents such as γ-valerolactone (GVL).[13] In a systematic, theoretical study of Palkovits *et al.*[14] and in experimental studies by Dumesic *et al.*[15–18], alkylphenol solvents were later shown to be very efficient solvents for the extraction of 5-HMF. The extraction property of an organic solvent can be expressed by a dimensionless physical chemical constant, the partitioning coefficient (P):

$$P = \frac{[X]_{org}}{[X]_{aq}} \quad (4.1)$$

where $[X]_{org}$ represents the concentration of solute X (in mol/L) in the organic phase and $[X]_{aq}$ the concentration of the solute (mol/L) in the aqueous phase.

In Chapter 3, we reported on the extraction of 5-HMF in biphasic systems (BS) with three different alkylphenols; 2-*iso*propylphenol (IPP), 4-propylguaiacol (PG) and 2-*sec*-butylphenol (SBP), showing higher 5-HMF extraction efficiency with increasing interfacial area. In the stirred (high interfacial area) BS, 84%, 91% and 100% of the 5-HMF could be extracted from the aqueous phase to PG, SBP and IPP respectively, in 1 h. An alternative method to create BS with high interfacial area is by emulsification. This is traditionally done by addition of surfactants, although more stable emulsions can be obtained by the addition of amphiphilic solid particles, creating so-called Pickering emulsions (PEs).

Water-in-oil (w/o) PEs formulated with the alkylphenol solvents and 2 wt% amphiphilic silica proved to be stable, using acidic and highly saline aqueous phases, for several hours at 100 °C (Figure 3.13 and Figure 3.14), opening up a window of reaction conditions relevant for sugar dehydration chemistry. Furthermore, the rate of partitioning of 5-HMF was found to be much higher in stirred than non-stirred BS, as a result of the generated higher interfacial area (Figure 3.16). In this PhD Thesis Chapter, the effect of 5-HMF partitioning on the dehydration reaction of fructose to 5-HMF was studied using PEs and non-stirred BS formulated with the IPP, PG and SBP alkylphenols. Fructose conversion, 5-HMF yield, 5-HMF extraction and 5-HMF selectivity were tracked over time, showing higher fructose conversion, 5-HMF yield and 5-HMF extraction in PEs than in BS, while maintaining 5-HMF selectivity in all three alkylphenols. IPP and SBP proved most efficient as extracting solvent, as 100% of the 5-HMF formed during reaction was extracted from the aqueous to the organic phase when PEs were used.

As noted above, 5-HMF is a versatile platform molecule and can be used for the production of high-value chemicals, e.g. by reduction or oxidation. For example, catalytic reduction of the formyl group of 5-HMF gives 2,5-dihydroxymethylfuran, which is used as a building block for polymers and polyurethane foams.[19] Additional reduction of the alcohol groups and the furanic double bonds result in the formation of 2,5-dimethylfuran (DMF) and 2.5-dimethyltetrahydrofuran (DMTHF) respectively, compounds with high energy densities, making them interesting biofuel components.[11,19,20] Selectively oxidizing the alcohol functionality of 5-HMF produces 2,5-diformylfuran (DFF), a precursor for polymers, pharmaceuticals and antifungal agents.[21] Selective oxidation of the formyl group to a carboxylic acid group, results in the formation of 5-hydroxymethyl-2-furancarboxylic acid

(HMFCA), which can be oxidized further to form 2,5-furandicarboxylic acid (FDCA).[21] This FDCA can be polymerized with ethylene glycol to form polyethylene 2,5-furandicarboxylate (PEF), a more sustainable and improved alternative for one of the most used synthetic polymers, polyethylene terephthalate (PET).[3,22] While the reactions listed above change the oxidation state of the functional groups, they leave the C_6 carbon skeleton unchanged. The possibility to vary the carbon chain length is important, however, as it multiplies the number of downstream applications that can be served with 5-HMF. Indeed, the 5-HMF structure also offers many opportunities for structure diversification by C-C coupling reactions, with the alcohol and aldehyde group of HMF being very susceptible to coupling reactions such as Wittig-type reactions, Baylis-Hillman reactions and aldol and other types of condensation reactions.[19] In Chapter 2 of this PhD Thesis, we coupled a base-catalyzed condensation reaction to an acid-catalyzed reaction, in a tandem reaction that could only be performed in PEs. Following up on that work, here we investigate the possibility to use PEs for the tandem (catalytic) reactions of fructose and allow one-pot further functionalization of 5-HMF.

The Knoevenagel condensation product of 5-HMF with Meldrum's acid (5-(hydroxymethyl) furfural-2-meldrum's acid (5-HMFMA, Figure 4.1), has been used as precursor for, e.g., the production of visible light organic photoswitches.[23–25] As the Knoevenagel condensation step is noncatalytic, this tandem reaction is an attractive first extension beyond the acid-catalyzed fructose dehydration reaction, on route towards tandem catalytic reactions in alkylphenol-formulated PEs.

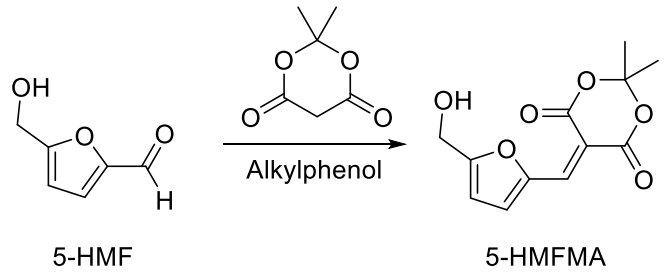

Figure 4.1: The (noncatalytic) Knoevenagel condensation between 5-HMF and Meldrum's acid yields 5-HMFMA, a precursor to organic photoswitches.

While Meldrum's acid is activated enough as substrate to allow for a non-catalytic Knoevenagel condensation, less reactive substrates typically require a base catalyst for efficient coupling. The Knoevenagel condensation of diethyl malonate with 5-HMF, for example will not give the product 5-(hydroxymethyl)furfural-2-diethyl malonate (5-HMFDEM) without a catalyst such as piperidine (Figure 4.2). The product 5-HFMDEM, an α,β-unsaturated furanic compound, has been identified as an important precursor for pharmaceuticals, chemicals for agriculture and cosmetics.[26–28]

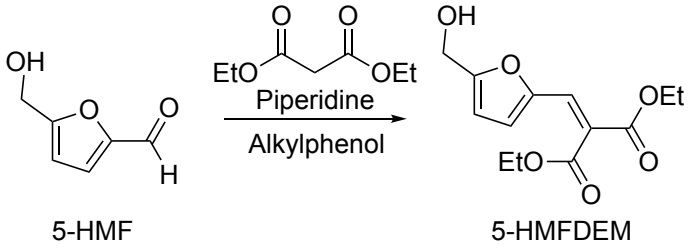

Figure 4.2: Base-catalyzed reaction between 5-HMF and diethylmalonate to form the Knoevenagel product 5-HMFDEM.

In Chapter 2 we showed that acid-base tandem catalytic deacetalization-Knoevenagel condensation can be run in PE systems and that PEs outperformed BS in the base-catalyzed Knoevenagel condensation reaction of benzaldehyde with malononitrile. In this Chapter we now extend this approach to the use of biobased substrates in tandem reactions that combine acid-catalyzed dehydration and (non-)catalytic Knoevenagel condensation. We report on a comparison of the efficiency of fructose dehydration in BS and PEs and of non-catalyzed and base-catalyzed Knoevenagel condensation reactions with 5-HMF to form 5-HMFMA and 5-HMFDEM, both, individually and coupled as (antagonistic) tandem catalytic reactions (Figure 4.3). While we show that antagonistic tandem catalytic conversion of biomass-derived building blocks is possible in PE, the results also demonstrate the added challenges of using more complex

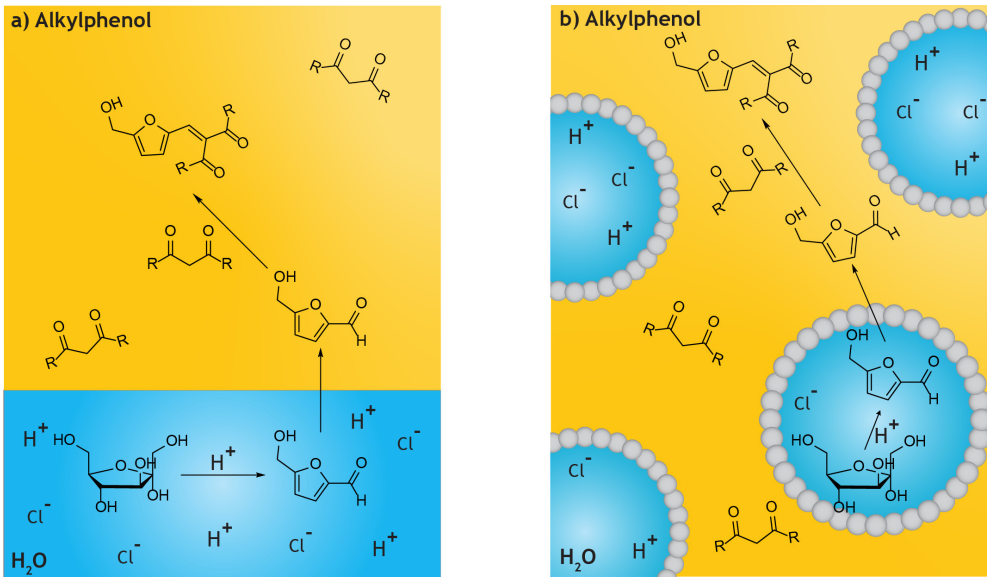

Figure 4.3: Tandem (catalytic) conversion of fructose to 5-HMF and 5-HMF derivatives in a) BS and b) PE.

substrates such as fructose and 5-HMF. For example, while the model deacetalization-Knoevenagel condensation reactions studied in Chapter 2 could be executed at room temperature, the reactions studied here require elevated temperatures (>80 °C), which impacts acid-base quenching by faster proton exchange,[29] and puts more strain on PE stability. The susceptibility of these substrates for side product formation still proved challenging, impacting lower yield, mass balance and product selectivity. Nevertheless, we further widen the window of application of PEs by showing that alkylphenol-formulated PEs are feasible reaction media for tandem catalytic biomass conversion.

4.2 Results and Discussion

4.2.1 Fructose to 5-HMF conversion and extraction

The three alkylphenols were previously shown to have a high extraction efficiency for 5-HMF, in both the high and low interfacial area systems (see Figure 3.16, Chapter 3). The high interfacial area systems showed 5-HMF extraction percentages of 84% to 100% at room temperature after 30 min, while in the low surface area systems much longer times are needed to reach the maximum extraction, *i.e.* after 1 h only 25% of the 5-HMF was extracted. To investigate the effect of this more rapid extraction on acid-catalyzed fructose dehydration, fructose conversion, 5-HMF yield, 5-HMF extraction to the organic phase and 5-HMF selectivity were followed over the course of 1 h in BS and PEs (Figure 4.4). A reaction time of 1 h was used, as the PEs were previously shown to be stable for at least this time at 100 °C, as shown in Chapter 3 (Figure 3.12).

The obtained fructose conversion profiles were similar for all three alkylphenol solvents. The higher fructose dehydration rate seen for PEs compared to BS is attributed to the higher extraction efficiency of PEs, pulling the reaction towards 5-HMF production. This resulted in a final conversion between 50 and 60% in the PEs and around 40% in the BS after 1 h. The higher 5-HMF yield in the PEs again reflect the excellent extraction abilities of the alkylphenol solvents in these systems with high interfacial area. Although the differences in conversion between the three alkylphenols are small, the yields differed considerably, with the highest 5-HMF yield being observed for the PE formulated with IPP (50%), while the yields in PG and SBP formulated PEs were 29 and 24%, respectively, after 1 h.

IPP and SBP were capable of extracting almost all formed 5-HMF out of the reactive aqueous phase in the PE (100% and 98% for IPP and SBP, respectively), showing that 5-HMF extraction is not limiting for this reaction. Again, PG showed to be a less efficient extracting solvent for 5-HMF of these three alkylphenol solvents, resulting in a final 5-HMF

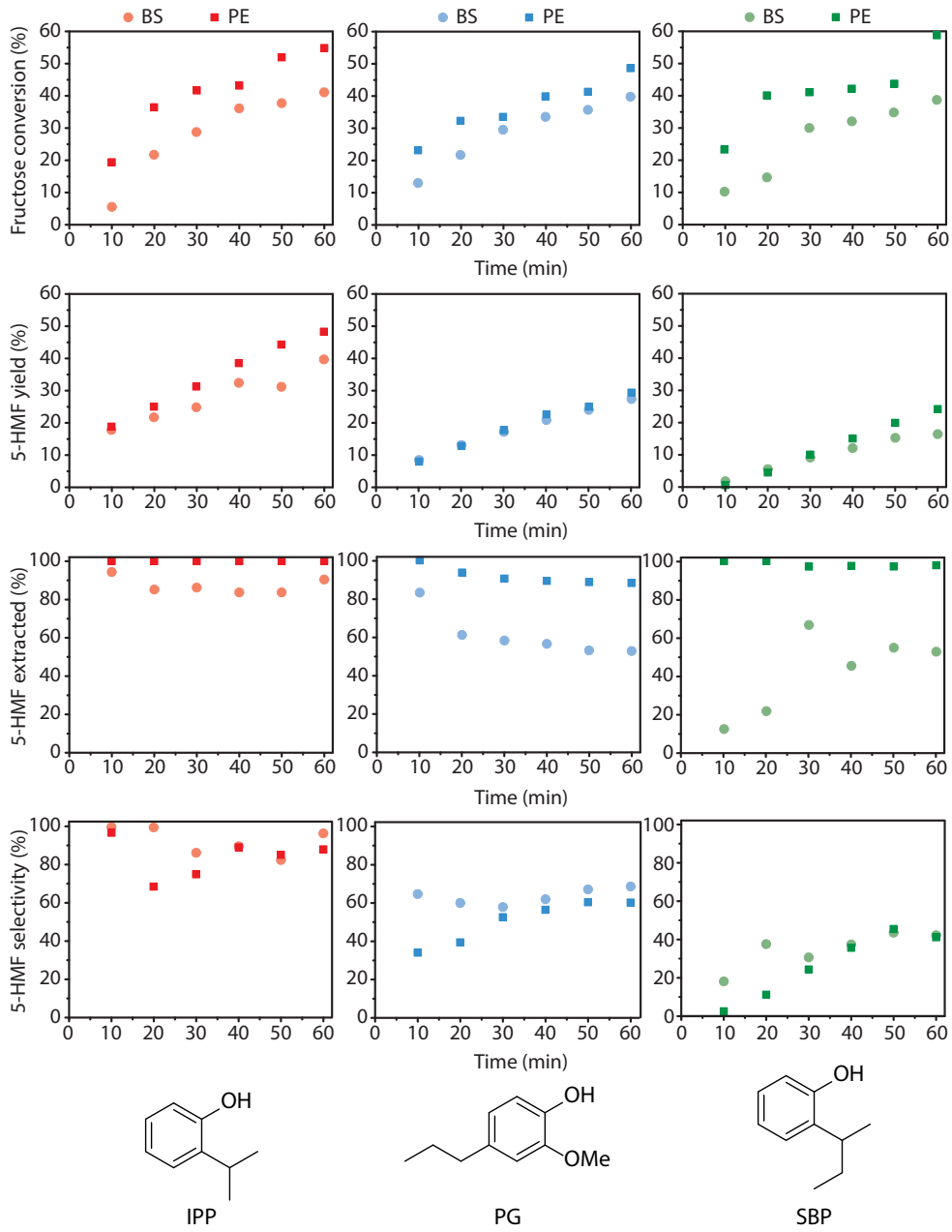

Figure 4.4: Conversion of fructose (top), yield of 5-HMF (second), percentage of extracted 5-HMF (third) and 5-HMF selectivity (bottom) followed over time in IPP (red), PG (blue) and SBP (green) in static biphasic systems (BS) and Pickering emulsions (PE). Reaction conditions: 6 mL alkylphenol solvent, 2 mL 0.1 M HCl sat. with NaCl, 1 mmol fructose, 100 °C, no stirring.

extraction of 88%. Nevertheless, the 5-HMF yield is the same in the PG formulated PE and BS, showing that 5-HMF is rather stable under these conditions for 1 h. The percentages of extracted 5-HMF are similar to those reported for the high interfacial area systems in Chapter 3 (i.e. 100% for IPP, 84% for PG and 91% for SBP, see Figure 3.16). Visual inspection of the reaction mixtures also showed the PE and BS system to behave differently. As highlighted in Figure 4.5, where the aqueous phases of the BS become yellow and orange over time while the aqueous phases of the PE stay transparent. All the colored components are extracted to the organic phase.

While higher conversions and a slightly enhanced 5-HMF yield were thus seen for the PEs, the presence of a larger interfacial area did not improve performance of the fructose dehydration in all ways anticipated. For example, the mass balances and 5-HMF selectivity are similar for both the BS and PE, suggesting that the amount of side product formation is not reduced. For both systems, selectivity was found to vary between the three alkylphenols, being lowest in the BS and PE formulated with SBP (approximately 35%), while the use of PG as organic phase gave a much higher selectivity of roughly 55%. The highest selectivity was obtained with IPP as organic phase, giving very high 5-HMF selectivities in the region of 85 to 95%. Such high selectivities, at even higher conversions (~94%), have been described before, but only for rather complex biphasic reaction media composed of water/DMSO mixtures as aqueous phase and MIBK/2-BuOH mixtures as organic phase.[30] Furthermore, at 75% 5-HMF extraction to the organic phase was only partial in these reported systems. As one of our aims is to eventually use the PE for tandem reactions, the alkylphenols thus proved very promising extractants.

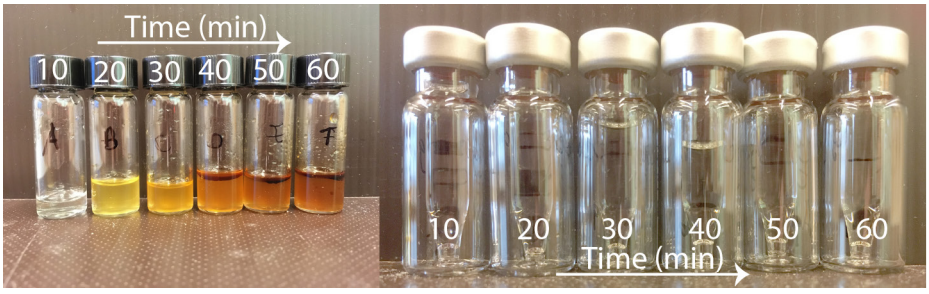

Figure 4.5: Appearance of aqueous phases of BS (left) and PEs (right) formulated with PG in the fructose dehydration reaction, samples taken after 10 to 60 min.

4.2.2 Tandem reactions starting from fructose

As a first step towards tandem reactions in PEs starting from carbohydrates, the Knoevenagel reaction of 5-HMF with Meldrum's acid was studied in a monophasic aqueous system. While the Knoevenagel condensation of 5-HMF with Meldrum's acid has

been reported at 75 °C with yields of around 75%, this temperature is not sufficient for the first fructose dehydration reaction targeted in the tandem conversion.[24] The tandem reaction was therefore run at 100 °C instead, for 2 h, a time frame for which the PEs have shown to be stable (see Chapter 3, Figure 3.12) Under the conditions applied, Meldrum's acid is supplied as a saturated aqueous solution, the product, 5-HMFMA is an oil and insoluble in water. The product distribution of the reaction mixture after 2 h is shown in Figure 4.6. In addition to 5-HMFMA, formic acid (FA) and levulinic acid (LA) were detected as side products. This in addition to humin formation, the extent of which could not be quantified by the GC or HLPC analysis methods used here. These humins are labeled as other and constitute the gap in the mass balance. Another side reaction that takes place and hampers the Knoevenagel condensation reaction, is the hydrolysis of Meldrum's acid to form malonic acid, a reaction that is already occurs at 75 °C. A practical coincidence hampering the quantification of the fructose conversion in the aqueous phase was the fact that malonic acid, a Meldrum's acid hydrolysis product[31], had the same retention time as fructose. To determine fructose conversions and the product distribution in the reactions starting from fructose the amount of malonic acid formed in the reactions starting from 5-HMF was subtracted from the fructose peak.

Starting from a single-phase, aqueous solution of 5-HMF at pH 7, 5-HMF conversion reached 90%. However, only 10% of 5-HMFMA was obtained resulting in a mass balance gap of 80%, which was attributed to humin formation. The low 5-HMFMA yield can be caused by the hydrolysis of Meldrum's acid as evidenced by the substantial formation of malonic acid (40% of the starting amount of Meldrum's acid). Using an acidic aqueous phase led to a 5-HMFMA yield of 21% at 88% 5-HMF conversion, and some formation of formic acid was observed. No 5-HMFMA was observed at all when fructose was used as starting compound. The low fructose conversion (36%) and 5-HMF yield (14%), are in accordance with the single, monophasic, fructose dehydration reaction, which showed

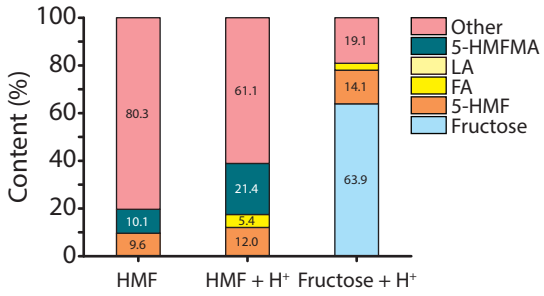

Figure 4.6: Content of reaction mixtures after reaction with Meldrum's acid starting from 5-HMF without and with acid (left and middle, respectively) and fructose (right) in a monophasic aqueous system. Reaction conditions: 2 mL 0.1 HCl or Milli-Q water sat. with NaCl, 1 mmol substrate, 2 mmol Meldrum's acid, 100 °C, 2 h, no stirring.

42% conversion and 20% yield. The low amount of 5-HMF formed in the reaction system, greatly limits the already poor subsequent Knoevenagel reaction.

BS were then tested by addition of one of the alkylphenols to an acidic aqueous phase containing either fructose or 5-HMF. To study the influence of the interfacial area on the (dehydration)-Knoevenagel condensation, three different systems where tested; static BS, stirred BS and static PEs (Figure 4.7).

The single step, noncatalytic Knoevenagel reaction between 5-HMF and Meldrum's acid in static BS did not lead to a big improvement, giving 5-HMFMA yields between 7 and 14% (Figure 4.7a). Apparently, the rate of 5-HMF extraction is lower than the rate of acid-catalyzed dehydration and polymerization which lead to poor performing systems, which is contradictive to what was observed for the single fructose dehydration reaction. Additionally, an average malonic acid yield of 40% was observed in the three static BS, reducing the amount of Meldrum's acid from a two-fold excess to almost stoichiometric amounts, diminishing the rate of the condensation reaction. Even though Meldrum's acid was fully soluble in IPP, this did not positively influence the 5-HMFMA yield.

Increasing the interfacial area by stirring the two phases led to an increase of the formation of 5-HMFMA, up to 22% in PG. As shown before in Chapter 3 (Figure 3.16), increasing the interfacial area enhances the 5-HMF extraction to the organic phase. The use of PEs rather than stirred BS gave lower product yields ranging from 8 and 14%, with the SBP formulated PE giving the highest yield and smallest extent of hydrolysis of Meldrum's acid. While 5-HMFMA formation did not improve, increasing the interfacial area did lead to a decrease of humin formation, due to more efficient 5-HMF extraction.

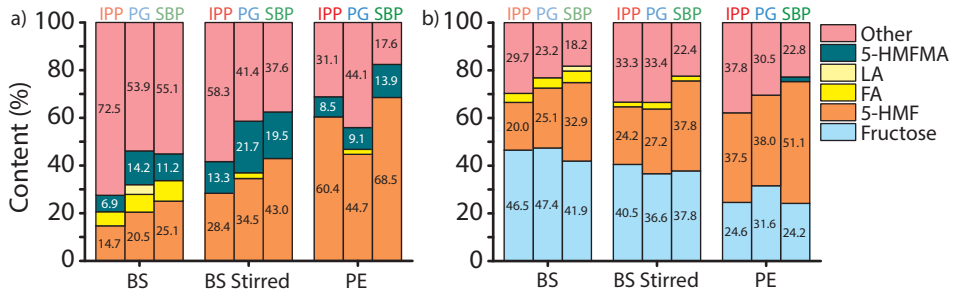

Figure 4.7: Content of reaction mixtures in BS, stirred BS and PEs containing IPP, PG or SBP as organic phase after the 5-HMF (a) and fructose (b) to 5-HMFMA reaction. Reaction conditions: 6 mL alkylphenol solvent, 2 mL 0.1 M aqueous HCl sat. with NaCl, 1 mmol substrate, 2 mmol Meldrum's acid, 100 °C, 2 h, stirring 750 rpm, PE: 2 wt% hydrophobic silica.

For the reactions starting from fructose (Figure 4.7b), no 5-HMFMA was observed at all except for the reaction in the PE formulated with SBP, in which just 2% of 5-HMFMA was detected. In the static and stirred biphasic reactions fructose conversions between 55 and 65% were obtained, resulting in 5-HMF yields between 20 and 38%. In the PEs, fructose conversions of 70 to 75% and 5-HMF yields of 38 to 51% were reached. At these extended reaction times of 2 h, lower 5-HMF selectivities were observed than during the kinetic experiments described above, evidence of enhanced side-product formation. The SBP formulated PE showed the lowest Meldrum's acid hydrolysis when compared to the IPP and PG PEs. In this system the highest 5-HMF yield (51%) was obtained as well, resulting in some 5-HMFMA formation.

An important factor inhibiting the performance of the Knoevenagel condensation of 5-HMF with Meldrum's acid is its acid-catalyzed hydrolysis, limiting the effect of using a twofold excess. Given that this Knoevenagel condensation reaction is non-catalytic few other means are left to influence the sluggish reactivity. A base-catalyzed Knoevenagel condensation step, such as those required for less active substrates such as diethyl malonate, could then offer more options to tune the rate of the second step in the targeted tandem reaction.

The base-catalyzed reaction between 5-HMF and diethyl malonate can be executed at 80 °C under neat conditions, according to literature.[27] As in our strategy the base-catalyzed Knoevenagel condensation reaction takes place in the continuous, organic, phase of the PE, the acid and base catalysts should be compartmentalized in the aqueous and organic phase, respectively (Figure 4.3). The tandem reaction with Meldrum's acid showed that accumulation of 5-HMF in the organic phase is necessary to obtain proper product yields. A strategy to reduce acid/base quenching and increase the 5-HMF concentration in the PE, in addition to the high salt concentrations used, could be to postpone addition of the base catalyst and the diethyl malonate. The kinetic traces of the fructose dehydration reaction, shown in Figure 4.4, indicated that a reasonable amount of 5-HMF is formed in the PEs after 1 h at 100 °C. Therefore, PEs containing just the acid catalyst and fructose were first left for 1 h at 100 °C, to accumulate the 5-HMF, after which the base catalyst and diethyl malonate were added and the reaction mixture was put at 80 °C for 1 h (Figure 4.8a) for 24 h (Figure 4.8b). Both BS and PEs were used with all three alkylphenol solvents to investigate the effect of 5-HMF extraction on the performance of the tandem reaction.

The reactions performed in the BS for 1 h at 100 °C followed by 1 h at 80 °C, resulted in similar fructose conversions for all three alkylphenols (~40%), in agreement with the kinetic results shown in Figure 4.4. However, no 5-HMFDEM was observed in these reaction mixtures at all. The PEs that were subjected to the same reaction conditions did

show some 5-HMFDEM formation, up to 5%, with IPP being at the upper end of the range, in line with its better 5-HMF extraction efficiency. Fructose conversion was higher with PG and SBP based PE, however.

The reaction time of the 80 °C step was increased to 24 h to see if yields could be improved. For the BS, no effect was observed, as similar fructose conversions and 5-HMF yields were obtained and again no 5-HMFDEM was present. Apparently, complete acid-base quenching occurs in these systems under these conditions and the BS were not further studied.

With the IPP and PG formulated PEs, elongation of the reaction time proved beneficial for performance of the tandem reaction. Both PEs showed 5-HMFDEM yields of approximately 16% while the fructose conversion also increased from 45% to 65% for IPP and from 58% to 70% for the reaction in PG. This decreasing fructose content shows that addition of base does not completely quench the acid catalyst in these PEs as this reaction proceeds in the 24 h at 80 °C. The reaction in the PG formulated PE showed less side products after the 24 h reaction compared to the 1 h reaction. This could indicate that, besides (irreversible) humin formation, part of the missing mass balance can be attributed to reaction intermediates.

The tandem catalytic experiments did show some 5-HMFDEM formation; however, the yields were clearly not optimal. To investigate whether the Knoevenagel condensation reaction of 5-HMF with diethyl malonate could be efficiently executed in PEs, with both acid and base catalysts present, this reaction was tested individually with different acid and base concentrations (Figure 4.9a). These reactions were performed at 80 °C for 32 h based on a literature procedure reporting the condensation between 5-HMF and diethyl

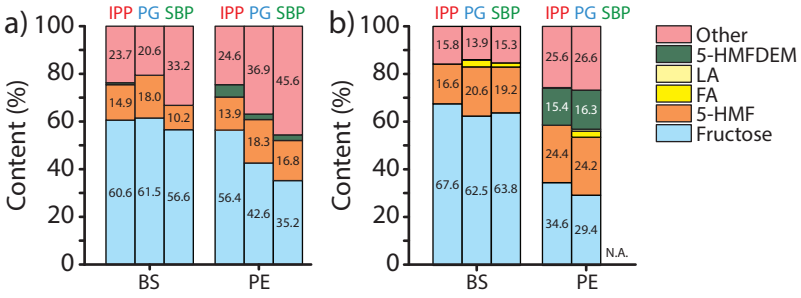

Figure 4.8: Content of reaction mixtures after fructose to 5-HMFDEM reaction in BS and PEs, base and diethyl malonate were added after 1 h reaction at 100 °C and reaction was proceeded at 80 °C for a) 1 h or b) 24 h. Reaction conditions: 6 mL alkylphenol solvent, 2 mL 0.1 M HCl sat. with NaCl, 1 mmol fructose, 2.5 mmol diethyl malonate, 20 mol% acid, 20 mol% base, 1 h 100 °C, 1 or 24 h 80 °C, BS: stirring 750 rpm, PE: 2 wt% silica.

malonate reaction under neat conditions.[27] Screening of acid and base concentrations was done with the most promising alkylphenol, PG.

As expected, an excess of base led to higher 5-HMFDEM yields than when an excess acid or equimolar amounts of acid and base were used. The highest 5-HMFDEM yield of 60% was obtained with 20 mol% acid and 50 mol% base, slightly lower than reported for the neat reaction in which a yield of 77% was obtained.[27] However, these conditions are not realistic for the tandem reaction as they would not allow for the fructose dehydration reaction to be performed. In Chapter 2, we showed that the antagonistic tandem catalytic reaction performed best using equimolar amounts of acid and base catalysts.[32] The reactions with 20 mol% of both catalysts and the reaction with 50 mol% of both catalysts gave similar 5-HMFDEM yields (approximately 42%), but the reaction with 20 mol% of both catalysts gave less side products. The same conditions were applied to PEs formulated with IPP and SBP (Figure 4.9b) showing similar 5-HMFDEM yields as in PG (~40%) at higher 5-HMF conversions and thus more side product formation. Nevertheless, these results show that the Knoevenagel condensation reaction can be performed with satisfactory yields in these PEs with both acid and base catalysts present.

Building on the insights obtained above, the tandem catalytic reaction was now performed in PEs formulated with PG at 80 °C and reaction times between 8 and 48 h, as shown in Figure 4.10. While fructose conversion did not change much anymore after 24 h of reaction time, the 5-HMF yield did increase up to 40 h, indicating that some of the undetected products collected under 'other' must be reaction intermediates from the fructose dehydration

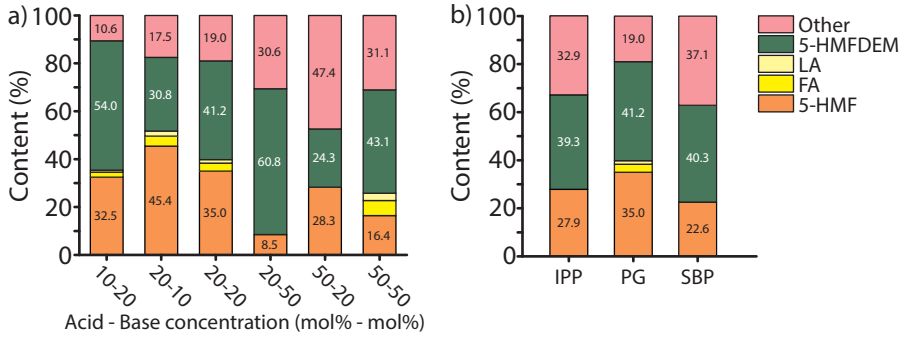

Figure 4.9: a) Content of PEs after 5-HMF to 5-HMFDEM reaction using various acid and base concentrations. Reaction conditions: 6 mL PG, 2wt% silica, 2 mL aqueous HCl, sat. with NaCl, 1 mmol 5-HMF, 2.5 mmol diethylmalonate, 80 °C, 32 h. b) Content of PEs formulated with IPP, PG or SBP after 5-HMF to 5-HMFDEM reaction using 20 mol% acid and 20 mol% base. Reaction conditions: 6 mL alkylphenol solvent, 2 wt% silica, 2 mL 0.2 M HCl sat. with NaCl. 1 mmol 5-HMF, 2.5 mmol diethylmalonate, 0.2 mmol piperidine, 80 °C, 32 h.

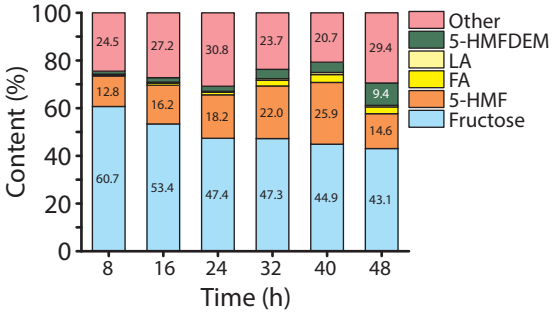

Figure 4.10: Content of PEs after the fructose to 5-HMFDEM tandem catalytic reaction at various reaction times using 20 mol% acid – 20 mol% base. Reaction conditions: 6 mL PG, 2wt% silica, 2 mL H_2O, sat. with NaCl, 1 mmol fructose, 2.5 mmol diethylmalonate, 80 °C.

reaction on way to 5-HMF. Although in modest amounts, 5-HMFDEM is formed already after 8 h of reaction. After 40 h the yield of the 5-HMF intermediate decreased, resulting in the increasing yield of final product, 5-HMFDEM. That the product distribution changes even after 48 h highlights that PEs are actually capable of compartmentalizing (part of) the antagonistic catalysts. However, the maximum 5-HMFDEM yield of 9% after 48 h of reaction is still rather low, for which we consider the relatively low 5-HMF concentrations in the reaction system are to blame. To increase the product yield and obtain a more reactive system, a different approach is required.

To increase the 5-HMF concentration in the PEs, we went back to the first strategy of postponing base and diethyl malonate addition. However, this time the reaction was started at 80 °C in attempt to decrease side product formation and base and diethyl malonate were added after 1, 2, 3, 4, 5, 6 or 24 h, whereafter the reaction was allowed to proceed for a total reaction time of 32 h (Figure 4.11). Such postponed addition of base and diethyl malonate indeed led to an increase of 5-HMFDEM yield, which strongly depended on the time of addition. Remarkably, fructose conversions and 5-HMF yields did not change between 1 and 6 h reaction before base and diethyl malonate addition. Extending the reaction much longer, for 24 h, resulted in an increase of the fructose conversion from 65 to 80%. This reaction showed the highest 5-HMFDEM content as well, 24%, even though this reaction had only 8 h for the base-catalyzed step. This is again indicative of the need for sufficiently high 5-HMF concentrations for the Knoevenagel condensation to proceed efficiently and, consequently, for the tandem catalytic reaction to run successfully.

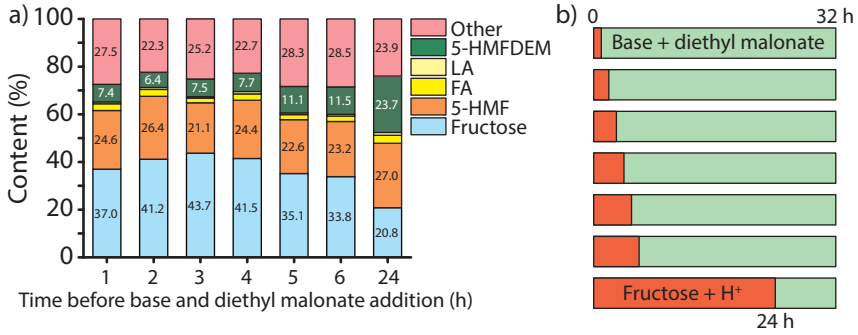

Figure 4.11: a) Content of PEs after fructose to 5-HMFDEM reaction with base and diethyl malonate addition after time indicated at x-axis, total reaction time of 32 h as schematically shown in b). Reaction conditions: 6 mL PG, 2wt% silica, 2 mL H_2O, sat. with NaCl, 1 mmol fructose, 2.5 mmol diethylmalonate, 20 mol% acid – 20 mol% base, 80 °C.

4.3 Conclusions

In this study we investigated the performance of alkylphenol-formulated biphasic reaction media for (tandem) reactions starting from fructose. The acid-catalyzed fructose dehydration reaction to 5-HMF was studied using IPP, PG and SBP as organic solvents in static BS and PEs, where PEs outperformed the BS in fructose conversion and 5-HMF extraction. Of the three alkylphenol solvents, IPP proved most suitable for this reaction, giving complete 5-HMF extraction and excellent 5-HMF selectivity (~90%) at a 5-HMF yield of 48%.

This high 5-HMF selectivity and 5-HMF extraction offered the opportunity to explore PEs as reaction media for tandem catalytic reactions over a wider window of process conditions. First, the non-catalytic Knoevenagel reaction between 5-HMF and Meldrum's acid proved not to work in either static and stirred BS and in PEs. The acid-catalyzed hydrolysis of Meldrum's acid to malonic acid was identified of one of the major factors inhibiting the performance of the tandem reaction. An antagonistic catalytic tandem dehydration-Knoevenagel condensation reaction did give the desired product, albeit in rather modest yield. As these reactions were performed at elevated temperatures, the extent of acid-base quenching proved more detrimental for the BS than for the PEs, with product only forming in the latter. Optimization studies showed that the sluggish, second Knoevenagel condensation required sufficiently high 5-HMF in the oil phase, which could be achieved by a delayed addition approach.

Although, the PEs formulated with alkylphenol solvents do appear promising for tandem catalytic reactions starting from fructose, e.g. because of the high 5-HMF selectivities,

quite some issues such as low intermediate concentration, substrate degradation or catalyst quenching do hamper overall efficiency. To utilize these PEs to their full potential further studies on substrate scope, reaction types and reaction conditions are therefore still needed.

4.4 Experimental procedures

4.4.1 Chemicals

All chemicals were used as received without any further purification. AEROSIL® 200 silica powder was purchased from Evonik Industries. Toluene was purchased from Interchema. Hydrochloric acid (HCl, 37%, analytical grade), chloro(trimethyl)silane (TMSCl, ≥ 98%), 2-*iso*propylphenol (IPP, 98%), 4-propylguaiacol (PG, ≥ 99%, food grade), 2-*sec*-butylphenol (SBP, 98%) and 5-(hydroxymethyl)furfural (5-HMF, ≥ 99%) were purchased from Sigma-Aldrich. Anisole (99%) and Citric acid (99.5%) were obtained from Acros Organics. D-fructose (99%) was purchased from Alfa Aesar. Sodium chloride (NaCl) was obtained from Merck.

4.4.2 Hydrophobization of silica

Silylated silica was prepared from an adapted procedure reported in literature.[33] A solution of TMSCl in toluene (10 wt%; V_T = 10 mL) was added to 1 g of silica powder AEROSIL® 200. The mixture was stirred for 2 h under reflux. The resulting silylated silica particles were filtered, washed twice with toluene and dried in air overnight, to give particles with a specific surface area of 174 m2·g-1.

4.4.3 Pickering emulsion preparation

All PEs were prepared by first dispersing a known mass of silylated silica particles into 6 mL of alkylphenol solvent (IPP, PG or SBP) using a VCX 130 Vibra-Cell Ultrasonic Processor equipped with a 3 mm diameter tip (Sonics, 20 kHz, 10 W, 2 min). During sonication, it was necessary to cool the vessel in an ice-bath. After the addition of 2 mL aqueous phase with appropriate NaCl concentration and required pH to the alkylphenol phase, the resulting mixture was emulsified using a UltraTurrax T25 homogenizer with a S25N-10G dispersing tool (IKA, 15200 rpm, 2 min).

4.4.4 Fructose to 5-HMF kinetics

15 mL Ace pressure tubes were loaded with 6 mL alkylphenol solvent and 2 mL of 0.1

M HCl in Milli-Q water saturated with NaCl containing 0.5 M fructose. For the reactions in PEs 2 wt% hydrophobized silica particles were added. The reactions were executed at 100 °C without stirring and stopped by putting in an ice bath after 10, 20, 30, 40, 50 and 60 min, respectively. The PEs were destabilized by centrifugation using a Rotina 38-R Hettich centrifuge (7500 rpm, 15 °C, 10 min) and samples from the organic and aqueous phase were taken for GC and HPLC analysis, respectively. HPLC analysis was performed on a Shimadzu HPLC system equipped with a Bio-Rad Aminex HPX-87H column, and a differential refractometer using citric acid as internal standard.

Conversions were defined as:

$$Conversion\ (\%) = \left(1 - \frac{m_{Fructose\ at\ t=x}}{m_{Fructose\ at\ t=0}}\right) \times 100 \tag{4.2}$$

5-HMF yields were defined as:

$$Yield\ (\%) = \frac{m_{5-HMF(org)\ at\ t=x} + m_{5-HMF(aq)\ at\ t=x}}{m_{Fructose\ at\ t=0}} \times 100 \tag{4.3}$$

5-HMF extractions were defined as:

$$extraction\ (\%) = \frac{m_{5-HMF(org)}}{m_{5-HMF(org)} + m_{5-HMF(aq)}} \times 100 \tag{4.4}$$

with $m_{fructose}$ is the amount of fructose in moles, $m_{5\text{-}HMF(org)}$ is the amount of 5-HMF in the organic phase in moles and $m_{5\text{-}HMF(aq)}$ is the amount of 5-HMF in the aqueous phase in moles.

4.4.5 5-HMFMA synthesis

5-HMF (500 mg, 4 mmol) and Meldrum's acid (600 mg, 4.1 mmol) were mixed with 10 mL Milli-Q water in a 25 mL round bottom flask. The mixture was heated for 2 h at 75 °C under stirring at 300 rpm. After cooling to room temperature chloroform was added to the reaction mixture, which was then washed 3 times with water in a separation funnel. Evaporation of the chloroform resulted in pure 5-HMFMA (>99% according to ^{1}H-NMR, data in line with [24]) as an brown/orange oil (150 mg, 16%).

4.4.6 5-HMFDEM synthesis

5-HMF (1 g, 7.9 mmol), diethyl malonate (2.5 mL, 16.4 mmol) and ethylene diamine (3 drops) were added to 20 mL of ethyl acetate and refluxed for 24 h. The mixture was cooled to room temperature and washed with a sulfuric acid solution. The organic phase was dried over Na_2SO_4, filtered and the solvent was removed by rotary evaporation. Purification was

done by column chromatography (Ethyl acetate : Petroleum ether 1:1) to give 5-HMFDEM (^{1}H-NMR data in line with [28]) as an brown/red oil (600 mg, 30%). This product was used for calibration of the GC.

4.4.7 Catalytic experiments

15 mL Ace pressure tubes were loaded with 6 mL alkylphenol solvent and 2 mL aqueous phase (0, 0.1, 0.2 or 0.5 M HCl in Milli-Q water saturated with NaCl) and 1 mmol of substrate (fructose or 5-HMF). For PE reactions 2 wt% of hydrophobized silica particles were used for stabilization. After preparation of the BS or PE, Meldrum's acid or diethyl malonate and base (0, 0.1, 0.2 or 0.5 mmol) were added. The reactions were left unstirred at 80 or 100 °C for a certain amount of time. PEs were destabilized by centrifugation as described before and analysis was performed by GC and HPLC.

Acknowledgements

Dr. Fuqiang Chang (Organic Chemistry and Catalysis, Utrecht University) is acknowledged for performing the solubility experiments of Meldrum's acid in the alkylphenols.

References

1 D. M. Alonso, J. Q. Bond and J. A. Dumesic, *Green Chem.*, **2010**, *12*, 1493.
2 C. E. Wyman, B. E. Dale, R. T. Elander, M. Holtzapple, M. R. Ladisch and Y. Y. Lee, *Bioresour. Technol.*, **2005**, *96*, 2026.
3 R. Van Putten, J. C. Van Der Waal, E. De Jong, C. B. Rasrendra, H. J. Heeres and J. G. De Vries, *Chem. Rev.*, **2013**, *113*, 1499.
4 K. I. Seri, Y. Inoue and H. Ishida, *Bull. Chem. Soc. Jpn.*, **2001**, *74*, 1145.
5 A. Chareonlimkun, V. Champreda, A. Shotipruk and N. Laosiripojana, *Bioresour. Technol.*, **2010**, *101*, 4179.
6 Y. Li, X. Lu, L. Yuan and X. Liu, *Biomass and Bioenergy*, **2009**, *33*, 1182.
7 F. S. Asghari and H. Yoshida, Carbohydr. Res., 2006, 341, 2379.
8 I. van Zandvoort, Y. Wang, C. B. Rasrendra, E. R. H. van Eck, P. C. A. Bruijnincx, H. J. Heeres, B. M. Weckhuysen, *ChemSusChem*, **2013**, *6*, 1745.
9 I. Van Zandvoort, E. R. H. Van Eck, P. De Peinder, H. J. Heeres, P. C. A. Bruijnincx, B. M. Weckhuysen, *ACS Sustain. Chem. Eng.*, **2015**, *3*, 533.
10 B. Saha and M. M. Abu-Omar, *Green Chem.*, **2014**, *16*, 24.
11 Y. Román-Leshkov, C. J. Barrett, Z. Y. Liu and J. A. Dumesic, *Nature*, **2007**, *447*, 982.
12 Y. Román-Leshkov and J. A. Dumesic, *Top. Catal.*, **2009**, *52*, 297.
13 J. M. R. Gallo, D. M. Alonso, M. A. Mellmer and J. A. Dumesic, *Green Chem.*, **2013**,

15, 85.
14 L. C. Blumenthal, C. M. Jens, J. Ulbrich, F. Schwering, V. Langrehr, T. Turek, U. Kunz, K. Leonhard and R. Palkovits, *ACS Sustain. Chem. Eng.*, **2016**, *4*, 228.
15 D. M. Alonso, S. G. Wettstein, J. Q. Bond, T. W. Root and J. A. Dumesic, *ChemSusChem*, **2011**, *4*, 1078.
16 E. I. Gürbüz, S. G. Wettstein and J. A. Dumesic, *ChemSusChem*, **2012**, *5*, 383.
17 P. Azadi, R. Carrasquillo-Flores, Y. J. Pagán-Torres, E. I. Gürbüz, R. Farnood and J. A. Dumesic, *Green Chem.*, **2012**, *14*, 1573.
18 Y. J. Pagán-Torres, T. Wang, J. M. R. Gallo, B. H. Shanks and J. A. Dumesic, *ACS Catal.*, **2012**, *2*, 930.
19 A. A. Rosatella, S. P. Simeonov, R. F. M. Frade and C. A. M. Afonso, *Green Chem.*, **2011**, *13*, 754.
20 M. R. Grochowski, W. Yang and A. Sen, *Chem. - A Eur. J.*, **2012**, *18*, 12363.
21 A. Brandolese, D. Ragno, G. Di Carmine, T. Bernardi, O. Bortolini, P. P. Giovannini, O. G. Pandoli, A. Altomare and A. Massi, *Org. Biomol. Chem.*, **2018**, *16*, 8955.
22 M. Sajid, X. Zhao and D. Liu, *Green Chem.*, **2018**, *20*, 5427.
23 S. Helmy, F. A. Leibfarth, S. Oh, J. E. Poelma, C. J. Hawker and J. R. De Alaniz, *J. Am. Chem. Soc.*, **2014**, *136*, 8169.
24 R. F. A. Gomes, Y. N. Mitrev, S. P. Simeonov and C. A. M. Afonso, *ChemSusChem*, **2018**, *11*, 1612.
25 M. M. Lerch, W. Szymański and B. L. Feringa, *Chem. Soc. Rev.*, **2018**, *47*, 1910.
26 US 8236972 B2, **2012**.
27 WO 2018/236218, **2018**.
28 J. Van Schijndel, L. A. Canalle, D. Molendijk and J. Meuldijk, *Synlett*, **2018**, *29*, 1983.
29 D. Mammoli, N. Salvi, J. Milani, R. Buratto, A. Bornet, A. A. Sehgal, E. Canet, P. Pelupessy, D. Carnevale, S. Jannin and G. Bodenhausen, *Phys. Chem. Chem. Phys.*, **2015**, *17*, 26819.
30 J. N. Chheda, Y. Roman-Leshkov and J. A. Dumesic, *Green Chem.*, **2007**, *9*, 342.
31 A. N. Meldrum, *J. Chem. Soc., Trans.*, **1908**, *93*, 598.
32 C. M. Vis, L. C. J. Smulders and P. C. A. Bruijnincx, *ChemSusChem*, **2019**, *12*, 2176.
33 M. C. Capel-Sanchez, L. Barrio, J. M. Campos-Martin and J. L. G. Fierro, *J. Colloid Interface Sci.*, **2004**, *277*, 146.

Chapter 5

Pickering Emulsion Catalysis with Mono- and Bifunctional Catalyst Particles

Pickering emulsions (PEs) have shown great potential as biphasic medium for catalysis, e.g. for application in acid-base tandem catalysis. To physically compartmentalize the antagonistic catalysts over the two phases of the PE and to avoid quenching, we immobilized the acid and base onto one or both of the two exposed faces of solid stabilizing particles to create monofunctional and bifunctional PE emulsifiers. Monodisperse Stöber-type spherical silica particles (450 nm) were synthesized, hydrophobized to ensure proper wetting and PE stabilization and finally functionalized with either sulfonic acid or amine groups to make acidic or basic particles, or, for the first time, both. For the latter, acid-base Janus particles, bearing both acid and base catalyst on one particle at different loadings, were synthesized through an etching and sulfonic acid grafting approach using wax/water colloidosomes of the amine-functionalized particles. The catalytic PE emulsifiers were used in the tandem dehydration-Knoevenagel condensation of fructose in water/4-propylguaiacol, with addition of the complementary homogeneous acid or base in case of the monofunctional materials. The mono-functional acid particles were poorly active, giving no 5-HMFDEM. The use of free amine-decorated particles resulted in acid-base quenching during PE preparation, but BOC-protected, in-situ activated amine particles did show some activity in the tandem reaction, yielding 11.1% 5-HMFDEM at 79% fructose conversion after 6 h reaction at 100 °C. Incomplete deprotection of the BOC-amine precluded more efficient conversion of the intermediate 5-HMF, which was the major product at 53.2%. The Janus particles performed best, yielding 5-HMFDEM in 17.3% after 24 h at 100 °C at 54.3% conversion. Acid loading proved important with higher acid concentration leading to an increase in conversion but at the expense of increased side product formation and not 5-HMFDEM yield. The use of mono- and bifunctional particles for antagonistic tandem reactions of fructose in PEs is thus shown to be feasible and promising, but further optimization, e.g. of the optimal balance between acid and base catalysts, is needed.

Based on: F.C. Chang*, C.M. Vis*, P.C.A. Bruijnincx, Bi-functional Janus Silica Spheres for Pickering Interfacial Tandem Catalysis, In preparation
* *These authors contributed equally*

5.1 Introduction

Biphasic oil/water systems have been extensively investigated for catalytic reactions, e.g. in biorefining.[1] Despite their extensive application, a general drawback of these systems is the low reaction efficiency due to the limited interfacial area. The interfacial area can be increased by emulsification of two the immiscible phases.[2] Solid particle-stabilized emulsions, so-called Pickering emulsions (PEs), are of particular interest as the solid particle emulsifiers provide superior stability, i.e. over a large temperature and composition window, and can be endowed with stimuli-responsiveness, something that classical surfactants cannot.[3] Moreover, the solid boundary layer in PEs serves to compartmentalize and protect the dispersed phase from the continuous phase, for example, allowing multiple reactions mediated by (antagonistic) catalysts to be conducted consequtively.[4–6]

Most research focusing on using PEs for catalysis make use of homogeneous catalysts, which was also the strategy in Chapters 2-4 of this PhD Thesis.[4] As shown in Chapter 2, for example, PE catalysis allowed for the antagonistic deacetalization-Knoevenagel condensation reaction in a PE at room temperature without (complete) catalyst quenching. However, reactions run at more elevated temperatures (100 °C), such as the dehydration-Knoevenagel condensation reaction of fructose (Chapter 4), do suffer from prohibitive acid-base quenching. A way to cope with this problem and make the system more robust would be to use heterogeneous catalyst particles that also operate as PE stabilizer. Using this method, the catalyst moieties are immersed in the liquids but cannot be removed from the surface, potentially resulting in less quenching. Another reason to use heterogeneous catalyst particles is the facile catalyst recycling as after reaction the PE can be destabilized, the catalytic particles recovered by centrifugation can be reused in a new PE.

The antagonistic tandem catalytic reactions discussed in the previous chapters, make use of differences in polarity of the substrate and products. In the dehydration-Knoevenagel condensation reaction of fructose, the fructose is soluble in the aqueous phase of the PE, where it is converted with the acid catalyst to 5-(hydroxymethyl)furfural (5-HMF). Generally, this dehydration reaction suffers from low yields and selectivities as 5-HMF can react further to form small organic acids or large insoluble polymers, so-called humins.[7] This side product formation can be reduced by extracting 5-HMF to the organic phase, where, with addition of a base catalyst and diethyl malonate, it can be converted in a Knoevenagel condensation reaction. The product of this tandem reaction, 5-(hydroxymethyl)furfural-2-diethyl malonate (5-HMFDEM), then ultimately resides in the organic phase. When using heterogeneous catalyst particles for this tandem reaction in PE, the catalyst should be available in the proper liquid phase, i.e. the acid in the aqueous

and the base in the organic phase.

In principle, the use of catalytically active solid emulsifiers for antagonistic tandem catalytic reaction in PEs can involve either mono- or bifunctional particles. Monofunctional particles, in this particular case covered with either acid or base functional groups, can then either be used separately, with the opposing catalyst being added as homogeneous version to the aqueous (acid) or organic (base) phase of the PE (Figure 5.1a and b respectively). Full heterogenization could be achieved by using a physical mixture (Figure 5.1c) or by having one bifunctional solid emulsifier (Figure 5.1d). The mixing of these particles in the former strategy would make them very susceptible to quenching, however.[8,9] Several types of bifunctional catalytic particles have been used for the execution of antagonistic tandem catalysis in reaction media other than PEs, using for example core-shell particles[10,11], porous silica or carbon materials grafted with acid and base functionalities[12,13] or crosslinked polymers with acid and base functional groups.[14] All these types of particles rely on the same strategy, i.e. to have the acid and base functionalities in close enough proximity to allow for improved tandem catalysis, but not quenching. In our PE strategy we aim to use so-called Janus particles as emulsifiers to specifically locate the acid and base functionalities into the two distinct liquid phases (Figure 5.1d). In addition to thus offering control over catalyst location, the Janus particles also offer great advantages in terms of PE stabilization itself, given that heir intrinsically distinct surface wettability makes them extremely efficient interfacial stabilizers.[15]

Recent studies strongly suggest that the geometry as well as the surface properties of Janus particles have a significant influence on their surface activity.[16] To date, Janus particles shaped as spheres[17,18] and nanosheets[19,20] have been reported for the successful stabilization of PEs. Janus spheres are ideal for designing interface-active solid catalysts, as the equilibrium orientation of the Janus boundary tends to get pinned at the oil-water interface when the apolar and polar hemispheres are exposed to the oil and water phases, respectively (Figure 5.1e).[21,22] By placing catalytically active groups on either the polar or the apolar hemisphere, the interfacial configuration of the Janus spheres can be precisely controlled, and thereby, the catalytic activity in a biphasic reaction system.[23–25] However, available examples of Janus spheres use in PE applications are mostly limited to mono-catalytic materials bearing metal nanoparticle functionalities, with the Janus nature improving stability and with the single patch decoration reducing the amount of metal nanoparticles required. Synthesizing Janus particles with antagonistic catalyst patches and to endow opposite wettability on different patches of the Janus spheres is still a major challenge and no examples of this are, to the best of our knowledge, currently available.

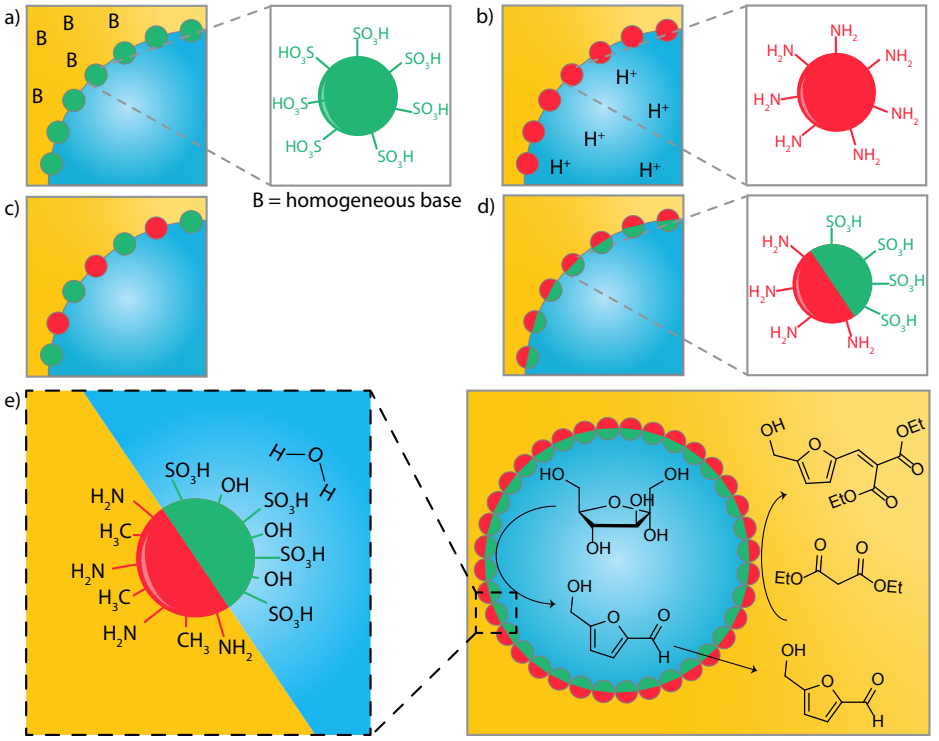

Figure 5.1: Heterogeneous catalytic approaches for antagonistic tandem catalysis in PEs using monofunctional (a-c) and bifunctional (d and e) catalyst particles. Blue: water droplet, yellow: continuous organic phase. a) PE stabilized by acid functionalized particles with homogeneous base in organic phase, b) PE stabilized by base functionalized particles with homogeneous acid in aqueous phase, c) PE stabilized by physical mixture of acid- and base-functionalized particles, d) acid and base bifunctional Janus particles, e) left: bifunctional Janus particles pinned at the oil-water interface due to polar and apolar sides. Polar hemisphere is functionalized with acid catalyst and apolar hemisphere is functionalized with base catalyst. Right: dehydration-Knoevenagel condensation reaction of fructose catalyzed by antagonistic Janus particles in PE.

In this PhD Thesis Chapter, we develop a strategy for bifunctional Janus PE emulsifiers and compare their application as heterogeneous catalyst particles in the acid-base tandem catalytic dehydration-Knoevenagel condensation of fructose with their monofunctional counterparts. Monodisperse silica particles of 450 nm, synthesized via the Stöber method, were successfully functionalized with either acidic (SO_3H), basic (NH_2) or BOC-protected basic (BOC-NH) groups. Bifunctional Janus particles were synthesized through a solidified wax PE method. Oil-in-water (o/w) PEs were prepared, using molten paraffin wax as the oil phase, stabilized by the amine-functionalized silica particles. After solidification, the exposed patch of the silica particles could be modified to bear acid functionalities. All

particles were capable of stabilizing w/o PEs formulated with 4-propylguaiacol (PG) as organic phase. The monofunctionalized particles still suffered from catalyst quenching during the antagonistic tandem reaction. Protecting the amine functionalized particles with BOC groups did lead to activity for the tandem reaction and some product, 5-HMFDEM, was formed. The use of antagonistic Janus particles resulted in higher product yield and selectivity as the acid and base catalysts are only exposed to the liquid phase they are required (Figure 5.1e).

5.2 Results and discussion

5.2.1 Synthesis of mono- and bifunctional catalytic solid emulsifiers

Monodispersed silica spheres (SiO_2) were synthesized using the Stöber method and further modified to obtain acid and base functionalized particles (Figure 5.2a). Figure 5.4a shows that the bare silica spheres synthesized were highly monodisperse and about 450 nm in diameter, at this size the particles were small enough to properly stabilize PEs while they are big enough to visualize any grafting by polymers with TEM.

The SiO_2 particles were grafted with 2-(4-chlorosulfonylphenyl)ethyltrimethoxysilane (CSPTMS) as acid group precursor. This group can be easily activated with HCl to obtain sulfonic acid groups (SiO_2-SO_3H). As previously reported by Freire et. al. the incorporation of phenyl sulfonic acids using this CSPTMS precursor led to a higher acid concentration and required less synthesis steps than when phenyltriethoxysilane or phenyltrimethoxysilane were used as precursor, which require sulfonation or chlorosulfonation steps in order to obtain acid functionality.[26] However, this procedure resulted in a poor sulfur content of 0.09 mmol·g-1 silica for the monofunctionalized particles, as determined by ICP-OES. The FT-IR spectra before and after modification, taken after drying for 30 min at 400 °C under vacuum, are shown in Figure 5.3. The drying procedure was less effective for the acid-functionalized particles than for the SiO_2 particles, resulting in the broad band from 3600 to 3000 cm^{-1} originating from water interacting with the silanol groups. The C-H stretch vibrations from the ethyl tail of the CSPTMS were observed at 3000-2700 cm^{-1} while the ring vibrations of the phenyl group were observed at ~1500 cm^{-1}.[26] Sulfonation was confirmed by the very weak band corresponding to S=O stretch vibrations at 1400-1350 cm^{-1}.

To obtain base-functionalized particles, the SiO_2 particles were grafted with (3-aminopropyl) triethoxysilane (APS) (Figure 5.2a). These SiO_2-NH_2 particles were hydrophobized using hexamethyldisilazane (HMDS) to obtain the SiO_2-NH_2-$OSi(CH_3)_3$ particles suitable for the stabilization of PG formulated PEs. Grafting with APS and HMDS was much more efficient

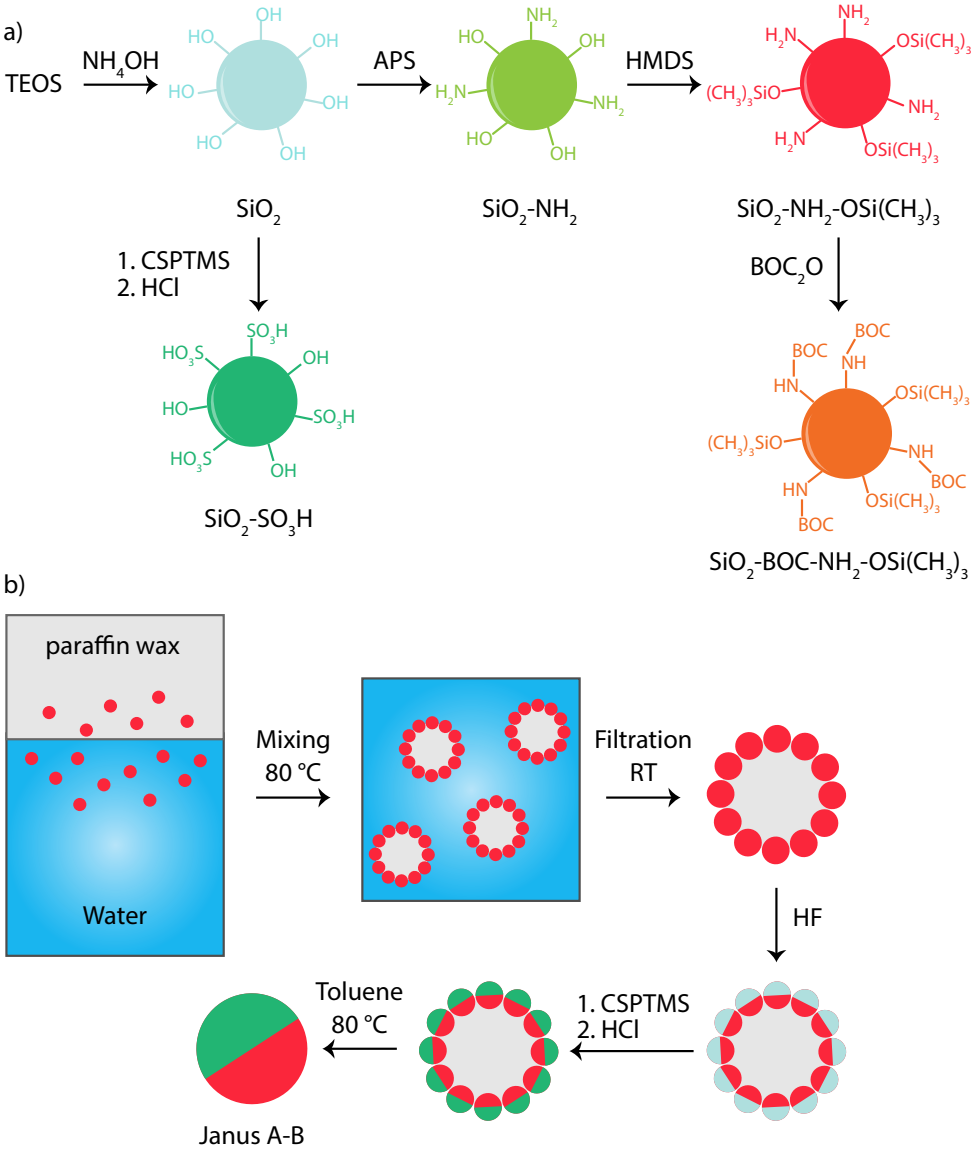

Figure 5.2: a) Schematic representation of all monofunctionalized particles synthesized from Stöber silica (SiO_2). CSPTMS = 2-(4-chlorosulfonylphenyl) ethyltrimethoxysilane, APS = (3-aminopropyl)triethoxysilane, HMDS = hexamethyldisilazane. b) Schematic representation of synthesis the acid-base functionalized Janus particles using the solidified wax procedure.

than grafting with CSPTMS, as loadings corresponding to 2.50 mmol·g-1 silica for N and 8.16 mmol·g-1 silica for C were obtained. The FT-IR spectrum of the particles, as shown in Figure 5.3, shows both the OH-stretch vibration of the silanol groups (3688 cm^{-1}) and

the N-H stretch vibration of the amine groups (3411 cm^{-1}). The hydrophobization was confirmed by the intense C-H stretch and C-H bending vibrations of the grafted methyl groups around 2800 and 1400 cm^{-1}.

To prevent potential quenching during PE preparation, the amine groups of the SiO_2-NH_2-$OSi(CH_3)_3$ particles were protected by tert-butyloxycarbonyl groups (BOC), yielding SiO_2-BOC-NH_2-$OSi(CH_3)_3$ particles. IR analysis of these materials gave only a weak signal, showing some C-H vibrations (2800 cm^{-1}) but no distinct N-H stretch and C=O vibrations were observed. In this case, sample drying was not very effective as indicated by the broad band in the OH-stretch region was observed. This could be due to the carbonyl of the BOC, which can strongly interact with water.

The SiO_2-NH_2-$OSi(CH_3)_3$ particles were used as starting materials for the synthesis of the acid-base Janus particles. These particles were mixed with water and molten paraffin wax at 80 °C to form a wax-in-water PE stabilized by the SiO_2-NH_2-$OSi(CH_3)_3$ particles, as

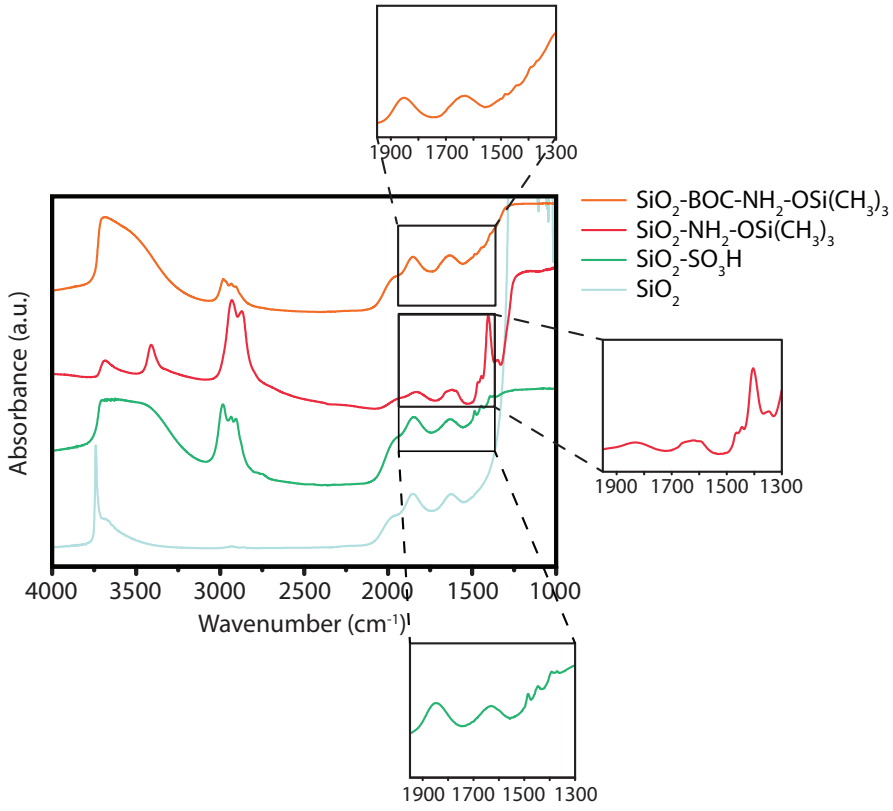

Figure 5.3: FT-IR spectra of SiO_2, SiO_2-SO_3H, SiO_2-NH_2-$OSi(CH_3)_3$ and SiO_2-BOC-NH_2-$OSi(CH_3)_3$, spectra measured at 400 °C under vacuum.

shown in Figure 5.2b. After cooling down to room temperature, and solidification of the paraffin wax, colloidosomes of paraffin wax covered with silica particles were obtained. These particles were partially embedded in the solidified wax, leaving only the exposed part of the silica spheres available for further modification (Figure 5.4b and c). This part of the silica spheres was then etched with 1 wt% HF to remove any surface functional groups and refunctionalized via covalent grafting with different concentrations of CSPTMS, to make Janus A-B particles with different acid concentrations. The etching thus removed the amine and hydrophobic groups of the exposed part of the colloidosome, so that the particles were converted from homogeneous hydrophobic spheres to amphiphilic ones. As can be seen in the TEM image in Figure 5.4b, the Janus silica particles are non-spherical after etching. The zoom of Figure 5.4b highlights the original size of the sphere before (indicated by black ring) and after etching (red ring). Interestingly, both the cap at the top that indicated the protected part inside solidified wax and etched part remain spherical with the diameter difference about 20 nm.

Visualization of grafting with APS and CSPTMS is not possible with e.g. electron microscopy techniques. Therefore, to show that the two parts of the Janus particle are in fact differently functionalized, the particles were modified by polymer grafting, as the polymeric materials should be visible in TEM. The aminated silica (SiO_2-NH_2) were coated with an acrylate layer using 3-(trimethoxysilyl)propyl methacrylate (TPM) as

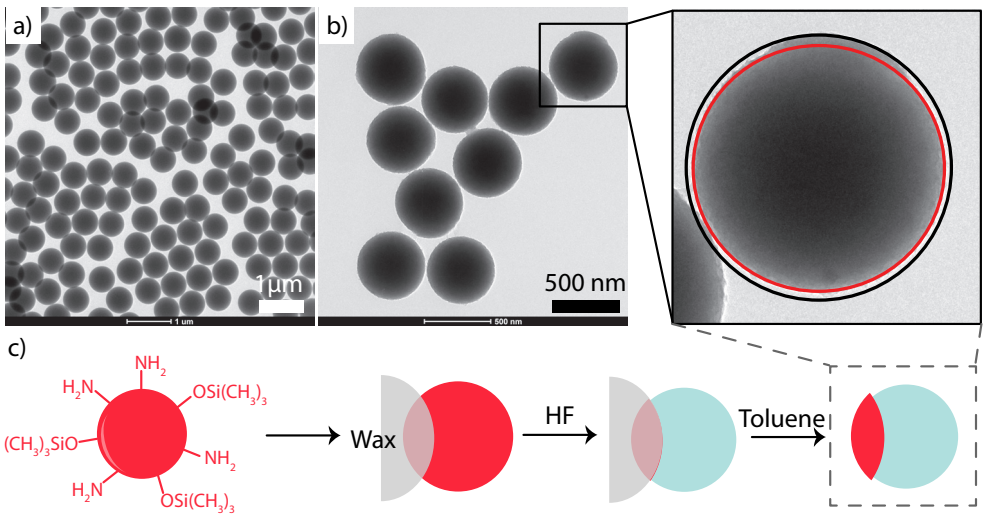

Figure 5.4: a) TEM image of SiO_2 particles synthesized via the Stöber method, scale bar = 1 µm. b) TEM image of partially etched SiO_2-NH_2-$OSi(CH_3)_3$ particles scale bar = 500 nm. Zoom shows the etched area of the particles, black ring corresponds to the original diameter of the particle, red ring corresponds to the diameter of the etched part of the particle. c) Schematic representation of etching procedure of SiO_2-NH_2-$OSi(CH_3)_3$ via the solidified wax method.

silane coupling agent, on which polystyrene (PS) was grafted by seeded polymerization. Without etching, PS was fully grown around the acrylate-coated SiO_2-NH_2 as shown on the left side of Figure 5.5, with the dark core corresponding to the silica sphere and the grey area corresponding to PS. When the particles were partially etched, no polystyrene was grown on the etched side of the particles, in as shown on the right side of Figure 5.5. The morphology of grafted PS varies from a spherical cap to irregular cluster-like structures on the surface of the silica core, as the polymerization procedure is very sensitive to the concentrations of acryl groups on the surface and the volume of monomers and initiators used.[27] As we are primarily interested in demonstrating the efficiency of bifunctional Janus particle synthesis, precise control over the shape of the grafted polystyrene was not necessary nor targeted. Indeed, the growth of PS shows that the silica particles can be selectively etched and grafted using this solidified paraffin wax method.

To further substantiate the influence of each modification step on the properties of the material, we simply observed the stability of the dispersion in water and toluene, indeed noting the changes in behavior anticipated for the specific modification. It was

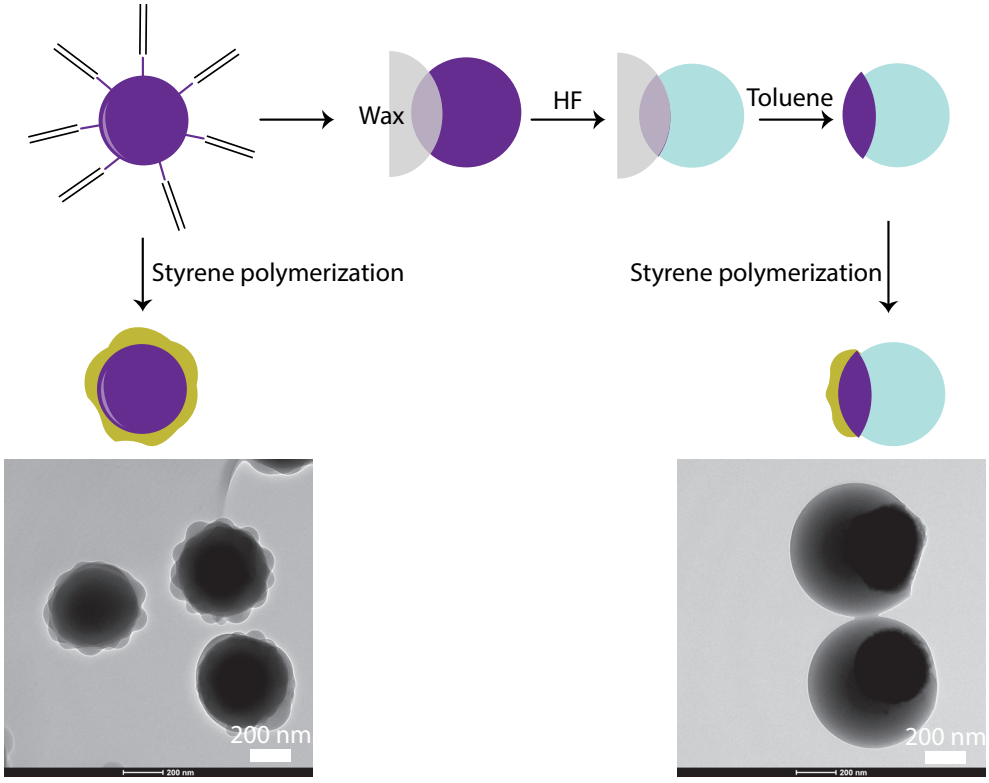

Figure 5.5: Schematic representation of styrene polymerization on vinyl terminated SiO_2 particles on homogeneous functionalized particles (left) and etched Janus particles (right) with corresponding TEM images after polymerization.

found that unmodified silica (SiO_2) and aminated silica particles (SiO_2-NH_2), due to their hydrophilic surface silanol and amine groups, could only be dispersed in the water phase (Figure 5.6a-d). Particles modified with HMDS (SiO_2-NH_2-$OSi(CH_3)_3$) were, as expected, found to disperse well only into the toluene phase (Figure 5.6e and f), as this modification resulted in a hydrophobic surface. However, Janus silica particles are not dispersed well into either water or toluene phase (Figure 5.6g and h) and rapidly transferred to the interface of water and toluene once water was added to the toluene dispersion (Figure 5.6i). These observations also corroborate that the desired Janus geometry was indeed achieved by the selective etching and coating strategy.

Four different functionalized silica particles were thus synthesized that can be used as PE stabilizing and catalytic particles containing sulfonic acid only, free amine only, BOC-protected amine only and a combination of spatially separated sulfonic acid-amine functional groups. The synthesis of the latter, i.e. bifunctional Janus particles with acid functionalization on the hydrophilic and base functionalization on the hydrophobic side of the particles using a solidified wax method has, to the best of our knowledge, has not been reported before.

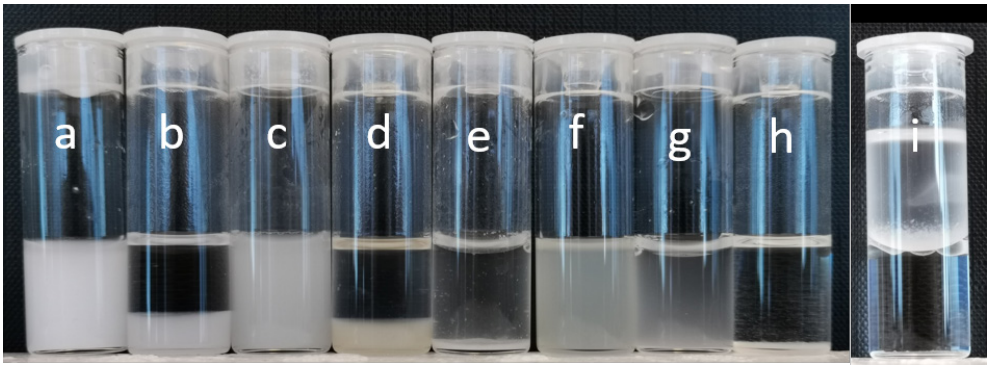

Figure 5.6: Unmodified silica SiO_2 dispersion in a) water and b) toluene; c) SiO_2-NH_2 in water and d) toluene; e) SiO_2-NH_2-$OSi(CH_3)_3$ in water and f) toluene; g) Janus A-B in water and h) toluene, i) amphiphilic Janus particles quickly adsorbed at the water-toluene interface.

5.2.2 Antagonistic tandem catalysis

With the monofunctional, SiO_2-NH_2-$OSi(CH_3)_3$, SiO_2-BOC-NH_2-$OSi(CH_3)_3$ and SiO_2-SO_3H and bifunctional Janus A-B emulsifiers in hand, we can use them as catalysts for the dehydration and Knoevenagel condensation reactions in PEs formulated with 4-propylguaiacol (PG) as organic phase. In Chapter 4, the optimal acid-base concentrations for antagonistic tandem catalytic reactions were determined to be 20 mol% acid and 20 mol% base and these (relative) loadings were used here as well.

First, the ability of SiO_2-NH_2-$OSi(CH_3)_3$ to perform the Knoevenagel condensation of 5-HMF and diethyl malonate was investigated (Figure 5.7, left). To reach a base concentration of 20 mol%, the amine-functionalized particles were diluted with non-catalytic hydrophobized silica particles. This PE system showed moderate activity and high selectivity as 50% of the 5-HMF was converted with a 5-HMFDEM yield of 39% after 24 h at 80 °C. This selectivity is similar to what was found in reaction with excess of homogeneous base catalyst (Chapter 4, Figure 4.9). Secondly, any influence of the monofunctionalized acid particles on the second Knoevenagel condensation step was tested. For this reaction, 20 mol% piperidine was used as homogeneous base catalyst. As the acid concentration on these particles was rather low at 0.09 mmol·g-1 silica the typical PE conditions of 2 wt% solid emulsifier, resulted in an acid loading of only 1 mol with respect to 5-HMF in these experiments. Even at this low acid concentration, an enormous influence on the product distribution was seen. After 24 h at 80 °C, 90% of the 5-HMF was converted while only 35% of 5-HMFDEM was obtained. The added acidity thus resulted in considerable side product formation

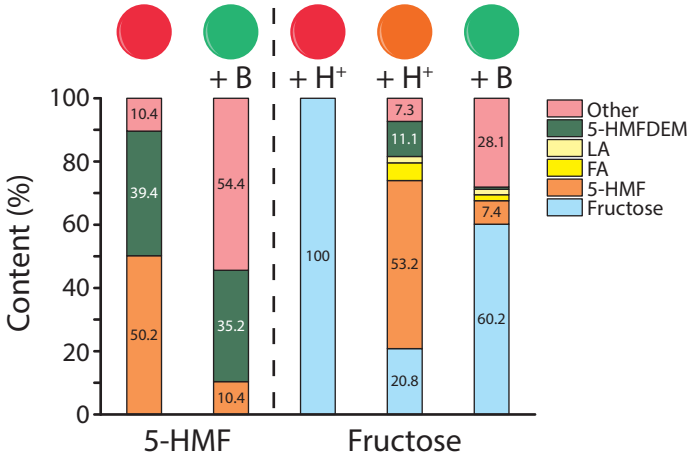

Figure 5.7: Left: Product distribution of Knoevenagel condensation reaction of 5-HMF with diethyl malonate in PEs stabilized by SiO_2-NH_2-$OSi(CH_3)_3$ (red ball) and SiO_2-SO_3H (green). Reaction conditions: SiO_2-NH_2-$OSi(CH_3)_3$: 6 mL PG, 2 wt% silica, 2 mL H_2O sat. with NaCl, 1 mmol 5-HMF, 2.5 mmol diethyl malonate, 20 mol% base, 80 °C, 24 h. SiO_2-SO_3H: 3 mL PG, 2 wt% silica, 1 mL H_2O sat. with NaCl, 0.5 mmol 5-HMF, 1.25 mmol diethyl malonate, 20 mol% piperidine (B), 80 °C, 24 h. Right: Product distribution of dehydration-Knoevenagel condensation of fructose with diethyl malonate in PEs stabilized with SiO_2-NH_2-$OSi(CH_3)_3$ (red), SiO_2-BOC-NH_2-$OSi(CH_3)_3$ (orange) and SiO_2-SO_3H (green). Reaction conditions: SiO_2-NH_2-$OSi(CH_3)_3$: 6 mL PG, 2 wt% silica, 2 mL 0.1 M aqueous HCl sat. with NaCl, 1 mmol fructose, 2.5 mmol diethyl malonate, 20 mol% base, 80 °C, 24 h. SiO_2-BOC-NH_2-$OSi(CH_3)_3$: 6 mL PG, 2 wt% silica, 2 mL 0.1 M aqueous HCl sat. with NaCl, 1 mmol fructose, 2.5 mmol diethyl malonate, 20 mol% base, 100 °C, 6 h. SiO_2-SO_3H: 3 mL PG, 2 wt% silica, 1 mL H_2O sat. with NaCl, 0.5 mmol fructose, 1.25 mmol diethyl malonate, 20 mol% piperidine (B), 80 °C, 24 h.

from 5-HMF. Another important thing to note is that due to the hydrophilic nature of the particles, the PEs were less stable than the PEs stabilized by partially hydrophobic particles. This could have benefited 5-HMFDEM formation, as the particles, and therefore the acid catalyst, for the most part reside on the bottom of the flask.

For the tandem catalytic dehydration-Knoevenagel condensation, both the acid and base catalysts are required. When SiO_2-NH_2-$OSi(CH_3)_3$ particles were used, aqueous HCl was used as counter catalyst. After 24 h of reaction at 80 °C, no conversion was observed (Figure 5.7, right), suggesting that the activity of the acid catalyst was fully quenched by the basic emulsifier particles. This quenching could be visualized using an optical microscope with a spectrometer measuring in the visible region and a pH indicator, methyl orange which is soluble in both water and PG. Above a pH of 4.4, methyl orange is yellow, while below 3.1 it has a red color (Figure 5.8a). A dispersion of the amine functionalized particles in PG is yellow (Figure 5.8b) with an absorption maximum (λ_{max}) at 440 nm. After addition of an acidic aqueous phase and emulsification, both the continuous and the dispersed phase became red with a λ_{max} around 530 nm (Figure 5.8c), showing a chemical reaction took place between the homogeneous acid and the base particles. As the aqueous phase is the dispersed phase, the homogeneous acid is by necessity always present during PE preparation, as post-emulsification addition of the acid is not possible. It is therefore difficult to avoid quenching of the free base-functionalized particles during PE preparation.

A way to circumvent this quenching during PE preparation is by protecting the amine group. However, after PE preparation, the protecting group should be readily cleaved to give the free amine required for the Knoevenagel condensation. If a thermally labile

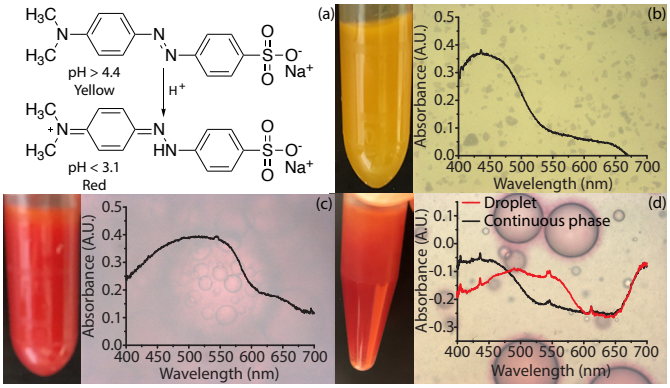

Figure 5.8: a) Reaction scheme of the protonation of methyl orange. b-d) Pictures and absorption spectra of methyl orange in b) amine functionalized particles dispersed in PG, c) PE stabilized with amine-functionalized particles formulated with PG and acidic water, d) PE stabilized with BOC-protected amine particles formulated with PG and acidic water.

protecting group is used, the base catalyst can simply be activated by heating to reaction temperature, omitting the need for addition of more reagents to the reaction mixture. The BOC protecting group, which is usually cleaved at elevated temperatures is a good candidate for this.[28] To determine if BOC protected amine particles stays intact during PE preparation and therefore protect against acid-base quenching, the phases were again stained with methyl orange (Figure 5.8d). Although the PE stabilized by BOC-protected amine functionalized particles appears to be completely red upon visual inspection, the microscope image clearly shows a yellow continuous phase (λ_{max}= 440 nm), with red droplets (λ_{max} = 530 nm) indicating that no reaction between the BOC-amine groups and the acid took place during PE preparation.

The tandem catalytic reaction using the BOC-protected amine particles was performed at 100 °C as this is the temperature that is typically used for BOC-protection and is also beneficial for fructose dehydration. However, side product formation occurs more rapidly at this temperature, therefore, the reaction time was shortened to 6 h, after which 79% fructose conversion with 53% 5-HMF and 11% 5-HMFDEM was obtained (Figure 5.7, right). The second Knoevenagel condensation reaction step therefore seems to be limiting, which could be due to several reasons; 1) the amine groups on the particles are not strong enough to catalyze the Knoevenagel condensation reaction efficiently enough, 2) the free amine is readily generated but the catalysts are quenched afterward or, 3) deprotection is relatively slow, limiting the availability of the free base during reaction. As these particles are synthesized from the SiO_2-NH_2-$OSi(CH_3)_3$ particles and those have shown to be able to perform the Knoevenagel condensation, 1) is very unlikely. If 2) would be true, the fructose conversion would not be this high. Incomplete or slow BOC removal can, however, not be excluded and requires further study.

In principle, another way to cope with the preparation method-induced quenching of the antagonistic catalysts is to add one of the catalysts after PE preparation, a method that we used before in Chapter 4. In this case, post-emulsification addition requires the catalyst located in the continuous phase, piperidine, to be added to a PE system prepared with the sulfonic acid functionalized particles. The hydrophilicity of these particles and their low acid loading of the sulfonic acid-decorated silica hampered this approach, resulting in limitedly stable PEs under reaction conditions and poor performance. A tandem reaction executed this way at 80 °C for 24 h indeed gave only 40% fructose conversion and 7% and 1% of 5-HMF and 5-HMFDEM, respectively.

As the Janus A-B particles have the acid and base catalysts spatially separated on two distinct patches of the particle, no precautions need to be taken to prevent quenching during PE preparation. Due to the amphiphilic nature of the particles, the particles furthermore

behave differently at the water-oil interface than the monofunctionalized ones. To form stable PEs with these Janus particles, 2 mL PG and 2 mL H_2O (30 wt% NaCl) was used stabilized with 7 wt% silica with respect to the organic phase. As acid-base quenching should not be an issue with these particles we decided to perform the reactions at the optimal temperature for fructose dehydration, 100 °C. Three different Janus A-B particles, with increasing acid concentration, were used for the tandem catalytic reaction. The Janus particles with the lowest acid concentration showed 54.3% conversion of fructose and 5-HMF and 5-HMFDEM yields of 12.9 and 17.3% respectively after 24 h (Figure 5.9). Increasing the acid concentration resulted as expected in higher fructose conversion, 62.6%, however, no increase in 5-HMF or 5-HMFDEM yield was observed, indicating an increase in humin side product formation. A further increase in acid loading resulted in very reactive catalyst particles as the PE became dark brown within 7 h, indicative of extensive humin formation, after which the reaction was stopped. Although the fructose conversion was quite high after such a short reaction time, 70.4%, the 5-HMFDEM yield was again lower as a result of side product formation and lack of 5-HMF accumulation.

The acid- and base functionalized particles could thus be used as Pickering stabilizers and heterogeneous catalysts for the tandem catalytic dehydration-Knoevenagel condensation reaction of fructose. Stable PEs could be formed with all particles, however,

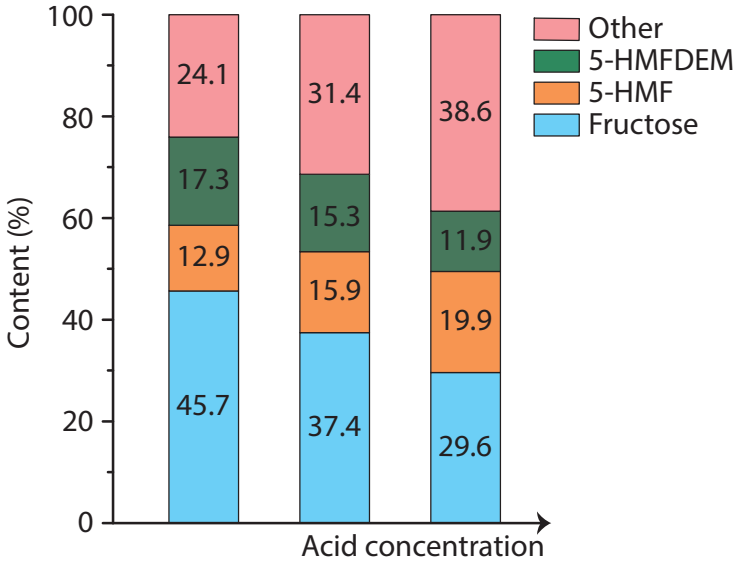

Figure 5.9: Product distribution of the fructose dehydration-Knoevenagel condensation tandem reaction in PEs stabilized with acid-base Janus particles with in increasing acid concentration. Reaction conditions: 2 mL PG, 7 wt% particles, 2 mL H_2O (30% NaCl), 100 °C, left and middle: 0.5 mmol fructose, 1.25 mmol diethylmalonate, 24 h, right: 1.0 mmol fructose, 2.5 mmol diethylmalonate, 7 h.

the SiO_2-SO_3H particles were not capable of stabilizing the PEs during the complete reaction time at high temperatures. The use of base-functionalized particles introduced another challenge, as acid-base quenching occurred during PE preparation, an issue that was addressed by BOC protection of the free amines. The results also show that the Janus particles are capable of catalyzing the tandem reaction, but also highlight that a fine balance needs to be struck to efficiently couple the individual steps. Careful control over the ratio of grafted functional groups is therefore needed in the synthesis of the Janus particles.

5.3 Conclusions

Here, we showed the successful synthesis of monodisperse silica particles of 450 nm using the Stöber method. These particles were hydrophobized to serve as solid emulsifiers for the stabilization of w/o PEs using PG as organic phase. To exploit these particles as heterogeneous catalysts, they were additionally functionalized with sulfonic acid or amine groups. For the acid-base reaction in the PE stabilized with amine functionalized particles, where HCl was added as homogeneous counter catalyst, no catalytic activity was observed due to mutual destruction of the catalyst, as also evidenced by indicator-based optical microscopy studies. Protecting the amine groups with BOC before PE preparation prevented quenching, and 79.2% fructose conversion and 11.1% 5-HMFDEM yield after 6 h reaction at 100 °C was reached. However, the BOC-protecting groups were not entirely removed during reaction, resulting in a 53.2% yield of the intermediate, 5-HMF. The use of silica particles functionalized with sulfonic acid groups showed only 40% conversion after 24 h reaction at 80 °C, without any product formation. The bifunctional Janus particles were synthesized with different acid concentrations by varying the amount of silylation agent. While increasing the acid concentration resulted in enhanced fructose conversions, it did not lead to increasing product formation, but more side products were formed. The lowest acid concentration resulted in 54.3% fructose conversion, 12.9% 5-HMF and 17.3% 5-HMFDEM in 24 h at 100 °C. To make use of the full potential of the Janus particles, better control over the grafting of the functional groups and the resulting acid-base balance is still required.

5.4 Experimental procedures

5.4.1 Chemicals

All chemicals were used as received without any purification. Hydrochloric acid (HCl, 37%, analytical grade), chloro(trimethyl)silane (TMSCl, ≥ 98%), 4-propylguaiacol (PG, ≥ 99%, food grade), methyl orange (85%), paraffin wax, 5-(hydroxymethyl)furfural (HMF, ≥ 99%),

sodium dodecyl sulfate (SDS), styrene, potassium persulfate (KPS), ethanol, tetraethyl orthosilicate (TEOS), (3-aminopropyl)triethoxysilane (APS, ≥ 99%), 3-(trimethoxysilyl) propyl methacrylate (TPM, 98%), hexamethyldisilazane (HMDS), di-*tert*-butyl dicarbonate, triethylamine (TEA), hydrofluoric acid (HF, 48%) and boric acid were purchased from Sigma-Aldrich. Anisole (99%), citric acid (99.5%),2-(4-chlorosulfonylphenyl)ethyltrimethoxysilane (CSPTMS, 50% in dichloromethane) and ammonium hydroxide (25%) were obtained from Acros Organics. D-fructose (99%) was purchased from Alfa Aesar. Sodium chloride (NaCl) was obtained from Merck.

5.4.2 Synthesis of monodispersed silica spheres (SiO_2)

The monodisperse surface functionalized silica spheres were synthesized using a modification of the method reported by Zhang *et al.*[29] In a 100 mL round bottom flask, 11.6 mL of ammonium hydroxide and 48.4 mL of ethanol were stirred at 400 rpm for 10 min. This is followed by the addition of a mixture of 1.5 mL TEOS and 6 mL of ethanol. To grow the silica particles into the desired size, 4 mL of TEOS in 20 mL of ethanol was added dropwise after 2 h reaction. The mixture was then mechanically stirred overnight for another 24 h at room temperature. Finally, the mixture was centrifuged and washed three times with 30 mL ethanol for the complete removal of reactants.

5.4.3 Synthesis of acid functionalized silica spheres (SiO_2-SO_3H)

Typically, 1 mL of CSPTMS and 0.5 mL ammonium hydroxide were added to 30 mL ethanol solution containing 3 g of silica spheres. The mixture was stirred for 24 h at room temperature after which the particles were washed three times with water. The resulting particles were dispersed in 30 mL 2 M HCl solution to activate the chlorosulfonyl groups.

5.4.4 Synthesis of amine or acrylate decorated silica spheres (SiO_2-NH_2)

Typically, 10 g of APS was added to 60 mL of toluene dispersion containing 3 g of silica spheres, and the suspension was subsequentially transferred to the oil bath to react for 24 h at 95 °C. Then the solid was collected by centrifugation and redispersion in 50 mL ethanol for three times and dried using a rotary evaporator.

Similarly, the modification of silica spheres whose external surfaces covered with acrylate groups were prepared using same method using TPM as silane coupling agent.

5.4.5 Hydrophobization of aminated silica spheres (SiO_2-NH_2-$OSi(CH_3)_3$)

HMDS (2 mL) was added to 50 mL SiO_2-NH_2 ethanol dispersion containing 3 g aminated silica spheres and the suspension was stirred for 24 h. After modification, the resulting particles were washed several times with 50 mL ethanol to remove unreacted chemicals and dried in the oven at 110 °C.

For hydrophobic, BOC-protected aminated silica spheres, 100 mg of SiO_2-NH_2-$OSi(CH_3)_3$ were dispersed in 35 mL of dichloromethane containing 120 mg di-*tert*-butyl dicarbonate (BOC_2O). After addition of 3 mg TEA the flask was placed in the ultrasonicate bath for 3 h. The resulting sample was washed for 3 times with 30 mL ethanol by centrifugation and redispersed in dichloromethane.

5.4.6 Preparation of wax-water colloidosome stabilized with silica spheres

The wax-water colloidosomes stabilized with silica spheres were prepared using a modification of a method first developed by Jiang *et al.*[30] 0.5 g of the hydrophobized aminated silica particles (SiO_2-NH_2-$OSi(CH_3)_3$) were dispersed in 10 g of paraffin wax at 80 °C, followed by addition of 50 mL preheated water (80 °C) under magnetic stirring at 1600 rpm. After stirring for 1 h, the wax-water PE was allowed to cool down to room temperature without stirring. The resulting solid colloidosomes stabilized by hydrophobized aminated silica particles creamed up forming a white layer of small spheres during cooling procedure. The colloidosomes were washed with water to remove particles in the aqueous solution as well as weakly attached particles, then washed with 50 mL ethanol for another 3 times and finally dried at room temperature.

5.4.7 Preparation of Janus silica via selective etching

10 g of the dried colloidosome spheres were immersed into 30 mL of 1 wt % aqueous HF for 12 h in a plastic test tube (caution: HF solution is very hazardous and corrosive and should be handled according to the MSDS guidelines), and the resulting etched Janus silica-covered colloidosomes were collected with filter paper and rinsed carefully and thoroughly with saturated boric acid aqueous solution and demi water multiple times. The colloidosomes were then dried inside the fume hood before further modification.

5.4.8 Synthesis of Janus silica with acid and base groups (Janus-A-B)

The etched colloidosomes were dispersed into 30 mL ethanol solution containing 1 mL of CSPTMS and 0.5 mL ammonium hydroxide (25 wt%) to modify the etched hemisphere. The mixture was stirred for 24 h after which the colloidosomes were washed with water three times, followed by dispersion in 30 mL 2 M HCl solution to activate the sulfonyl groups. Finally, to release these modified silica particles from the paraffin wax, the colloidosome were dispersed in toluene at 80 °C. Janus-A-B with different surface coverages of acid catalysts were achieved by adjusting the amount of 2-(4-chlorosulfonylphenyl) ethyl trimethoxysilane introduced to the coating procedure (100, 50 or 30%, with respect to the procedure described above).

5.4.9 Synthesis of Janus SiO_2/PS composite colloids

10 mg of the Janus colloid, 4 µL of 20 wt% SDS solution and 0.1 mL styrene were added to 2 mL water. The mixture was purged with nitrogen to remove oxygen then emulsified with ultrasonication for 30 s. The polymerization was initiated by 200 µL KPS aqueous solution (1 wt%) in the oil bath at 70 °C for 10 h. The product was separated by centrifugation and washed three times each with water and ethanol.

5.4.10 Characterization of particles

Transmission electron microscopy (TEM) pictures were taken with a Philips Tecnai10 electron microscope typically operating at 100 kV. The samples were prepared by drying a drop of diluted aqueous dispersion on top of polymer-coated copper grids. Scanning electron microscopy (SEM) images were taken with a Philips SEM XL PEG 30 typically operating at 5 – 10 kV.
The silica particles were analyzed by Fourier-Transformed Infrared (FT-IR) for which self-supported wafers of ~20 mg were mounted in an FT-IR cell connected to an oven. The wafer was dried by heating the sample to 400 °C with a heating rate of 5 °C/min under vacuum. A Perkin-Elmer System 2000 instrument was used to record the FT-IR spectra in transmission mode in the spectral range of 4000 to 1000 cm^{-1}. For each spectrum 32 scans were collected with a spectral resolution of 4 cm^{-1}.

5.4.11 Visualization of catalyst quenching using optical microscopy

A solution of 0.05 wt% methyl orange in 1 mL 4-PG was added to 20 mg particles (SiO_2-NH_2-$OSi(CH_3)_3$ or SiO_2-NHBOC-$OSi(CH_3)_3$) in an Eppendorf and the particles were dispersed using the ultrasonic bath (37 Hz, 30 min). A PE was prepared by addition of 0.3 mL 0.1 M HCl

(30 wt% NaCl) and by shaking the mixture. The well of a microscopy slide was filled with PE and covered with a cover glass. Optical microspectroscopy studies were performed in reflectance mode by using an Olympus BX41M upright microscope, equipped with a 50x0.5NA objective lens. Illumination of the sample was performed with a 30 W halogen lamp. The microscopy setup was equipped with a 50/50 double-viewport tube, which accommodated a CCD video camera (ColorView IIIu, Soft Imaging System GmbH) and an optical fiber mount. The microscope was connected to a CCD Visible spectrometer (AvaSpec-2048TEC, Avantes) by a 200 mm core fiber and absorption spectra were obtained using an average of 25 measurements with an integration time of 400 ms.

5.4.12 PE preparation

All PEs were prepared by first dispersing a known mass of particles into PG using a VCX 130 Vibra-Cell Ultrasonic Processor equipped with a 3 mm diameter tip (Sonics, 20 kHz, 10 W, 2 min). During sonication, it was necessary to cool the vessel in an ice-bath. After the addition of 2 mL aqueous phase with appropriate NaCl concentration and required pH to the dispersion, the resulting mixture was emulsified using a UltraTurrax T25 homogenizer with a S25N-10G dispersing tool (IKA, 15200 rpm, 2 min).

5.4.13 Tandem catalytic reactions

15 mL Ace pressure tubes were loaded with PEs stabilized by mono- or bifunctional particles. Fructose or 5-HMF were dissolved in the aqueous phase before PE preparation while diethylmalonate (and piperidine when necessary) were added after PE preparation. The PEs were left for reaction at 100 °C without stirring for the applied reaction time. After the reaction time was complete, the mixture was cooled to room temperature in air and 1 mL of citric acid solution was added (15 mg/mL) and the PE was destabilized by centrifugation using a Rotina 38-R Hettich centrifuge (11000 rpm, 4 °C, 10 min). The aqueous phase was analyzed by HPLC analysis performed on a Shimadzu HPLC system equipped with a Bio-Rad Aminex HPX-87H column, and a differential refractometer using citric acid as internal standard. The organic phase was analyzed on a Varian GC equipped with a VF-5 ms capillary column and an FID detector.

Acknowledgements

Silvia Zanoni (Inorganic Chemistry and Catalysis, Utrecht University) is acknowledged for performing FT-IR experiments and the pellet preparation involved. Arnold van Dijk and ing. Helen de Waard (GeoLab, UU) are acknowledged for the ICP measurements.

References

1 P. Azadi, R. Carrasquillo-Flores, Y. J. Pagán-Torres, E. I. Gürbüz, R. Farnood and J. A. Dumesic, *Green Chem.*, **2012**, *14*, 1573.

2 W. Zhang, L. Fu and H. Yang, *ChemSusChem*, **2014**, *7*, 391.

3 J. Wu and G. H. Ma, *Small*, **2016**, *12*, 4633.

4 M. Pera-Titus, L. Leclercq, J. M. Clacens, F. De Campo and V. Nardello-Rataj, *Angew. Chem.- Int. Ed.*, **2015**, *54*, 2006.

5 C. T. Womble, M. Kuepfert and M. Weck, *Macromol. Rapid Commun.*, **2019**, *40*, 1.

6 C. M. Vis, L. C. J. Smulders and P. C. A. Bruijnincx, *ChemSusChem*, **2019**, *12*, 2176.

7 I. Van Zandvoort, Y. Wang, C. B. Rasrendra, E. R. H. Van Eck, P. C. A. Bruijnincx, H. J. Heeres and B. M. Weckhuysen, *ChemSusChem*, **2013**, *6*, 1745.

8 M. Giesbers, J. M. Kleijn and M. A. Cohen Stuart, *J. Colloid Interface Sci.*, **2002**, *252*, 138.

9 J. Gao, X. Zhang, Y. Lu, S. Liu and J. Liu, *Chem. - A Eur. J.*, **2015**, *21*, 7403.

10 L. C. Lee, J. Lu, M. Weck and C. W. Jones, *ACS Catal.*, **2016**, *6*, 784.

11 M. H. Qi, M. L. Gao, L. Liu and Z. B. Han, *Inorg. Chem.*, **2018**, *57*, 14467.

12 L. Zhong, C. Anand, K. S. Lakhi, G. Lawrence and A. Vinu, *Sci. Rep.*, **2015**, *5*, 1.

13 Z. Weng, T. Yu and F. Zaera, *ACS Catal.*, **2018**, *8*, 2870.

14 Z. Jia, K. Wang, B. Tan and Y. Gu, *ACS Catal.*, **2017**, *7*, 3693.

15 L. C. Bradley, W. H. Chen, K. J. Stebe and D. Lee, *Curr. Opin. Colloid Interface Sci.*, **2017**, *30*, 25.

16 B. J. Park and D. Lee, *Soft Matter*, **2012**, *8*, 7690.

17 T. M. Ruhland, A. H. Gröschel, N. Ballard, T. S. Skelhon, A. Walther, A. H. E. Müller and S. A. F. Bon, *Langmuir*, **2013**, *29*, 1388.

18 F. Tu and D. Lee, *Chem. Commun.*, **2014**, *50*, 15549.

19 A. F. Mejia, A. Diaz, S. Pullela, Y. W. Chang, M. Simonetty, C. Carpenter, J. D. Batteas, M. S. Mannan, A. Clearfield and Z. Cheng, *Soft Matter*, **2012**, *8*, 10245.

20 Z. Cao, G. Wang, Y. Chen, F. Liang and Z. Yang, *Macromolecules*, **2015**, *48*, 7256.

21 B. P. Binks and P. D. I. Fletcher, *Langmuir*, **2001**, *17*, 4708.

22 B. J. Park, T. Brugarolas and D. Lee, *Soft Matter*, **2011**, *7*, 6413.

23 J. Faria, M. P. Ruiz and D. E. Resasco, *Adv. Synth. Catal.*, **2010**, *352*, 2359.

24 A. Kirillova, C. Schliebe, G. Stoychev, A. Jakob, H. Lang and A. Synytska, *ACS Appl. Mater. Interfaces*, **2015**, *7*, 21218.

25 J. Cho, J. Cho, H. Kim, M. Lim, H. Jo, H. Kim, S.-J. Min, H. Rhee and J. W. Kim, *Green Chem.*, **2018**, *20*, 2840.

26 M. M. Aboelhassan, A. F. Peixoto and C. Freire, *New J. Chem.*, **2017**, *41*, 3595.

27 B. Liu, C. Zhang, J. Liu, X. Qu and Z. Yang, *Chem. Commun.*, **2009**, *26*, 3871.

28 P. G. M. Wuts, in *Greene's Protective Groups in Organic Synthesis*, Wiley, Fifth Edit.,

2014, pp. 895.
29 J. H. Zhang, P. Zhan, Z. L. Wang, W. Y. Zhang and N. B. Ming, *J. Mater. Res.*, **2003**, *18*, 649.
30 L. Hong, S. Jiang and S. Granick, *Langmuir*, **2006**, *22*, 9495.

Chapter 6

Continuous Flow Pickering Emulsion Catalysis in Droplet Microfluidics studied with In-situ Raman Microscopy

Pickering emulsions (PEs), emulsions stabilized by solid particles located at the liquid-liquid interface, have shown to be a versatile tool for catalysis, amongst others allowing for antagonistic tandem catalysis. Most examples of PE catalysis are performed in batch, which has some disadvantages from an application point of view and hampers fundamental studies of transport, reactivity and reaction mechanism. Alternatively, some continuous flow applications of PE (FPE) catalysis are emerging, and here we report a droplet microfluidic approach for continuous flow water-in-oil (w/o) PE catalysis. This microfluidic setup allowed in-situ analysis of the catalytic process with Raman spectroscopy. This is demonstrated for the acid-catalyzed deacetalization of benzaldehyde dimethyl acetal, for which the formation of the product, benzaldehyde, was followed by tracking the C=O stretch vibration in the Raman spectra. A ninefold increase in yield was observed for this reaction using FPEs when compared to flow biphasic systems (FBS). Furthermore, coupling an antagonistic set of reactions, in this case the sequential deacetalization-Knoevenagel condensation, could only be achieved with FPEs, as quenching of acid and base catalysts occurred in the FBS. In this microfluidic setup, the FPE system gave full conversion of the benzaldehyde dimethyl acetal and 25% of product in a maximum reaction time of 34 min. This droplet microfluidic setup is a versatile system to study catalytic reactions in FPE with in-situ and ex-situ analysis techniques.

This chapter is based on: C.M. Vis*, A.-E. Nieuwelink*, B.M. Weckhuysen, P.C.A. Bruijnincx, Continuous Flow Pickering Emulsion Catalysis in Droplet Microfluidics with In-situ Raman Spectroscopy *Chemistry – A European Journal* Accepted

* *These authors contributed equally*

6.1 Introduction

Biphasic catalysis has shown to be a great tool for efficient chemical transformations, for instance in the commercial Shell Higher Olefin Process (SHOP)[1] and the Ruhrchemie/Rhone–Poulenc Process (RCRPP)[2]. In these processes, reactions take place in an aqueous solution of substrate and catalyst, resulting in the formation of an insoluble product phase. The reactive and product phase can be easily separated, facilitating catalyst recycling. Another reason to use biphasic reaction media in catalysis is to improve selectivity: by extracting products from the reactive phase unwanted consecutive reactions can be prevented, reducing side product formation.[3] A major drawback of classical biphasic systems is the low interfacial area between the two phases, resulting in low activity for events that need this interface. Indeed, an increase of the interfacial area of a biphasic system usually leads to an increase in reactivity and extraction.[4,5] This can, for example, be accomplished by addition of emulsifying agents, such as surfactants, or when more stable emulsions are targeted, amphiphilic solid particles. These so-called Pickering emulsions (PEs) are stabilized by adsorption of the particles on to the liquid-liquid interface, typically creating either water-in-oil or oil-in-water emulsions depending on the affinity (hydrophilic or hydrophobic) for one of the two phases.[6,7] Whereas for surfactant-stabilized emulsions it is difficult to recover the surfactants and to separate the organic and aqueous phase, this can be easily done for PEs. Various methods for PE destabilization are available, making them suitable reversible reaction media. The most versatile destabilization method is to use centrifugation, but when responsive particles are used, changing the pH[8–10] or applying a magnetic field[11,12] can also cause PE destabilization.

Previous research has mainly focused on the formation and stability of PEs[13–18] in order to replace the classical surfactant-stabilized emulsions for pharmaceutical and cosmetic applications.[19] More recently, interest has been shown in using PEs as reaction media for catalysis.[20–24] However, most examples in literature focus on catalytic reactions performed in batch PE, a reactor setup that comes with some experimental challenges. For example, the vigorous stirring that is used to make the batch PEs results in broad droplet size distributions, making it hard to measure kinetics based on, for instance, interfacial area. Another challenge is to measure the partitioning of a substrate over the two phases as function of time, as this happens instantly upon the vigorous stirring during PE preparation. Sampling and sample work up require destabilization of the PE, making it impossible to investigate what exactly happens inside the system.

To deal with the complexity of the analysis and to make PE catalysis more industrially relevant, continuous flow water-in-oil (w/o) PEs were developed by the group of Yang *et al.* as a liquid equivalent of a packed bed reactor.[25,26] In this system the catalyst was

contained inside the water droplets. At the interface, an oil soluble reactant is converted by this catalyst by flowing through the droplet packed column. The oil phase containing the product could then be collected at the bottom of the column. These flow PEs (FPEs) were found to be stable over 1000 h time on stream. The flow speed, and therefore the residence and reaction time, was shown to be dependent on gravity as well as on the droplet size, with smaller droplets leading to a longer residence time. However, controlling the droplet size of these FPEs is still not trivial, as FPE preparation is similar to batch PEs, *i.e.* by vigorous stirring. Analysis of reactions performed in these FPEs was done ex-situ by collecting the oil phase dropping out of the reactor, leaving little room for changing parameters during reaction or for measuring kinetics. A way to potentially better monitor the reaction is to use a spectroscopic technique to determine substrate and product concentrations at different heights of the column. However, this is not readily done in a normal flow PE, due to scattering of radiation at the solid particles and the droplet surface. To overcome the various challenges offered by the currently available batch and flow PEs a droplet microfluidic device could be used.

Droplet microfluidics provides an easy way to gain control over the droplet size, and thus creates a more homogeneous system.[27] This rapidly growing field of research is based on small channel systems in the micrometer range. Droplets can be created when two immiscible fluids are combined at a T-junction, flow focusing or co-flow geometry in the channel system. The viscosity, interfacial tension and the flow rate ratio of both liquids determine the local flow field and therefore the pinch off of droplets and with that, their size.[28] Depending on the nature of the channel walls, water-in-oil or oil-in-water droplets can be created, as the properties of the walls can be matched with the wetting and non-wetting properties of the continuous and dispersed phase, respectively. The micrometer scale of these systems gives the channels special features regarding mixing, temperature control and homogeneity. The enhanced mixing is due to the convectional flow in- and outside the droplets that is caused by their movement through the microchannel. Furthermore, droplets in a microchannel are more stable compared to bulk biphasic systems and can exist without the use of surfactants due to their regular spacing. Surfactants are often added, however, to achieve the desired stability and prevent droplet coalescence in case two droplets do collide. To a lesser extent, solids have been used as stabilizing agents in microfluidics and most literature examples focus solely on the stability[29–31] or applicability for the food and biomedical industry[32,33]. One of the difficulties in preparing such in-flow PEs is the lack of shear, which causes particle adsorption at the interface to be very slow. To prepare stabilized droplets, sufficient time is needed for the droplets to be covered by particles before the droplets encounter each other.[34]

Here, we made use of a tube-in-tube co-flow microfluidic setup for the production of

water-in-oil droplets with or without the use of stabilizing particles, to prepare FPEs (Figure 6.1). The use of chemically resistant and optically transparent polymer tubing allows for visual observation of the formation and stability of droplets over the full course of the tubing, and it enables the execution of in-situ spectroscopic studies, which, to the best of our knowledge, has not been shown before in flow biphasic system (FBS) and FPE experiments. By measuring Raman spectra at different positions in the flow channel, the composition of the reaction mixture can be monitored at various reaction times, and hence kinetic profiling of reactants and reaction products can be performed. The reaction time can be easily controlled by either changing the total flow rate or by changing the length of the tubing, making this setup a versatile reaction system. Furthermore, one of the advantages of FPEs over bulk PEs is the automatic phase separation after the tubing's outlet.[19] This makes post analysis of both phases relatively easy.

This microfluidic system was used to demonstrate the advantage of using Pickering stabilized droplets over non-stabilized droplets for biphasic flow catalysis, using the acid-base catalyzed deacetalization-Knoevenagel condensation reaction of benzaldehyde dimethyl acetal as probe reaction. In Chapter 2 of this PhD thesis, we showed the positive influence of PEs on the performance of this reaction in a batch system.[23] In this

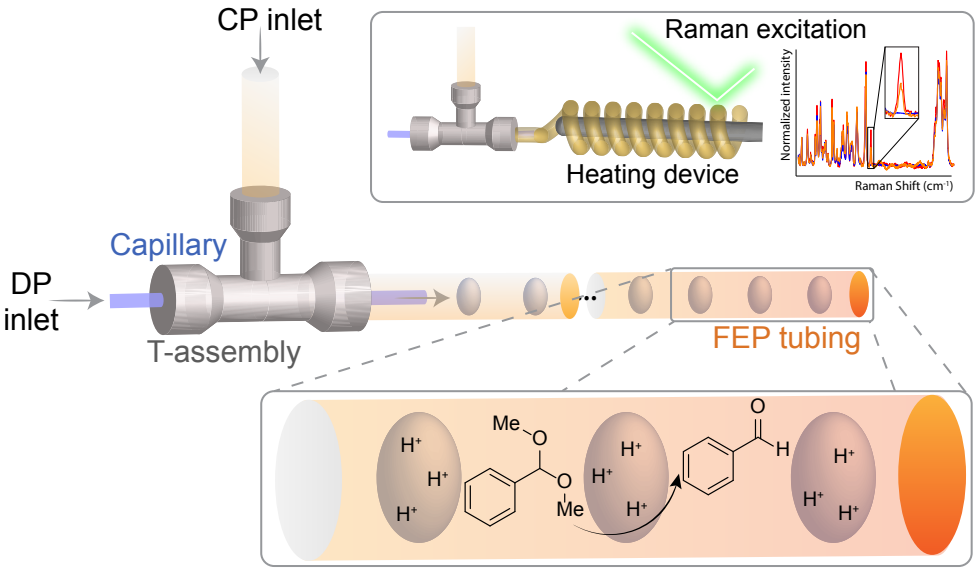

Figure 6.1: Droplet microfluidic approach for the tandem catalytic deacetalization-Knoevenagel condensation reaction with 4-propylguaiacol as continuous phase (CP) and water as dispersed phase (DP). Top inset: The deacetalization reaction can be monitored in-situ using Raman spectroscopy, bottom inset: schematic representation of the deacetalization-Knoevenagel condensation reaction inside the tubing.

microfluidic system, the acid-catalyzed deacetalization reaction could be followed in-situ with Raman spectroscopy. Tracking the C=O stretch vibration of the benzaldehyde product allowed kinetic profiles for this reaction at various temperatures using stabilized and non-stabilized droplets to be determined. Secondly, a positive effect of Pickering stabilization of a microfluidic flow system was shown for the antagonistic tandem reaction using ex-situ GC analysis.

6.2 Results and Discussion

A tube-in-tube co-flow microfluidic setup constructed with hydrophobic outer tubing (FEP) and hydrophilic inner tubing (fused silica) was used to create droplets, using acidic water as aqueous phase and 4-propylguaiacol (PG) as oil phase (Experimental procedure, Figure 6.7). This system configuration ensured that water-in-oil (w/o) droplets formed with a homogeneous size distribution, with or without the addition of solid emulsifiers. Although addition of silica to form the PE led to an increase in viscosity of the continuous phase, this did not change the droplet size significantly. In both systems spherical droplets with sizes approximately equal to the inner diameter of the tubing were observed. However, changes in composition of the reaction mixture possible led to different velocities of the droplets, in which case contact between two droplets could occur. Without addition of stabilizing particles this resulted in droplet coalescence, while in the PE system the droplets remained stable and no coalescence was observed.

The FPE system and reaction mixture were uniformly heated by coiling the tubing around a cylindrical heating device. Its temperature accuracy was tested using luminescence thermometry, using $NaYF_4$ particles doped with 18% Yb^{3+} and 2% Er^{3+} which were synthesized as described earlier.[35] As described by Geitenbeek *et al.* these particles can be used in various microfluidic systems to accurately determine the temperature inside the system.[36] The exact temperature inside the tubing was close to the temperature set on the heating device, showing a maximum deviation of 2.2 °C.

6.2.1 Deacetalization reaction followed by in-situ Raman spectroscopy

As shown in Figure 6.1, the deacetalization reaction was started with benzaldehyde dimethyl acetal in the organic phase which could be converted by contact with the acidic water droplets to form benzaldehyde. In order to obtain a proper droplet spacing, *i.e.* a space of one droplet diameter between two droplets, flow rates of 20 and 5 µL/min were used for the continuous organic and dispersed aqueous phases respectively. With the substrate and catalyst concentrations used, these flow rates resulted in 25 mol% of catalyst with respect to the substrate.

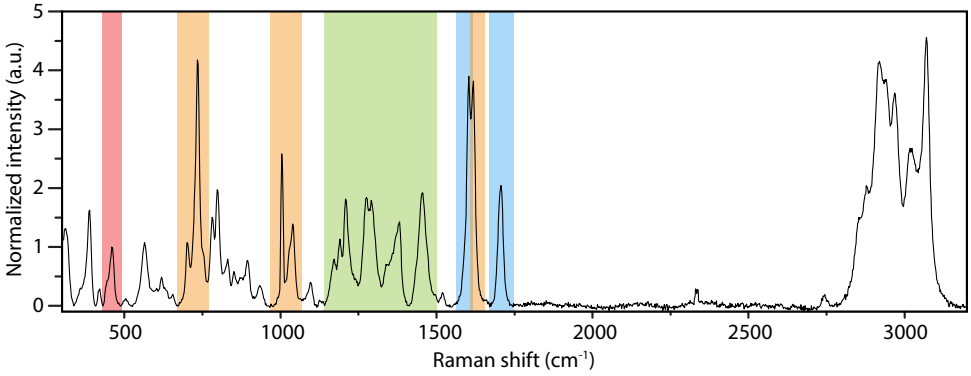

Figure 6.2: Full Raman spectrum of 1 M benzaldehyde (blue) and 0.5 M CCl_4 (red) in 4-propylguaiacol (orange) in measured through FEP tubing (green).

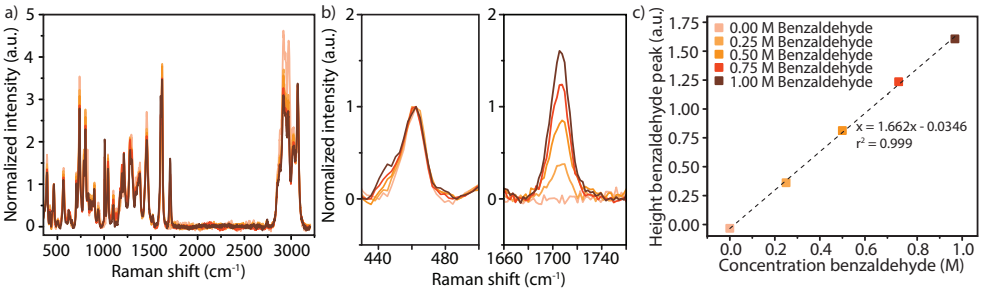

Figure 6.3: Calibration of benzaldehyde in Raman spectroscopy using 0.5 M CCl_4 as internal standard, a) full Raman spectra, b) Raman spectra of the CCl_4 peak at 460 cm^{-1} and benzaldehyde peak at 1700 cm^{-1}, c) calibration curve based on benzaldehyde peak at 1700 cm^{-1}.

Probing the reaction with a 532 nm in-situ Raman laser, gave a spectrum as shown in Figure 6.2. The FEP tubing has some very distinct peaks in the region 1150-1500 cm^{-1}, labeled with green, these peaks were used to ensure the correct focusing of the Raman laser inside the tubing. The PG solvent peaks are labeled in orange, showing the C-C chain vibration of the propyl side group at 750 cm^{-1}, and the C=C stretch vibrations at 1000 and 1600 cm^{-1} originated from the aromatic ring. These same ring vibration peaks are visible for benzaldehyde (blue), for which the 1600 cm^{-1} peak is slightly shifted to lower wavenumbers. The C=O stretch vibration of benzaldehyde shows a very distinct peak at 1700 cm^{-1}, therefore this peak was used for the quantification of benzaldehyde. Carbon tetrachloride (CCl_4), showing a distinct peak at 460 cm^{-1} (red), was added as internal standard. As the peaks of the substrate, benzaldehyde dimethyl acetal overlap with the solvent peaks, this compound could not be traced with Raman spectroscopy.

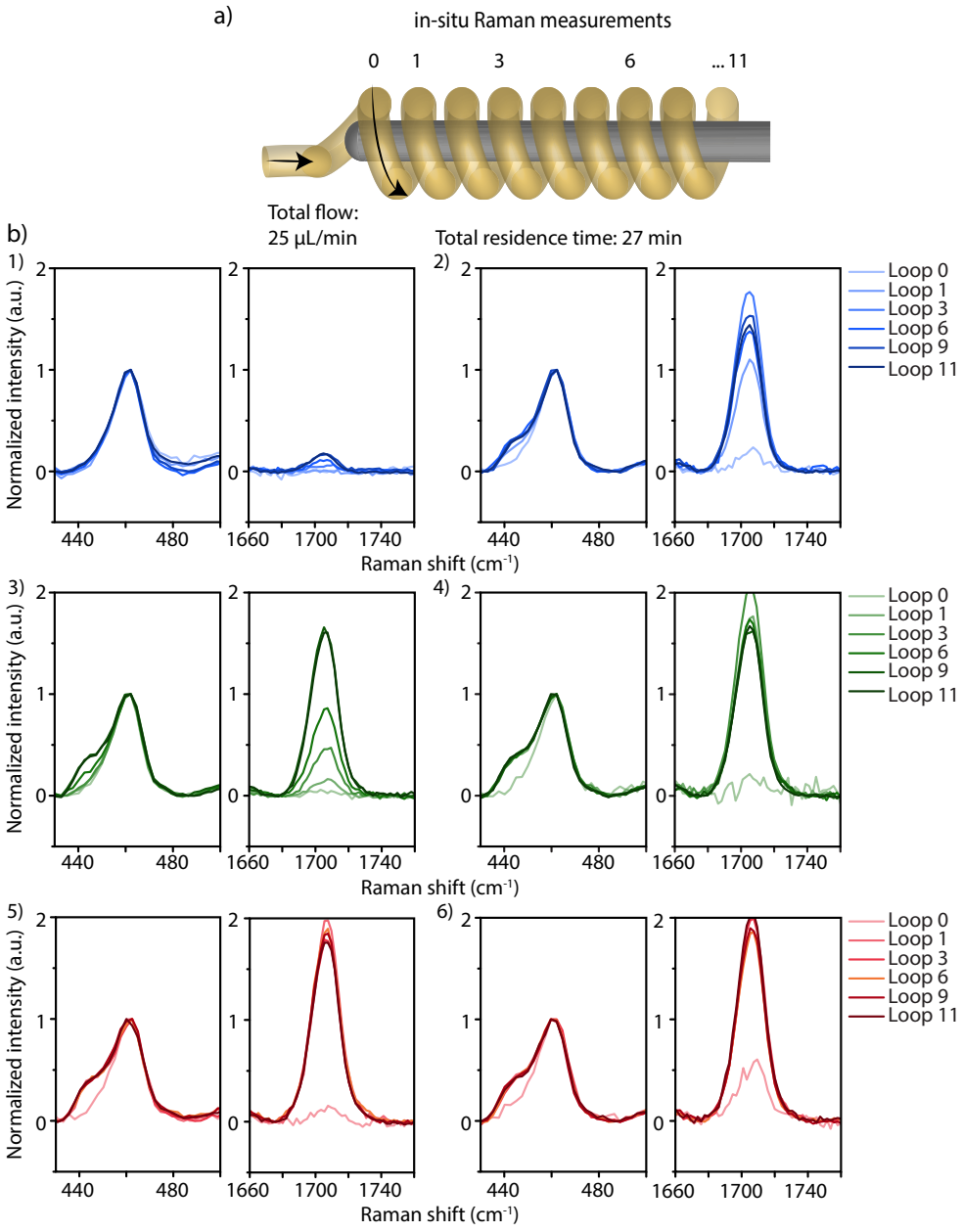

Figure 6.4: a) Schematic representation of the in-situ Raman spectroscopy analysis loops, b) online monitoring of the continuous phase (PE) deacetalization reaction: CCl_4 peak (460 cm^{-1}) and benzaldehyde peak (1700 cm^{-1}) in the Raman spectra at different positions in the tubing at room temperature (1, 2), 60 °C (3, 4) and 90 °C (5, 6) without silica (1, 3, 5) and with 2 wt% silica (2, 4, 6).

To obtain the correct benzaldehyde concentrations from the Raman spectra a calibration was performed. The full Raman spectra, zooms of the relevant Raman peaks at 460 and 1700 cm^{-1} and the resulting calibration curve, showing a linear response over the tested concentration range, are shown in Figure 6.3.

The catalytic reaction was followed in time by measuring at different loops of the tubing. At a total flow of 25 µL/min, the reaction time after each loop was approximately 2 min and the total reaction time was 27 minutes (Figure 6.4a). At loop 0, which is almost directly after droplet formation, the reaction time is 5 s. The presence of silica in the reaction mixture did not influence the Raman measurements. The Raman spectra as function of position in the tubing and temperature are shown in Figure 6.4b. In the Raman spectra at 60 and 90 °C, a shoulder originating from benzaldehyde can be observed at the 460 cm^{-1} peak, growing in concomitantly with the peak at 1700 cm^{-1}.[37]

The kinetic profiles of benzaldehyde formation at all temperatures and with and without silica are shown in Figure 6.5. At room temperature without any silica present, the reaction proceeds very slowly, yielding only 10% of benzaldehyde after 22 min. Increasing the reaction temperature from RT to 60 °C led to a significant increase in reaction rate, with full conversion reached after approximately 18 min. At 90 °C, full conversion is already reached after 2 min. Addition of silica to the reaction mixture had a clear positive effect on the reactions run at room temperature and 60 °C. At room temperature, silica addition resulted in a jump in activity, increasing the yield from 10% in the normal biphasic system (BS) to 90% in the PE after 22 min. At 60 °C full conversion was reached within 2 min, whereas for the BS only a 10% yield was observed after the same time. At 90 °C, the reaction was too fast to measure any differences between the BS and PE. A control experiment, with only silica and no HCl, showed no significant benzaldehyde formation,

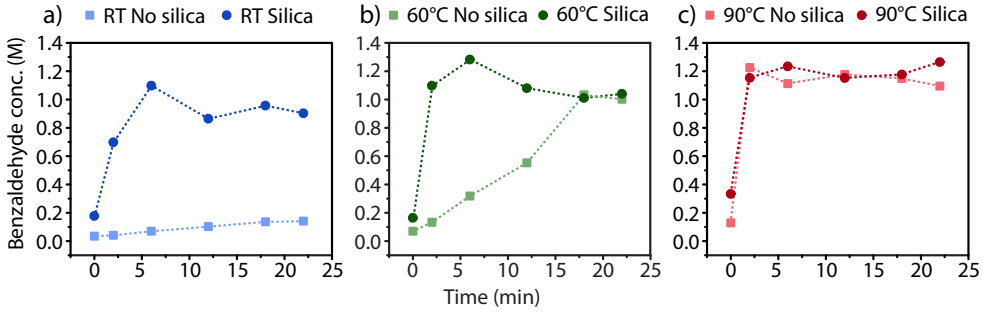

Figure 6.5: Concentration of benzaldehyde during the acid catalyzed deacetalization reaction of benzaldehyde dimethyl acetal followed over time by in-situ Raman spectroscopy at RT (a), 60 °C (b) and 90 °C (c). Reaction conditions: 1.0 M benzaldehyde dimethyl acetal and 0.5 M CCl_4 in 4-propylguaiacol (and 2 wt% silica), 0.1 M HCl in water, total flow 25 µL/min.

indicating that the higher droplet stability and therefore higher interfacial area in the PE are causing the enhanced reactivity.

This simple microfluidic setup thus enabled the facile, real-time analysis of a reaction in a continuous flow catalytic BS or PE system, in this case the deacetalization of benzaldehyde dimethyl acetal, demonstrating the advantage of using PEs for biphasic catalysis. The use of in-situ Raman spectroscopy eliminates the need for (time consuming) work-up procedures as are used for batch BS and PEs, resulting in more opportunities for data collection and more accurate kinetic profiles.

6.2.2 Antagonistic tandem catalytic deacetalization-Knoevenagel condensation reaction

After investigating the single acid-catalyzed reaction, the effect of silica addition on the performance of the antagonistic tandem catalytic reaction from benzaldehyde dimethyl acetal to benzylidene malononitrile was studied. As the destructive and unwanted reaction between acids and bases is a very fast process, droplet stabilization by addition of silica was expected to be beneficial for this tandem reaction as this hinders instant acid-base recombination by the formation of a physical barrier, a phenomenon that was also observed in the batch PE reactions.[23,24]

The use of excess of the second substrate, malononitrile, and addition of the base catalyst, 2-(1-ethylpropyl)piperidine, resulted in a slight increase of the viscosity of the organic phase. As a result, the droplets formed were found to be unstable at the flow rates that were used for the deacetalization reaction. To again obtain a similar droplet spacing and a stable system, the flow rates were adjusted to 10 µL/min for the aqueous and 10 µL/min for the organic phase, giving a total reaction time of 34 min. As the Knoevenagel condensation reaction is rather slow at room temperature[23], the tandem reaction was carried out at 90 °C. The molar ratio of acid and base catalyst with respect to the substrate was screened and a combination of 20 mol% acid and 10 mol% base was determined to be the most effective. The product distribution of the tandem catalytic reactions under these conditions, in the FBS and FPE are shown in Figure 6.6. Unfortunately, deprotonated malononitrile is highly fluorescent when irradiated with the Raman laser, making in-situ analysis with Raman spectroscopy impossible for this reaction.

In the FBS, *i.e.* the reaction mixture without any stabilizing particles added, only 34% of the substrate benzaldehyde dimethyl acetal was converted, resulting in yields of the intermediate benzaldehyde and the final product benzylidene malononitrile of 10% and 17% respectively. The use of an FPE system proved highly beneficial, as full conversion of benzaldehyde dimethyl acetal could be achieved under identical conditions, with

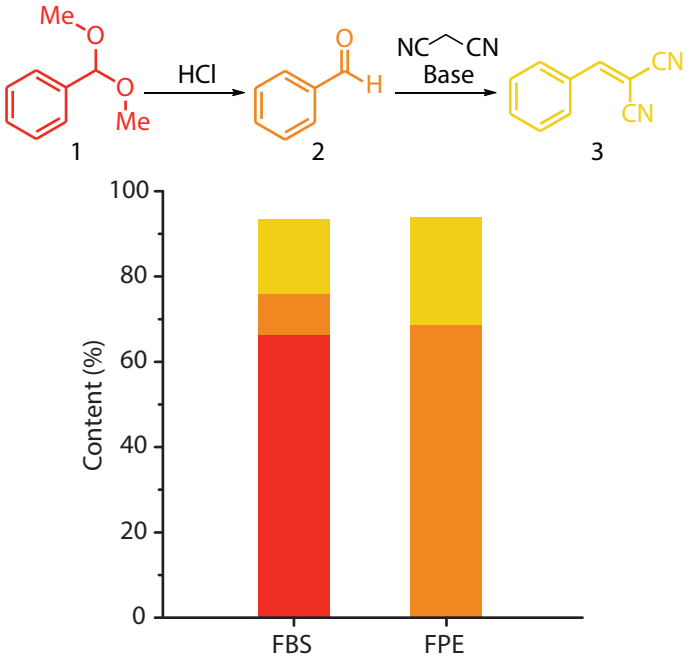

Figure 6.6: Product distribution compared to the starting amount 1 of the tandem catalytic reaction without (FBS) and with addition of silica (FPE). Red bars show of benzaldehyde dimethyl acetal (1), orange bars benzaldehyde (2) and yellow bars benzylidene malononitrile (3) content in the sample. Reaction conditions: 0.16 M 1, 0.4 M malononitrile, 0.016 M 2-(1-ethylpropyl)piperidine in 4-propylguaiacol, 0.032 M HCl in water, T = 90 °C, total flow: 20 µL/min, reaction time: 34 min. Addition of silica: 2 wt% with respect to organic phase.

69% benzaldehyde and 25% final product, benzylidene malononitrile. The yield of final product is limited in this case by the available short reaction time, dictated by the number of loops that could be coiled around the heating device. Residence time of the reactants in the microchannel can, however, in principle be extended by simply extending the tube length.

Again, the use of stabilizing particles showed to be beneficial for the performance of flow biphasic catalysis. Reaction mixtures are easily separable after leaving the microfluidic setup, resulting in an easier work-up procedure compared to conventional batch PEs. Previously reported examples of flow PEs e.g. as described by Yang *et al.* required vigorous stirring for PE preparation resulting in broad droplet distributions while in this droplet microfluidic setup the droplet size is determined by the diameter of the tubing, producing monodisperse droplets.

6.3 Conclusions

In conclusion, we report the first use of a tube-in-tube co-flow microfluidic setup for continuous flow BS and PE reactions. The formation of an FPE by addition of silica stabilizing particles, led to an increase in stability of the w/o droplets. This increased stability was shown to be beneficial for the reactivity of the system. The use of transparent tubing enabled reaction monitoring by in-situ Raman spectroscopy. As the residence time of the reaction mixture inside the tubing corresponds with the reaction time, this setup allowed for the analysis of reaction progress over time by recording Raman spectra at different positions in the tubing.

The acid catalyzed deacetalization reaction of benzaldehyde dimethyl acetal performed much better in an FPE than in the FBS. This effect was most pronounced at room temperature where a ninefold increase in yield was observed. At 60 °C the Pickering stabilization lead to a 9-times increase in yield after 2 min. At 90 °C the reaction occurs instantly, and no difference was observed between the BS and PE. The higher reactivity of the PE was attributed to high droplet stability as this is correlated to the high interfacial area which is required for this reaction.

The formation of FPE was also beneficial for the performance of the antagonistic deacetalization-Knoevenagel condensation tandem reaction of benzaldehyde dimethyl acetal to benzylidene malononitrile. In the FBS low conversion of the substrate was observed as fast acid-base quenching occurred. Pickering stabilization however, inhibited the mutual destruction of acid and base catalyst which resulted in full conversion of the substrate. The yield of end product could be increased by elongation of the reaction time.

6.4 Experimental procedures

6.4.1 Chemicals and Materials

All chemicals were used as received without any further purification. Benzaldehyde dimethyl acetal (≥ 98%), benzylidene malononitrile (98%), hydrochloric acid (37%, analytical grade), 2-(1-ethylpropyl)piperidine and 4-propylguaiacol (>99%) were obtained via Sigma-Aldrich. Malononitrile (99%), carbon tetrachloride (p.a) and anisole (99%) were obtained from Acros Organics. Benzaldehyde (≥ 99%) was obtained from Fluka Analytical. Hydrophobic silica (HDK® H20) was obtained from Wacker Chemie.

6.4.2 Microfluidic Setup

The droplet microfluidic setup was built using FEP tubing (OD 1/16", ID 1/32") and fused silica capillary tubing (OD 360 µm, ID 100 µm) in a coaxial flow geometry using an IDEC T-assembly (P-712), as shown in Figure 6.7. After the coaxial junction, 150 cm of the FEP tubing was coiled around a cylindrical heating device (Max Pro Twist 32 mm) of which the temperature could be regulated per 5 °C between 60 and 180 °C. The two liquid phases were introduced using two ProSense NE1000 syringe pump, equipped with 5 mL polypropylene syringes, at flow rates of 20 and 5 µL/min for the aqueous and organic phase, respectively.

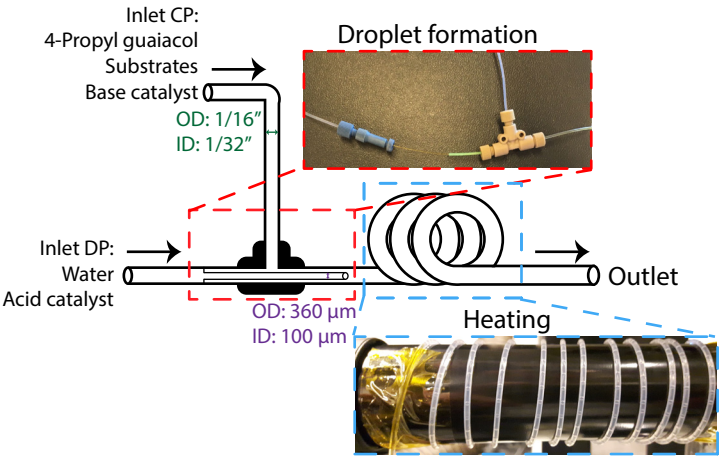

Figure 6.7: Schematic representation of the microfluidic setup illustrating the dimensions of the tubing and the combination of T-assembly to the tubing. All inlets are connected to syringes driven by syringe pumps. Top image shows the configuration at the T-assembly where droplets are formed, bottom picture shows how tubing was coiled around the heating device.

6.4.3 Thermoluminescence Measurements

A dispersion of NaYF4 particles, prepared according to Geitenbeek *et al.*, in cyclohexane was brought inside the microfluidic setup, allowing the relevant temperature setting for the PE experiments to be determined.[35,36] To exclude any influence of the solvent on the heat transfer, the system was allowed to equilibrate before measurement. The luminescence experiments were performed using an MDL-III laser of 500 mW with an excitation wavelength of 980 nm. Upon excitation, light was collected via a fiber patch chord and a short pass filter on an OceanOptics QEPro CCD. The temperature was measured at 7 different setpoints and several positions along the microchannel, resulting in a maximum deviation of 2.2 K from the set temperature (see Table 6.1), which is within

the error margin for this method.[35]

Table 6.1: Temperature measured inside the tubing using luminescence thermometry

T_{set} (°C)	$T_{measured}$ (°C)
RT	29.4
60	60.1
65	66.3
70	69.6
75	73.8
80	77.8

6.4.4 Deacetalization Reaction

In the acid-catalyzed deacetalization reactions, the organic phase consisted of 1 M benzaldehyde dimethyl acetal and 0.5 M CCl_4 (as internal standard) in 4-propylguaiacol. These experiments were followed over time by Raman spectroscopy. In experiments with silica, 2 wt% HDK® H20 with respect to the organic phase was dispersed in the 4-propylguaiacol mixture using a VCX 130 Vibra-Cell Ultrasonic Processor equipped with a 3 mm diameter tip (Sonics, 20 kHz, 10 W, 2 min). The aqueous phase contained 0.1 M HCl in water. The reaction was followed over time with Raman spectra being collected at different loops of the tubing coiled around the heating device. Due to the length of the tubing, the diameter of the heating device and the total flow of 25 µL/min used, every loop represented approximately 2 min of reaction time. Raman spectra were taken at loop 0 (directly after droplet formation), loop 1, loop 3, loop 6, loop 9 and loop 11. To avoid any influence of acid staining of the FEP tubing on the reactions, the system was flushed with NaOH solution and water between measurements at different temperatures. The Raman spectra were obtained with a Renishaw InVia Raman microscope, using a 532 nm laser through a 50x objective and a laser power of 50%. A sequence of 5 accumulated scans of 10 s exposure time were recorded on a CCD, taken over an extended range of 300 to 3200 cm^{-1} and using a grating of 1200 lines per mm. The spectra were baseline corrected manually and normalized on the CCl_4 peak at 460 cm^{-1}. To obtain the benzaldehyde concentrations, calibration standards of known concentration were made and measured.

6.4.5 Deacetalization-Knoevenagel Condensation Tandem reaction

The organic phase contained 0.16 M benzaldehyde dimethyl acetal, 0.016 M 2-(1-ethylpropyl)piperidine and 0.09 M anisole (as internal standard for GC) in 4-propylguaiacol. In experiments with silica, 2 wt% HDK® H20 silica was dispersed as described before. The aqueous phase contained 0.032 M HCl in tap water. The droplets

were formed using a flow rate ratio of 10 to 10 µL/min of organic to aqueous phase, pumped by a ProSense NE-1000 syringe pump. The reaction mixtures were collected at the end of the tubing in a vial containing HCl to separate the organic and aqueous phase directly, this vial was cooled in an ice bath to stop the reaction. After collection of the sample, the organic phase was filtered over a syringe filter to remove any silica or other contaminants. The sample was directly analyzed with GC (Varian GC equipped with a VF-5 ms capillary column and an FID).

Acknowledgements

Thomas van Swieten (Soft Condensed Matter, Utrecht University) is acknowledged for his help with the thermoluminescence experiments. Dr. Jeroen Vollenbroek (Biomedical and Environmental Sensorsystems, University of Twente) and Dr. Mathieu Odijk (UT) are acknowledged for their input and fruitful discussions. This work was supported by a VIDI grant of the Dutch Research Council (NWO) as well as by the Netherlands Center for Multiscale Catalytic Energy Conversion (MCEC), an NWO gravitation program funded by the Ministry of Education, Culture and Science of the government of the Netherlands and by the Dutch Research Council (NWO).

References

1 W. Keim, *Angew. Chem.- Int. Ed.*, **2013**, *52*, 12492.
2 C. W. Kohlpaintner, R. W. Fischer and B. Cornils, *Appl. Catal. A Gen.*, **2001**, *221*, 219.
3 Y. J. Pagán-Torres, T. Wang, J. M. R. Gallo, B. H. Shanks and J. A. Dumesic, *ACS Catal.*, **2012**, *2*, 930.
4 D. S. Flett, *Acc. Chem. Res.*, **1977**, *10*, 99.
5 L. Wei, M. Zhang, X. Zhang, H. Xin and H. Yang, *ACS Sustain. Chem. Eng.*, **2016**, *4*, 6838.
6 Y. Chevalier and M. A. Bolzinger, *Colloids Surfaces A Physicochem. Eng. Asp.*, **2013**, *439*, 23.
7 R. Aveyard, B. P. Binks and J. H. Clint, *Adv. Colloid Interface Sci.*, **2003**, *100–102*, 503.
8 F. Tu and D. Lee, *J. Am. Chem. Soc.*, **2014**, *136*, 9999.
9 W.-L. Jiang, Q.-J. Fu, B.-J. Yao, L.-G. Ding, C.-X. Liu and Y.-B. Dong, *ACS Appl. Mater. Interfaces*, **2017**, *9*, 36438.
10 J. Huang, F. Cheng, B. P. Binks and H. Yang, *J. Am. Chem. Soc.*, **2015**, *137*, 15015.
11 D. Suzuki and H. Kawaguchi, *Colloid Polym. Sci.*, **2006**, *284*, 1443.
12 H. Kim, J. J. Cho, J. J. Cho, B. J. Park and J. W. Kim, *ACS Appl. Mater. Interfaces*, **2018**, *10*, 1408.

13 N. M. Briggs, J. S. Weston, B. Li, D. Venkataramani, C. P. Aichele, J. H. Harwell and S. P. Crossley, *Langmuir*, **2015**, *31*, 13077.
14 M. Shen and D. E. Resasco, *Langmuir*, **2009**, *25*, 10843.
15 M. Zhang, A. Wang, J. Li, N. Song, Y. Song and R. He, *Mater. Sci. Eng. C*, **2017**, *70*, 396.
16 D. E. Tambe and M. M. Sharma, *J. Colloid Interface Sci.*, **1993**, *157*, 244.
17 B. P. Binks and S. O. Lumsdon, *Langmuir*, **2000**, *16*, 8622.
18 B. P. Binks, J. Philip and J. A. Rodrigues, *Langmuir*, **2005**, *21*, 3296.
19 C. Albert, M. Beladjine, N. Tsapis, E. Fattal, F. Agnely and N. Huang, *J. Control. Release*, **2019**, *309*, 302.
20 Y. Chi, S. T. Scroggins and J. M. J. Fréchet, *J. Am. Chem. Soc.*, **2008**, *130*, 6322.
21 J. Faria, M. Pilar Ruiz and D. E. Resasco, *ACS Catal.*, **2015**, *5*, 4761.
22 J. Faria, M. P. Ruiz and D. E. Resasco, *Adv. Synth. Catal.*, **2010**, *352*, 2359.
23 C. M. Vis, L. C. J. Smulders and P. C. A. Bruijnincx, *ChemSusChem*, **2019**, *12*, 2176.
24 H. Yang, L. Fu, L. Wei, J. Liang and B. P. Binks, *J. Am. Chem. Soc.*, **2015**, *137*, 1362.
25 H. Chen, H. Zou, Y. Hao and H. Yang, *ChemSusChem*, **2017**, *10*, 1989.
26 M. Zhang, L. Wei, H. Chen, Z. Du, B. P. Binks and H. Yang, *J. Am. Chem. Soc.*, **2016**, *138*, 10173.
27 X. Casadevall i Solvas and A. deMello, *Chem. Commun.*, **2011**, *47*, 1936.
28 C. N. Baroud, F. Gallaire and R. Dangla, *Lab Chip*, **2010**, *10*, 2032.
29 C. Priest, M. D. Reid and C. P. Whitby, *J. Colloid Interface Sci.*, **2011**, *363*, 301.
30 Z. Nie, Z. Nie, J. Il Park, J. Il Park, W. Li, W. Li, S. a F. Bon, S. a F. Bon, E. Kumacheva and E. Kumacheva, *J. Am. Chem. Soc.*, **2008**, *130*, 16508.
31 M. Pan, L. Rosenfeld, M. Kim, M. Xu, E. Lin, R. Derda and S. K. Y. Tang, *ACS Appl. Mater. Interfaces*, **2014**, *6*, 21446.
32 A. Schröder, J. Sprakel, K. Schroën, J. N. Spaen and C. C. Berton-Carabin, *J. Food Eng.*, **2018**, *234*, 63.
33 R. Al nuumani, G. T. Vladisavljević, M. Kasprzak and B. Wolf, *J. Food Eng.*, **2020**, *267*, 109701.
34 Q. Y. Xu, M. Nakajima and B. P. Binks, *Colloids Surfaces A Physicochem. Eng. Asp.*, **2005**, *262*, 94.
35 R. G. Geitenbeek, P. T. Prins, W. Albrecht, A. Van Blaaderen, B. M. Weckhuysen and A. Meijerink, *J. Phys. Chem. C*, **2017**, *121*, 3503.
36 R. G. Geitenbeek, J. C. Vollenbroek, H. M. H. Weijgertze, C. B. M. Tregouet, A.-E. Nieuwelink, C. L. Kennedy, B. M. Weckhhuysen, D. Lohse, A. van Blaaderen, A. van den Berg, M. Odijk and A. Meijerink, *Lab Chip*, **2019**, *19*, 1236.
37 WinChembase, Raman spectrum Benzaldehyde, https://www.chemicalbook.com/SpectrumEN_100-52-7_Raman.htm, (accessed 27 March 2020).

Chapter 7

Summary, Concluding Remarks and Outlook

7.1 Summary

The work in this PhD Thesis focused on the separation of incompatible reagents and catalysts in Pickering Emulsions (PEs) as compartmentalized reaction media, inspired by nature's strategy of compartmentalization. For instance, a living cell contains all kind of physically separated compartments in which multiple parallel and consecutive reactions can take place without interfering with each other. Here, we use PEs to mimic this strategy, emulsions stabilized by solid micro- or nanoparticles rather than surfactants as is the case for classical emulsions. The benefit of using PEs over classical emulsions, is the higher stability of the former, due to the strong adsorption of the particles at the liquid-liquid interface. Two general types of PEs can be distinguished, the water-in-oil (w/o) and the oil-in-water (o/w) type of emulsion. Which type of emulsion is obtained, depends on the wettability of the particles, and therefore on the contact angle of the particles with the liquid phases. Hydrophobic stabilizing particles are more easily wetted by oil than by water, resulting in a contact angle > 90° with water, giving w/o PEs. The opposite is the case for hydrophilic particles. All research described in this PhD Thesis was performed in w/o PEs stabilized by (partially) hydrophobic silica particles.

In Chapter 2 the ability for compartmentalization was demonstrated by performing a simple acid-base catalyzed probe reaction. W/o PEs were formulated with toluene as continuous organic phase and water as dispersed aqueous phase, stabilized by commercially available hydrophobic fumed silica. The deacetalization-Knoevenagel condensation reaction of benzaldehyde dimethyl acetal was chosen as probe reaction as this reaction is fast and can be performed at room temperature. The acid catalyst was confined in the aqueous phase while the reagents and base catalysts were located in the organic phase. The higher interfacial area of the PEs relative to conventional biphasic systems (BS), showed to be of great importance for the single deacetalization reaction as the reaction proceeded much faster in PEs. The antagonistic tandem catalytic reaction was performed in both static BS and PEs using different acid-base ratios. The PEs clearly outperformed the BS as mutual destruction of acid and base catalysts occurred instantly in the BS while in the PE 76% of product was obtained using equimolar amounts of acid and base catalysts. These results showed that PEs are promising reaction media for antagonistic tandem reactions.

In Chapter 3 and Chapter 4 the use of PEs formulated with alkylphenols as reaction media for tandem (catalytic) conversion of fructose was explored. The acid-catalyzed dehydration of fructose to 5-(hydroxymethyl)furfural (5-HMF), a compound that is considered an important platform molecule for the production of biobased chemicals, suffers from low yields due to the large amounts of side products that are typically formed. Indeed, 5-HMF is very susceptible towards further dehydration or polymerization induced by the acid

catalyst. By extracting 5-HMF from the reactive aqueous phase to an organic phase during reaction, this side product formation can be reduced.

Previously, multiple studies identified alkylphenols as very efficient 5-HMF extracting solvents and we therefore chose these alkylphenols as oil phase for the PE catalysis studies. In Chapter 3 the stability of PEs formulated with 2-*iso*propylphenol (IPP), 4-propylguaiacol (PG) and 2-sec-butylphenol (SBP) as organic phases was studied. First, a theoretical assessment of the stability was made based on measured physicochemical properties of the solvents, such as three-phase contact angle, interfacial tension and viscosity, suggesting that SBP and PG would give the most and least stable PEs, respectively. However, due to the small differences in the physicochemical properties between the three alkylphenols, no difference in stability was observed in the experimental study. The stability was experimentally studied as a function of solid stabilizer concentration, salinity and pH of the aqueous phase, temperature and pressure. PEs stabilized with 2 wt% hydrophobic fumed silica were found to be stable for over a month at room temperature. Using an acidic aqueous phase (pH 2) with high salt concentrations (30 wt% NaCl), conditions relevant for catalytic sugar dehydration reactions, did not affect the stability. The PEs were also moderately stable for at least 1 day at 100 °C under atmospheric pressure. The influence of the interfacial area of BS on the extraction of 5-HMF was tested in stirred and non-stirred BS with the three alkylphenols. In the stirred, high interfacial area, BS, high 5-HMF extractions were obtained within 30 min. IPP showed the highest extraction capacity with all 5-HMF being extracted to the organic phase, followed by SBP (91%) and PG (84%). Expectedly, in the non-stirred, low interfacial area BS, considerably less 5-HMF could be extracted. The results obtained with the high interfacial area BS with alkylphenols as organic phase, used here as model for the PEs, seemed very promising for PE tandem (catalytic) reactions starting from fructose.

In Chapter 4 the alkylphenol formulated PEs were tested as reaction media for fructose dehydration and subsequent Knoevenagel condensation reactions. The performance of the PEs for the single fructose dehydration reaction was compared to that of conventional, non-stirred BS. The PEs outperformed the BS in terms of fructose dehydration and 5-HMF extraction. This high extraction rate could then be utilized for subsequent reactions by putting a second substrate (and catalyst) in the organic phase. Meldrum's acid was tested as substrate for a non-catalytic Knoevenagel condensation reaction, but its hydrolysis hampered the execution of the tandem reaction. The use of the less activated Knoevenagel substrate diethyl malonate, asked for the use of a base catalyst. The combined antagonistic dehydration-Knoevenagel condensation tandem catalytic reaction proved, again, to only be possible in PEs. In the BS mutual destruction of acid and base catalyst was observed, while after optimization of reaction conditions 24% of product could be obtained in the

PE with 27% of the intermediate 5-HMF.

While the previous chapters dealt with homogeneous catalysts, a heterogeneous approach was demonstrated in Chapter 5. Monodisperse silica particles were prepared using the Stöber method, and monofunctionalized acid or base groups. Besides these monofunctional particles, bifunctional Janus particles, with one patch being hydrophilic and acidic and the other being hydrophobic and basic, were synthesized for the first time. Due to the hydrophilic and hydrophobic sides of the particles, the particles are trapped at the interface and the catalysts are located in the liquid phase where they are needed. All particles were used as catalytic stabilizing particles for the acid-base catalyzed dehydration-Knoevenagel condensation reaction of fructose. The use of monofunctionalized particles as catalytic stabilizing particles led to some practical issues, as quenching occurred during PE preparation, which was solved by addition of a protecting group. The use of the Janus particles resulted in active reaction systems for the antagonistic dehydration-Knoevenagel condensation of fructose. Further improvements in catalytic performance will require optimization of the acid-base ratio on the particles.

A continuous flow approach for PE catalysis using droplet microfluidics was demonstrated in Chapter 6. A tube-in-tube co-flow microfluidic setup was used for the preparation of w/o droplets. Due to the laminar flow inside the small tubing, stable droplets could be made with or without addition of stabilizing particles. However, non-stabilized droplets could coalesce upon collision while stabilized droplets stay intact. This droplet microfluidic setup was used for the execution of deacetalization and deacetalization-Knoevenagel condensation reactions of benzaldehyde dimethyl acetal. The transparent tubing enabled in-situ analysis of the deacetalization reaction with Raman spectroscopy, allowing the reactions to be monitored directly as function of residence time. In typical batch setups this cannot be done as the particles stabilizing the droplets scatter incoming light hampering spectroscopic analysis. Similar as was shown in Chapter 2, droplet stabilization by solid emulsifiers led to an increase of the reaction rate for the deacetalization reaction. Without addition of stabilizing particles, the antagonistic deacetalization-Knoevenagel condensation reaction could not be performed, as mutual destruction of acid and base catalysts occurred. The use of Pickering stabilizing particles resulted in full substrate conversion and 34% of product yield.

7.2 Concluding remarks

In this thesis we have shown some applications and benefits of the use of PEs as reaction media for catalysis. First the advantage of using PEs for antagonistic tandem reactions was shown with a simple acid-base probe reaction in Chapter 2. The use of stabilizing

particles resulted in the formation of a physical boundary between the aqueous and organic phase, confining the acid and base catalysts, respectively. This physical boundary inhibited full mutual destruction of acid and base catalysts and allowed the antagonistic tandem catalytic reaction to be performed.

To broaden the window of operation of catalysis in PEs, more demanding reactions, in view of PE composition and reaction temperature were tested, such as the fructose dehydration and subsequent conversion of 5-HMF. For these reactions, w/o PEs formulated with alkylphenol solvents were employed, as a new type of PE system. The PEs proved to be stable under the required reaction conditions, i.e. at elevated reaction temperature, high salinity of aqueous phase and low pH. However, acid-base quenching was more severe and unavoidable at the elevated reaction temperatures, something that could be partially solved by postponing the addition of base catalyst. Another strategy to prevent acid-base quenching is by using bifunctional Janus particles as was done in Chapter 5.

Performing catalytic reactions in a continuous flow system, rather than in batch systems, enables control over residence time and concentrations of reagents and catalysts and of course a continuous means of production. Besides that, reactions performed in batch PEs can only be analyzed ex-situ as the PEs require destabilization in order to determine substrate and product concentrations in both phases. In Chapter 6, a droplet microfluidic approach was shown for performing catalytic conversions in continuous flow PEs and enabling in-situ analysis by Raman spectroscopy.

7.3 Outlook

With the work described in this thesis we have shown some new applications for PEs as compartmentalized reaction media for catalysis, a novel and emerging field of research. Although progress has been made in broadening the window of application of these PEs, both in type and in operating conditions, advances on the topic of reaction scope, stabilizing materials and process design are still required to make the use of PEs viable on larger scale. Here, we will discuss some research directions that address some of the open challenges in these three aspects of PE catalysis.

7.3.1 Advances in reactivity

In Chapters 2-4 we demonstrated that PEs do allow for the execution of antagonistic tandem catalytic reactions using homogeneous catalysts, but it is also clear that substrate conversions and product yields are yet to be improved. Especially performing reactions at elevated temperatures mutual destruction of antagonistic catalysts is a serious issue,

hampering catalytic performance. Limiting the reaction temperature may therefore lead to better tandem reaction performance. Recently, Held *et al.* reported that on the replacement of the aqueous phase of a biphasic system, with an ionic liquid, which lowered the required reaction temperature for fructose dehydration reaction to 70 °C[1], which may reduce the acid-base quenching. Another hypothetical method to reduce homogeneous catalyst quenching could be by making a more rigid layer of particles around the droplet, for instance by cross-linking the stabilizing particles as was done by Schmidt *et al.* for w/w emulsions.[2] The PEs, after cross-linking polydopamine particles, showed to be much more stable than without cross-linking. However, a cross-linked, less porous, shell around the droplets would be disadvantageous for the extraction of products from the dispersed to the continuous phase. A better solution would be to use positively charged particles, such as the positively charged polystyrene particles described by Shen *et al.*[3], to stabilize the acidic aqueous droplets, creating a proton gradient throughout the droplet with low proton concentrations at the liquid-liquid interface and high proton concentrations in the bulk phase. This would decrease acid-base interaction at the interface while keeping the reactivity inside the droplets.

In this PhD Thesis we have focused on the use of PEs for acid-base catalyzed reactions, however, this approach can be applied much more broadly. In thermoregulated phase-transfer biphasic catalysis, compartmentalization has already been used, for example, as strategy confining homogeneous catalysts in the aqueous phase.[4] PEs could be applied here to increase the interfacial area during reaction, after which the catalyst can be separated from the products and be reused. Another class of reactions that could benefit from using w/o PEs as reaction medium are reactions in which water is used as a reagent or the so-called "on-water" reactions.[5] For reactions using water as a reagent, the reaction could then be run such that it is self-terminating when the droplets are depleted, resulting in a product phase without any phase separation.

7.3.2 Advances in stabilizing materials

In Chapter 5 we developed a new class of catalytic stabilizing particles in the form of acid-base Janus particles. While these particles did show catalytic activity, the acid-base balance of the particles was not yet optimal, resulting in modest substrate conversions and product yields. As the particles were prepared via the solidified wax method, the area of the particle trapped inside the wax determines the balance between the polar and apolar surface areas that can be synthetically addressed, and therefore the balance between acid and base groups on the surface of the resulting Janus particle. The polar/apolar ratio of the particles could therefore be tuned by changing the area trapped inside the wax colloidosome, which can be achieved by tuning the hydrophobicity of the

particles before colloidosome preparation.[6] Functionalization of silica Janus particles is of course not limited to acid and base groups. Resasco *et al.* reported on the use of Pd-containing Janus particles which were utilized for phase-selective hydrogenation.[7] By functionalizing the other side of the Janus particles with another catalyst, for instance an acid catalyst, these particles can be used as Pickering stabilizing particles for dehydration-hydrogenation reactions of fructose, resulting in products that can be used as building blocks for polymerizations.[8] As there are many examples of catalyst grafted on silica, many more bifunctional catalytic Janus particles can be imagined. In Chapter 1, we discussed the use of responsive PE stabilizing particles, for example. Such functionality, e.g. temperature or magnetic field responsiveness, could be added to the Janus particles to make switchable, bifunctional reaction systems. The use of polymer-based particles would be very interesting to use as Pickering stabilizer. As also noted above, by cross-linking the polymers after PE formation, a permanent PE could be formed.[2] In this case, the droplets can be easily removed from the reaction phase, e.g. by filtration, and immediately used in a new continuous phase, containing fresh substrate. These permanent PEs could in principle also be used for continuous flow processes.

7.3.3 Advances in process design

Using PEs as compartmentalized reaction media also opens opportunities on the side of process design. By confining a catalyst in the dispersed phase of a PE a homogeneous analogue can be constructed of a continuous plug-flow reactor, such as those commonly used in heterogeneous catalysis. This method offers a new way of immobilizing homogeneous catalysts and has the advantage of higher space-time yields, as well as the ability to analyze the stability of the system and the influence of different reaction parameters without having to destroy the PE by destabilization. Recently, the first exciting examples of this approach have been reported by the groups of Yang[9,10] and Song[11]. Quite some experimental challenges remain to be addressed though to fully exploit the potential continuous flow PE catalysis. Using bulk PE flow setups, the flow of the continuous phase over the catalyst containing dispersed phase is determined by gravitational forces and the droplet size, therefore changing the flow during reaction is not trivial. Small droplets result in a condensed packing of the column, resulting in a lower flow than with larger droplets. As PEs are usually prepared by fast stirring, a polydisperse droplet size distribution is obtained which can differ per preparation cycle, resulting in different flow behavior in every experiment. A method in which flow behavior and droplet size can in fact be carefully controlled is by making use of droplet microfluidics, a rapidly growing field of research. Droplet microfluidics offers many possibilities for use as PE reaction system. The reaction conditions can be easily controlled by factors inside the reactor, e.g. by tuning the flow of the two phases, or by factors outside the reactor,

e.g. by changing the temperature or by applying an external (e.g. magnetic) field.[12,13] Another advantage of microfluidic devices, is the ability to do sequential reactions by placing multiple reactors in series.[14,15] We have employed a droplet microfluidic setup to monitor reactions with in-situ analysis methods, as described in Chapter 6. This strategy does not only allow monitoring the progress of catalytic reactions, but can also be used to monitor physicochemical changes in a reaction mixture, including transport phenomena such as liquid-liquid extraction.[16] Microfluidic setups are thus promising in their own right as reactor configuration for PE catalysis and can serve as very useful model systems to study processes occurring when chemistry or catalysis is done in bulk PE. Furthermore, droplet microfluidics can also aid our understanding of the formation and compositional evolution of PEs. In the next section we show some preliminary work on the combined use of droplet microfluidics and microscopy to study the formation and stabilization of PEs.

7.3.4 PE formation and stabilization in droplet microfluidics

Knowledge on and control over the stability of PEs is of great importance to further their application as reaction media for catalysis. Macroscopic stability can be studied by observing and measuring the emulsion phase over time as was for example done in Chapter 3 of this PhD Thesis. However, studying the stability on a microscopic scale, i.e. investigating coalescence of neighboring droplets or particle attaching and detaching, is more challenging. Sampling from a bulk PE with a needle, pipette or spatula result in breaking of the droplets due to squeezing and any sample obtained may thus not be representative for the PE under study. Therefore, a method for the generation of Pickering stabilized droplets with the possibility for in-situ analysis of the stability should be developed. One such a method could be found in microfluidics.

In Chapter 6, we showed that Pickering stabilized droplets can easily and very homogeneously be generated in a microfluidic device. However, the setup used, a tube-in-tube co-flow reactor, did not allow for the collection of these solid-stabilized droplets for further observation. Another, often-used microfluidic approach may be better suited for this, i.e. to use a microfluidic chip,[17] e.g. one made of cheap and easily moldable polydimethylsiloxane (PDMS). In these chips droplet generation usually proceeds via the T-junction or flow-focusing channel geometry (Figure 7.1).[18] The wettability of the channel walls determines the type of droplets formed, hydrophobic channels will have preferential interaction with apolar phases, resulting in water in oil droplets. The opposite is the case for hydrophilic channel walls.

The few studies that are available on the stability of PE in microfluidic systems mainly focused on the formation of o/w PEs[19–21], while for our research on the tandem catalytic conversion of fructose, w/o PEs were much more of interest. The packing density, or surface coverage of

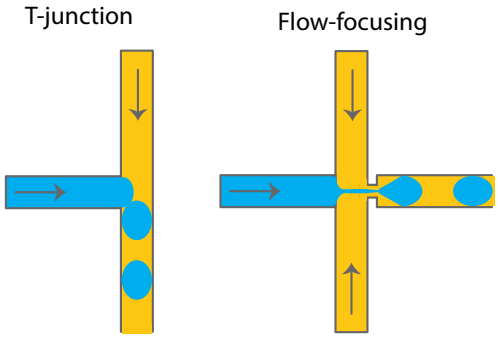

Figure 7.1: Droplet formation via T-junction and flow-focusing geometries inside microfluidic chips.

the particles on the droplet surface is an important parameter to study when investigating droplet stability. Droplets with a low surface coverage are more likely to coalesce upon collision than droplets with a high surface coverage. In previous literature examples, the packing density was determined either by small-angle X-ray scattering (SAXS)[19] or an estimation was made based on the droplet size, shape and particle concentration.[20,21] The packing density has been experimentally determined, for instance by visualization of the particles at the interface by fluorescence microscopy (FM).[22] By making use of a confocal fluorescent microscope (CFM) the focus depth can be changed, by changing the pinhole. A stack of images at different heights can be made, which can be reconstructed into a 3D image.[23] This can be used to image the complete surface of PE droplets and obtain the surface coverage. However, this is only possible when a monolayer of droplets is obtained. In this section, we provide some preliminary results and an outlook on the combined use of a microfluidic setup and CFM to study the formation and stability of w/o PEs.

Microfluidic chip design

We decided to make use of PDMS chip as they are, as mentioned before, cheap and easily moldable. Another benefit is the hydrophobicity of PDMS, which would induce the desired formation of w/o droplets. The PDMS microreactors were fabricated with standard soft- and photolithography methods as described by Whitesides *et al.*[24] One mask fit a total of eight microreactor templates (Figure 7.2), enabling some variation of the height and width of the channel and some different designs to be made at once. The zoom of Figure 7.2 shows the flow direction, the possible in- and outlets and the reservoir of the microreactor.

All microreactor designs included a T-junction for the formation of droplets, a serpentine, to increase the channel length on the PDMS chip, and a reservoir, where droplets could be collected, and assembly of the solid emulsifiers and PE stabilization could be

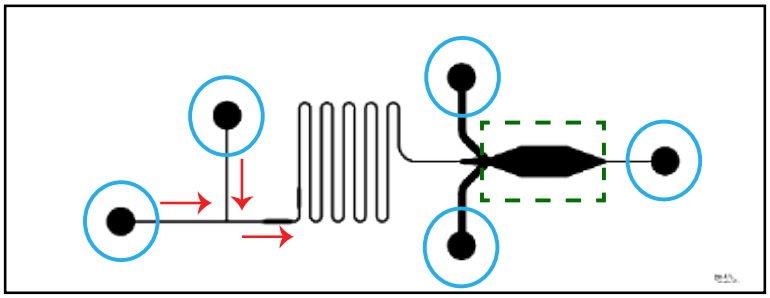

Figure 7.2: General microreactor designs. Zoom: red arrows indicate flow direction in the microreactor, dots indicated with blue circles indicate in- and outlets of the reactors, reservoir is indicated by the green dashed rectangle.

followed over time. The size of the droplets is as function of the size of the channels in these designs. To ensure that a similar number of droplets fit inside the reservoir, the size of the reservoir was adjusted based on the channel size. The preparation method of the mask dictates a uniform height over the chip, leaving only the length in the x and y direction to be variable. The width of the reservoir was designed to be 7.5 times the height of the channels to at least fit 7 spherical droplets in one row. The two outlets on the left side of the reservoirs could be used to remove oil from the reservoir and increase the droplet concentration, as was described by Wan *et al.*[25]

Another parameter that should be considered when designing the microreactors, is the aspect ratio of the channels. Initial test experiments showed that slug-shaped droplets were formed at the T-junction. When these droplets reach the reservoir, these particles

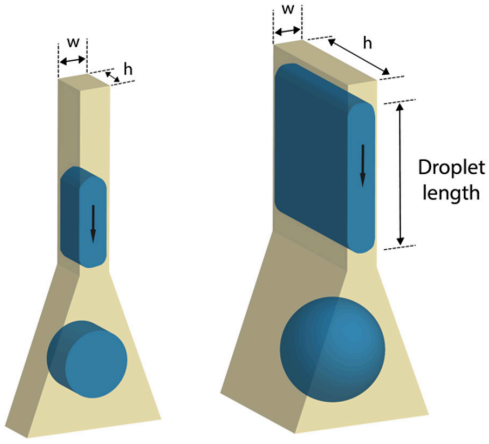

Figure 7.3: Slug shaped droplets become disk shaped or spherical depending on the channel height/width ratio.

will become disk shaped rather than spherical as is desired (Figure 7.3, left). A way to cope with this is to change the height/width ratio of the channels from 1 to 3 (Figure 7.3, right).[26]

PE components

As our intent was to study the stability and packing of the droplets with CFM, the particles must be fluorescent. Therefore, silica particles, containing a fluorescein-based core, were synthesized via a modified Stöber method. Fluorescein can be excited using a 488 nm or 534 nm laser. To be large enough to properly observe individual particles with CFM and small enough to flow easily through the channels of the microreactor, particle with sizes of > 400 nm and ≤ 800 nm were synthesized. Similar to batch w/o PE preparation, in which hydrophobic particles are dispersed in the organic phase after which the aqueous phase is added, the fluorescein-based silica particles were hydrophobized and added to the organic phase.

Besides the particles used to stabilize the droplets, the combination of polar and apolar liquid is also of great importance. First of all, the liquid phases should be compatible with PDMS to prevent swelling of the PDMS, leading to channel blocking. Scattering of the light due to the curvature of the droplet can decrease resolution in CFM. This can be prevented by using liquid phases and particles with matching refractive indices.[26] The left image in Figure 7.4 shows water in octadecene droplets, showing a meniscus due to differences in refractive indices. When these refractive indices are matched as with water/glycerol droplets in liquid PDMS (Figure 7.4, right image), no meniscus is observed. The actual PE systems present an additional challenge in this sense, as the refractive index of the fluorescein-based silica particles (~1.45) also needs to be matched by the liquids. By variation of the water/glycerol ratio, the refractive index of the water phase could indeed be matched to 1.45. The use of liquid PDMS proved impractical for PE formation, however, given its already highly viscosity, which became worse upon addition of the solid emulsifiers. Variation of the oil phase revealed that a squalene/cyclohexane mixture to be best suited for PE formation and for CFM analysis.

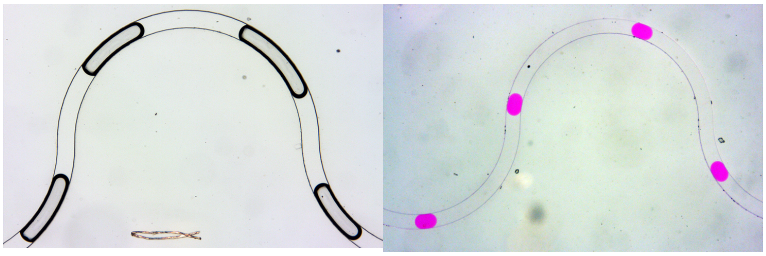

Figure 7.4: Left: Water droplets (n = 1.33) in octadecene (n = 1.44), Right: water/glycerol droplets (n = 1.42) in liquid PDMS (n = 1.42). Aqueous droplets are stained with Rhodamine B for clarification.

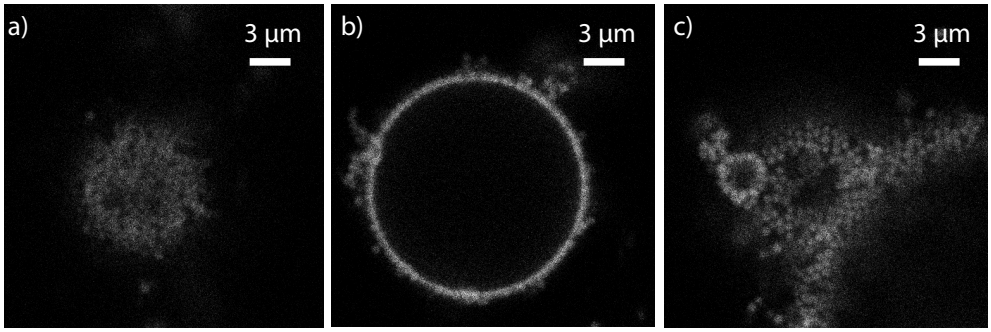

Figure 7.5: CFM images at the a) bottom, b) center and c) top of a water/glycerol droplet in a squalane/cyclohexane mixture stabilized by 1 wt% hydrophobic fluorescein-based silica (fluorescein core = 500 nm).

Having established a suitable w/o system and with the fluorescent solid emulsifiers in hand, the chips with the reservoirs were studied for PE formation. Figure 7.5 shows the CFM images of the bottom, center and top of a droplet stabilized by fluorescein-based silica particles in a system without any flow. The individual particles can indeed be observed, and a packing density could now, in principle, be calculated. These images show that this combined microfluidic/CFM approach can be used to study the formation and stability of PE droplets. However, some challenges still remain, e.g. to prevent fast coalescence with other droplets or droplets directly flowing out of the reservoir, the flow had to be stopped once a droplet was collected inside the reservoir, which resulted in settling of the droplet at the bottom of the microreactor.

These preliminary results thus show that a microfluidic reactor can be used to study the (dynamic) packing of Pickering stabilized droplets. However, the method developed is rather specific in terms of solvents and particles that can be used, having been developed with the specific CFM requirements in mind, limiting its broader applicability. In particular, the refractive indices had to be matched to be able to observe single particles at the liquid-liquid interface, resulting in the identification of the solvent combination of water/glycerol and squalene/cyclohexane. This combination allowed a proof-of-principle but is not a representative solvent combination used in PE catalysis. Indeed, although the use of this system could lead to general observations about particle adsorption and self-assembly at w/o droplets, the fluid behavior of a different solvent combination can be completely different, affecting these processes.

Before this method can be used as a model system to study the formation and stability of PEs, more research is needed. Using the current, functioning, solvent combination, the influence of, for example, particle concentration, size and surface functionalization on

the packing density could be tested. However, increasing the particle concentration in the organic phase, besides increasing the possibility of channel clogging, increases the viscosity and the pressure required to push the liquid through the small channels. As changing the viscosity also influences the formation of the droplets, flow PEs prepared with different solid concentrations cannot be compared one-to-one as the size of the droplets may differ. While one needs to be aware of the influence on stability of such small changes in the system, the microfluidic chip approach to studying PEs does offer considerable potential for gaining new insights and achieving high level of control over various aspects of the PE, including the homogeneity of the system, warranting further pursuit of this research direction.

Acknowledgements

Peter Schut (Inorganic Chemistry and Catalysis, Utrecht University) is acknowledged for performing the microfluidic chip experiments. Relinde van Dijk-Moes (Soft Condensed Matter, UU) is acknowledged for her help with the synthesis of the fluorescein-based silica particles. Dr. Jeroen Vollenbroek and Johan Bomer (Biomedical and Environmental Sensorsystems, Twente University) are acknowledged for their help with the microreactor design and production of the mask. Anne-Eva Nieuwelink (ICC, UU) and Prof. dr. Alfons van Blaaderen (SCM, UU) are acknowledged for fruitful discussions.

References

1 M. Knierbein, M. Voges and C. Held, *Org. Process Res. Dev.*, **2020**, *24*, 1052.
2 J. Zhang, J. Hwang, M. Antonietti and B. V. K. J. Schmidt, *Biomacromolecules*, **2019**, *20*, 204.
3 W. Chen, Y. Shen, Y. Ling, Y. Peng, M. Ge and Z. Pan, *ACS Omega*, **2019**, *4*, 6669.
4 C. Liu, X. Li and Z. Jin, *Catal. Today*, **2015**, *247*, 82.
5 N. A. Harry, S. Radhika, M. Neetha and G. Anilkumar, *ChemistrySelect*, **2019**, *4*, 12337.
6 S. Jiang, Q. Chen, M. Tripathy, E. Luijten, K. S. Schweizer and S. Granick, *Adv. Mater.*, **2010**, *22*, 1060.
7 J. Faria, M. P. Ruiz and D. E. *Resasco*, *Adv. Synth. Catal.*, **2010**, *352*, 2359.
8 J. J. Wiesfeld, M. Kim, K. Nakajima and E. J. M. Hensen, *Green Chem.*, **2020**, *22*, 1229.
9 M. Zhang, L. Wei, H. Chen, Z. Du, B. P. Binks and H. Yang, *J. Am. Chem. Soc.*, **2016**, *138*, 10173.
10 Z. Meng, M. Zhang and H. Yang, *Green Chem.*, **2019**, *21*, 627.
11 X. Tang, Y. Hou, Q. B. Meng, G. Zhang, F. Liang and X. M. Song, *Colloids Surfaces A*

Physicochem. Eng. Asp., **2019**, *570*, 191.
12 S. Y. Teh, R. Lin, L. H. Hung and A. P. Lee, *Lab Chip*, **2008**, *8*, 198.
13 M. Solsona, A. E. Nieuwelink, F. Meirer, L. Abelmann, M. Odijk, W. Olthuis, B. M. Weckhuysen and A. van den Berg, *Angew. Chem.- Int. Ed.*, **2018**, *57*, 10589.
14 U. Gross, P. Koos, M. O'brien, A. Polyzos and S. V. Ley, *European J. Org. Chem.*, *2014*, **2014**, 6418.
15 H. P. L. Gemoets, G. Laudadio, K. Verstraete, V. Hessel and T. Noël, *Angew. Chem.- Int. Ed.*, **2017**, *56*, 7161.
16 P. Mary, V. Studer and P. Tabeling, *Anal. Chem.*, **2008**, *80*, 2680.
17 H. N. Joensson and H. Andersson Svahn, *Angew. Chem.- Int. Ed.*, **2012**, *51*, 12176.
18 X. Casadevall i Solvas and A. deMello, *Chem. Commun.*, **2011**, *47*, 1936.
19 S. Fouilloux, F. Malloggi, J. Daillant and A. Thill, *Soft Matter*, **2016**, *12*, 900.
20 X. Yao, Z. Liu, M. Ma, Y. Chao, Y. Gao and T. Kong, *Small*, **2018**, *14*, 1.
21 A. Schröder, J. Sprakel, K. Schroën, J. N. Spaen and C. C. Berton-Carabin, J. *Food Eng.*, **2018**, *234*, 63.
22 L. S. Roach, H. Song and R. F. Ismagilov, *Anal. Chem.*, **2005**, *77*, 785.
23 A. Diaspro, F. Federici and M. Robello, *Appl. Opt.*, **2002**, *41*, 685.
24 D. B. Weibel, W. R. DiLuzio and G. M. Whitesides, *Nat. Rev. Microbiol.*, **2007**, *5*, 209.
25 K. S. Koppula, R. Fan, K. R. Veerapalli and J. Wan, *J. Colloid Interface Sci.*, **2016**, *466*, 162.
26 M. Musterd, V. Van Steijn, C. R. Kleijn and M. T. Kreutzer, *RSC Adv.*, **2015**, *5*, 16042.

Chapter 8

Nederlandse Samenvatting, Publications, Presentation, Dankwoord & Curriculum Vitea

Nederlandse samenvatting

Het onderzoek beschreven in deze PhD Thesis gaat over het gebruik van Pickering emulsies als reactiemedia voor katalyse. In dit hoofdstuk wordt het onderzoek op een begrijpelijke manier uitgelegd voor mensen zonder achtergrond in de scheikunde. Hiervoor wordt eerst uitgelegd wat katalyse inhoudt, gevolgd door een uitleg over Pickering emulsies. Vervolgens zal een korte samenvatting van de belangrijkste bevindingen per hoofdstuk worden gegeven.

Katalyse

Katalyse is een essentieel voor de chemische industrie. Bijna alle materialen en chemicaliën om je heen worden gemaakt met behulp van een katalysator. Een katalysator is een stof die wordt toegevoegd tijdens een chemische reactie met als doel deze te versnellen, naar het goede product te leiden of om een reactie die normaal gesproken niet zou plaatsvinden wel te laten gebeuren. De katalysator helpt de reactie op weg, maar wordt tijdens deze reactie zelf niet verbruikt. Wat een katalysator wel doet, is verlagen van de activeringsenergie; de energie die nodig is om een reactie te laten plaatsvinden. Eén van de bekendste voorbeelden van een katalysator is de autokatalysator. Deze katalysator bevindt zich in de uitlaat van de auto en zorgt ervoor dat uitlaatgassen volledig verbranden tot koolstofdioxide, stikstof en water. De temperatuur die nodig is voor deze verbranding is veel hoger dan de temperatuur van de motor. Door het gebruik van de katalysator kunnen deze reacties bij lagere temperatuur plaatsvinden: de activeringsenergie is verlaagd. Niet alleen vindt de reactie nu plaats onder mildere omstandigheden, de reactie is ook schoner. Zonder deze katalysator zouden er allerlei giftige gassen en roetdeeltjes ontstaan, die slecht zijn voor het milieu.

Er bestaan grofweg twee soorten katalyse, homogene en heterogene katalyse. Bij homogene katalyse bevindt de katalysator zich in dezelfde toestand als de reactanten, de uitgangsstoffen. De toestand van een stof kan vloeibaar, vast of gas zijn. In homogene katalyse bevinden de reactanten en katalysator zich meestal in oplossing in een vloeistof. Bij heterogene katalyse bevindt de katalysator zich in een andere toestand dan de reactanten. Meestal, zoals ook in het geval van de autokatalysator, bevinden de reactanten zich in de gastoestand (de uitlaatgassen die uit de motor komen) en is de katalysator een vaste stof (het katalysatorblok in de uitlaat). Hierdoor kunnen de producten van de reactie na afloop makkelijk gescheiden worden van de katalysator, waarna de katalysator kan worden hergebruikt. In het onderzoek dat is beschreven in deze PhD Thesis wordt gebruik gemaakt van zowel homogene als heterogene katalysatoren.

Pickering emulsies

De reactiemengsels die gebruikt worden in dit onderzoek zijn zogenaamde Pickering emulsies. Emulsies zijn mengsels van twee vloeistoffen die niet mengbaar zijn met elkaar, zoals olie en water. Bekende emulsies zijn mayonaise, melk en margarine. Deze emulsies zijn uit zichzelf niet stabiel, het mengen van de twee stoffen zal al snel weer gevolgd worden tot ontmengen en het vormen van de originele olie- en waterlaag. Daarom wordt er vaak een stof toegevoegd die ervoor zorgt dat de twee vloeistoffen beter met elkaar gemengd blijven, een emulgator of surfactant (een samenvoeging van het Engelse surface-active agent). Deze surfactant is een stof die voor een gedeelte oplosbaar is in water en voor het andere gedeelte in olie. Na roeren van het mengsel zal de surfactant daarom op het grensvlak van de olie en water gaan zitten (zie Figuur 1). In Figuur 1, bestaat de emulsie uit olie met waterdruppels. Het omgekeerde, een emulsie van water met oliedruppels, kan ook. In dit onderzoek worden alleen water-in-olie-emulsies gebruikt.

Een andere manier om emulsies te stabiliseren, werd in het begin van de vorige eeuw ontdekt door de onderzoeker S.U. Pickering. Hij, en ook de onderzoeker Ramsden vier jaar

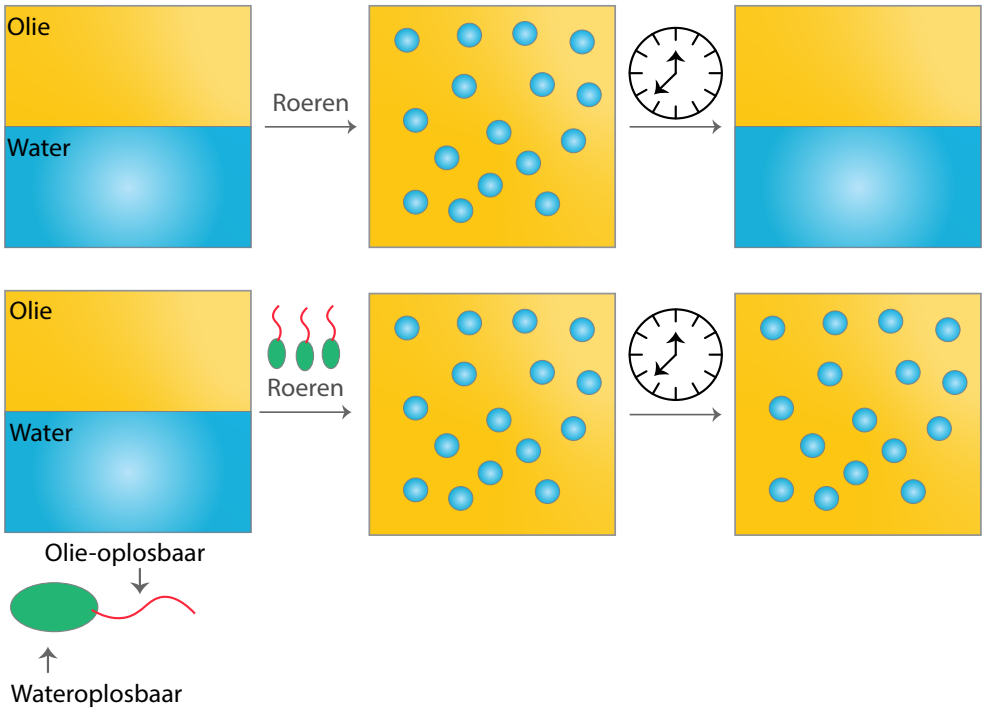

Figuur 1: Boven: Niet gestabiliseerde emulsies vallen na verloop van tijd weer uit elkaar. Onder: Emulsies gestabiliseerd met surfactanten blijven stabiel over tijd.

daarvoor, ontdekten dat olie-en-watermengsels ook gestabiliseerd kunnen worden met micro- en nanodeeltjes. Deze deeltjes zijn zo klein dat je ze niet of nauwelijks kunt zien met het blote oog. Een enkele menselijke haar is bijvoorbeeld ongeveer 40 micrometer (µm), een nanodeeltje is nog eens duizend keer zo klein. Deze deeltjes kunnen zich hechten aan het water-olie oppervlak waardoor er een beschermend laagje van deeltjes om een druppel heen vormt. Daardoor kunnen de druppels niet meer uiteenvallen. De emulsies die op deze manier gestabiliseerd worden, worden Pickering emulsies (PEs) genoemd.

Door het laagje micro- of nanodeeltjes dat zich om de druppel heen vormt, worden de oliefase en de waterfase gescheiden in zogenaamde compartimenten. Deze compartimenten zouden gebruikt kunnen worden voor het uitvoeren van verschillende chemische en katalytische reacties in een reactiesysteem, bijvoorbeeld om reactanten of katalysatoren die eigenlijk niet bij elkaar in de buurt zouden moeten komen van elkaar gescheiden te houden. Deze strategie wordt bijvoorbeeld gebruikt door de natuur. Een levende cel bestaat uit allerlei kleine onderdeeltjes en compartimenten waarin verschillende reacties kunnen plaatsvinden, zonder dat ze elkaar hinderen.

In deze PhD Thesis zullen PEs gebruikt worden om reacties uit te voeren waarin twee katalysatoren nodig zijn die eigenlijk niet samen in een mengsel kunnen overleven. Deze katalysatoren zijn een zuur en een base katalysator. Een zuur en een base zijn tegengesteld aan elkaar, vergelijkbaar met warm en koud water. Als je een bak warm water mengt met eenzelfde soort bak met koud water, zal de temperatuur van het mengsel in het midden van het warme en koude water liggen. Hetzelfde gebeurt wanneer een zure stof en een basische stof met elkaar in aanraking komen: de zure eigenschappen worden tenietgedaan door de basische stof, en andersom. Met als resultaat dat alle reactiviteit verdwijnt. Door de zure en de basische katalysator van elkaar te scheiden in de waterfase en de oliefase van de PE, kan dit worden voorkomen.

In Hoofdstuk 2 hebben we een eerste voorbeeld laten zien waarin PEs gebruikt worden als reactiemedium voor een combinatie van reacties die zowel een zuur als een base als katalysatoren nodig heeft. De gekozen reactie is een simpele omzetting van een reactant in de oliefase, die met het zuur uit de waterfase reageert tot een tussenproduct. Dit tussenproduct kan vervolgens met de base en een tweede reactant in de oliefase reageren tot het eindproduct. Deze gehele reactie kan plaatsvinden op kamertemperatuur. Voor de eerste reactie, de zuurgekatalyseerde reactie, is veel interactie tussen de oliefase en de waterfase nodig. In de PE is, door het vormen van de kleine druppels, het grensvlak veel hoger dan in een gewoon tweefasesysteem. Het voordeel van dit hoge grensvlak was duidelijk te zien in de resultaten van de zuurgekatalyseerde reactie. Deze reactie gaat veel sneller in de PE dan in het gewone tweefasesysteem. De gecombineerde

zuur-base-reactie was alleen mogelijk in de PE en niet in het tweefasesysteem. De laag deeltjes op het grensvlak kon (gedeeltelijk) voorkomen dat het zuur en de base met elkaar in contact kwamen. In het gewone tweefasesysteem konden de twee katalysatoren wel met elkaar in contact komen, waardoor alle reactiviteit verdween.

In Hoofdstuk 3 en Hoofdstuk 4 werd gefocust op het gebruik van PEs voor de omzetting van suikers naar soortgelijke producten die normaal uit olie gemaakt worden. Fructose, opgelost in de waterfase, kan met een zuurkatalysator, ook in de waterfase, worden omgezet naar 5-(hydroxymethyl)furfural (5-HMF). Dit is een stof die een grote rol kan gaan spelen als belangrijk duurzaam platformmolecuul, een molecuul waaruit veel andere stoffen gemaakt kunnen worden. Het probleem met deze reactie is echter dat de 5-HMF die wordt gevormd, gemakkelijk verder reageert met de zuurkatalysator waardoor veel bijproducten worden gevormd. Om deze ongewenste vorming van zijproducten te verminderen kan de 5-HMF worden geëxtraheerd, d.w.z. onttrokken aan de waterfase en naar de oliefase gebracht. Alkylfenolen zijn specifieke categorie oliën die door meerdere onderzoeksgroepen zijn aangewezen als efficiënte oplosmiddelen voor de extractie van 5-HMF.

In Hoofdstuk 3 werd de stabiliteit van PEs met drie verschillende alkylfenolen, 2-*iso*propylfenol (IPP, van het Engelse 2-*iso*propylphenol), 4-propylguaiacol (PG) en 2-*sec*-butylfenol (SBP, van het Engelse 2-*sec*-butylphenol) als oliefase getest. Eerst werd een theoretische beoordeling gemaakt, gebaseerd op fysisch-chemische eigenschappen als contacthoek, oppervlaktespanning en viscositeit. Op basis van deze gegevens zou de PE met SBP als oliefase de meest stabiele emulsie geven en die met PG als oliefase de minst stabiele. De verschillen in eigenschappen waren echter zo klein dat tijdens de experimentele studie dit verschil niet zichtbaar was. PEs gestabiliseerd met 2 gewichtsprocent (wt%) deeltjes ten opzichte van de oliefase, waren meer dan een maand stabiel. De stabiliteit werd niet beïnvloed door toevoeging van zuur aan de waterfase, wat nodig is voor de katalytische reactie, of door zout aan de waterfase, wat nodig is voor een meer efficiënte 5-HMF-extractie. De PEs waren ook vrij stabiel bij 100 °C, de temperatuur die nodig is voor deze reactie. Verder werd de extractie van 5-HMF bestudeerd in tweefase systemen met een hoog en een laag grensvlak. Hiervoor werden normale tweefasesystemen en geroerde tweefasesystemen gebruikt. De extractie bleek, als verwacht, veel efficiënter in tweefasesystemen met een hoog grensvlak. Deze resultaten waren veelbelovend voor het uitvoeren van zuur-base-katalyse in PEs.

In Hoofdstuk 4 werden de PEs met de alkylfenolen als oliefase getest als reactiemedia voor de katalytische omzetting van fructose. Voor de zuurgekatalyseerde reactie van fructose naar 5-HMF presteerde de PE beter dan het gewone tweefasesysteem als het gaat om

fructose conversie en 5-HMF-extractie. De koppeling van deze reactie aan een tweede (basegekatalyseerde) reactie bleek echter niet zo makkelijk. Omdat deze reacties op hoge temperatuur plaatsvinden, gaf de laag deeltjes over de druppels niet meer voldoende bescherming. Gedeeltelijke zuur-base interactie was voor deze reactie niet te voorkomen. Toch werd er in PEs wel product gevormd terwijl in de gewone tweefase systemen de reactie niet verliep.

In Hoofdstuk 5 werden voor het eerst heterogene katalysatordeeltjes gebruikt. Deze deeltjes konden naast het katalyseren van de reacties ook gebruikt worden voor het stabiliseren van de PEs. Hiervoor werden deeltjes uitgerust met zuur- en/of base-groepen. Naast deeltjes met enkel zuur of enkel base groepen, werden door ons voor het eerst silicadeeltjes gemaakt die aan een kant zuurgroepen en aan de andere kant basegroepen bevatten. Deze zogenaamde Janusdeeltjes, bleken actief voor de gecombineerde zuur-base reacties, maar verdere optimalisatie van de hoeveelheid zuur- en basegroepen op de deeltjes is nodig om de prestaties en opbrengst te verbeteren.

Alle experimenten beschreven in Hoofdstuk 2 tot Hoofdstuk 5 werden uitgevoerd als losse reacties in reageerbuizen. In Hoofdstuk 6 werd een opstelling gebruikt waarin PEs in een continue stroom kunnen worden gevormd en geanalyseerd. Hiervoor werd een zogenaamd microfluïdisch systeem gebruikt, m.b.v. buisjes met een diameter op de micrometer schaal (de dikte van een aantal haren). In dit systeem kunnen continu druppels gevormd worden die vervolgens door de buisjes stromen. Door reactanten en katalysatoren toe te voegen aan de olie- en de waterfase wordt een katalytische PE gemaakt en vindt de reactie plaats tijdens het stromen. Omdat de buisjes transparant zijn kan de reactie worden gevolgd door analyses te doen op verschillende plekken. Een techniek die hiervoor zeer geschikt is, is spectroscopie. In spectroscopie wordt de interactie van licht met materie bestudeerd. Wanneer het reactiemengsel beschenen wordt met een lichtbron waarvan de eigenschappen zoals kleur en intensiteit precies bekend zijn, kunnen de veranderingen in deze eigenschappen, die optreden door de interactie tussen het licht en het reactiemengsel, gerelateerd worden aan wat er in het reactiemengsel gebeurt. Op deze manier kan worden bepaald of de concentratie van de reactanten afneemt en de concentratie van het product toeneemt. Ook in dit onderzoek bleken gestabiliseerde water-in-olie-druppels, PEs, efficiënter in het uitvoeren van enkel de zuurgekatalyseerde en de gecombineerde zuur-base-gekatalyseerde reactie dan niet gestabiliseerde druppels.

In dit onderzoek hebben we laten zien dat PEs gebruikt kunnen worden als reactiemedium voor het uitvoeren van katalytische reacties die zowel een zuur- als een basekatalysator nodig hebben. Hiervoor zijn zowel homogene als heterogene katalysatoren gebruikt.

Hoewel de tegenstrijdige katalysatoren normaal gesproken niet kunnen overleven in één reactievat, kunnen ze in PEs worden gescheiden door het laagje vaste stofdeeltjes dat zich op de rand van de druppel bevindt. Hierdoor wordt de reactiviteit van beide katalysatoren behouden. Deze methode werkte zeer goed voor reacties die uitgevoerd kunnen worden bij kamertemperatuur, maar bij het uitvoeren van reacties op hogere temperatuur bleek het lastig om zuur-base interactie te voorkomen. De beste methode om dit te voorkomen lijkt het gebruik van heterogene katalysatoren, en dan voornamelijk het gebruik van deeltjes die zowel zuur- als basegroepen bevatten. De balans tussen de hoeveelheid zuurgroepen en de hoeveelheid basegroepen moet daarvoor nog verder worden onderzocht.

Publications and Presentations

List of publications based on Chapters in this Thesis

C.M. Vis, L.C.J. Smulders, P.C.A. Bruijnincx, ***Tandem Catalysis with Antagonistic Catalysts Compartmentalized in the Dispersed and Continuous Phases of a Pickering Emulsion,*** *ChemSusChem* **2019**, *12*, 2176.

C.M. Vis*, A.-E. Nieuwelink*, B.M. Weckhuysen, P.C.A. Bruijnincx, ***Continuous Flow Pickering Emulsion Catalysis in Droplet Microfluidics with In-situ Raman Spectroscopy,*** *Chem.- A European Journal,* **2020**, DOI 10.1002/chem.202002479

* *These authors contributed equally*

Co-author publications

D. Fu, J.E. Schmidt, P. Pletcher, P. Karakiliç, X. Ye, C.M. Vis, P.C.A. Bruijnincx, M. Filez, L.D.B. Mandemaker, L. Winnubst, B.M. Weckhuysen, ***Uniformly Oriented Zeolite ZSM-5 Membranes with Tunable Wettability on a Porous Ceramic,*** *Angew. Chem. -Int. Ed.* **2018**, *57*, 12458.

L.D.B. Mandemaker, M. Rivera-Torrente, R. Geitner, C.M. Vis, B.M. Weckhuysen, ***In Situ Spectroscopy of Calcium Fluoride Anchored Metal–Organic Framework Thin Films during Gas Sorption***, *Angew. Chem. -Int. Ed.* **2020**, DOI 10.1002/anie.202006347

List of oral presentations by the author

Acid-Base Catalyzed Tandem Reaction in a Pickering Emulsion, *Netherlands' Catalysis and Chemistry Conference*, **2018**, Noordwijkerhout, the Netherlands

Pickering Emulsions as Compartmentalized Reaction Media for Catalysis, *CHAINS*, **2018**, Vekthoven, the Netherlands

Antagonistic Tandem Catalysis in Pickering Emulsions using Droplet Microfluidics, *Netherlands' Catalysis and Chemistry Conference*, **2019**, Noordwijkerhout, the Netherlands

Pickering Emulsions as Compartmentalized Reaction Media for Catalysis, *International Symposium on Green Chemistry*, **2019**, La Rochelle, France

List of poster presentations by the author

Towards Tandem Catalytic Biomass Conversion in Pickering Emulsions, *Netherlands' Chemistry and Catalysis Conference*, **2017**, Noordwijkershout, the Netherlands

Towards Tandem Catalytic Biomass Conversion in Pickering Emulsions, *3rd International Symposium on Green Catalysis*, **2017**, Rennes, France – Awarded with RSC Green Chemistry poster prize

Pickering Emulsions as Compartmentalized Reaction Media for Antagonistic Tandem Catalysis, *EuropaCat*, **2019**, Aachen, Germany

Dankwoord

Na vijf jaar komt mijn PhD avontuur in Utrecht ten einde. Een tijd waarin ik heel veel heb geleerd, over de wetenschap, maar ook over mezelf. Het is een hele leuke maar ook vermoeiende tijd geweest, met dit proefschrift als eindresultaat. Dit had ik nooit gekund zonder de hulp en aanwezigheid van een aantal personen.

Pieter, jij bent de eerste die ik wil bedanken. Bedankt alle hulp de afgelopen jaren, als ik weer eens met mijn handen in het haar zat omdat ik geen wijs meer kon worden uit alles wat ik aan het doen was, hielp jij me weer het overzicht terug te krijgen en me de juiste richting te wijzen. Ik heb heel veel van je geleerd over het systematisch doen van onderzoek en het positieve zien in resultaten, ook al komen hypotheses niet altijd uit. Ik wil je bedanken dat je zo benaderbaar bent, hoe druk je het ook had, er was altijd wel een gaatje te vinden.

I also want to thank my co-workers on the Pickering emulsion projects. Pierre-François, we started together in 2015 and had to figure out what Pickering emulsions were and how to make them. Your hard work on studying the stability of the alkylphenol PEs were very useful and essential for Chapter 3. Wirawan, I've had a lot of fun with you while working in the lab, and I enjoyed the chats about Pickering emulsions and their strange behavior sometimes. You are one of the kindest people I know, I wish you all the best in the future! Fuqiang, your knowledge about particle synthesis was something that we really missed in the team. Thank you for all the hours of trying to make the perfect Janus spheres, which resulted in Chapter 5. That would not have been there without all your work.

Al die wetenschappelijke hulp is heel fijn maar er is nog een heel team, of eigenlijk in mijn geval twee teams, die ik graag wil bedanken. Dymph en Ilonka bedankt voor al jullie hulp betreffende de organisatorische en administratieve taken. Zonder jullie hulp kan een grote onderzoeksgroep als ICC niet bestaan. Daarnaast wil ik Silvia bedanken voor de hulp in de laatste paar maanden van het promotietraject. Verder wil ik de hele technische staf van ICC bedanken met in het bijzonder Ad, Pascal, Oscar en Ramon. Bedankt voor al jullie hulp met HPLC's en GC's, het aanleggen van gasleidingen, het ergens vandaan toveren van waterslangen, het veilig houden van het lab etc. En natuurlijk mag ik Thomas en Johann niet vergeten, het was voor mij even zoeken welke wegen ik moest bewandelen na de wisseling van ICC naar OCC, maar samen met jullie is dat gelukt, bedankt!

Verder ben ik heel dankbaar voor alle studenten die ik heb mogen begeleiden gedurende het promotietraject. Kristiaan, Tjom, het was leuk om jullie te begeleiden tijdens jullie eerste zelfstandige onderzoek bij ICC, een plek waar jullie zijn terug gekomen voor verdere

onderzoeksprojecten. Bedankt voor jullie harde werk en de bijdragen aan mijn onderzoek. Tweedejaars studenten; Bart, Jan-Willem, Jochem v.d. M., Jochem P., Lars, Marlous, Storm en Zhou Zhou, bedankt voor jullie enthousiasme (en slechte teamnamen). Matthijs, een bachelor student als geen andere, het was heel fijn om jou, met al je leergierigheid, te begeleiden. Peter, jouw eigenwijze ideeën hebben geleid tot mooie resultaten die beschreven zijn in de outlook van deze thesis. Je mag trots zijn op wat je allemaal hebt bereikt!

Luc, jij was mijn eerste student en wat vond ik dat spannend. We hadden vanaf het begin af aan een goede klik en we staken elkaar aan met ons enthousiasme. Jouw harde werken heeft geleid tot het werk beschreven in hoofdstuk 2 en in een publicatie in ChemSusChem. Ik ben heel trots op je dat je nu zelf een PhD aan het doen bent bij ICC en vond het heel leuk dat ik je nog een paar maanden als bureaubuurman mocht hebben. Nog leuker vind ik het dat je mijn paranimf wil zijn!

Anne-Eva, natuurlijk moest jij ook mijn paranimf worden! We zijn bijna tegelijk begonnen met onze PhD, bijna gelijk geëindigd en hebben in de tussentijd een goede vriendschap opgebouwd. Ik heb daardoor intens genoten van onze samenwerking, lekker priegelen met stukjes tubing, krultangen en in het donker meten. Wat kunnen twee mensen toch blij worden van een paar druppeltjes. Daarnaast konden we heerlijk kletsen over dansen, samen meezingen op het lab, theedrinken (heb je nog steeds een Pavlov reactie als je iets hoort rinkelen?), fietsen tegen de wind in en nog veel meer. Het was fijn om een maatje te hebben waarbij ik altijd even mijn frustratie of blijheid kwijt kon. Bedankt voor alles!

Marjolein, jij was ook zo'n persoon bij wie ik altijd even terecht kon. Jij bent echt een voorbeeld voor mij geweest, altijd hard werken om het beste uit jezelf te halen maar daarnaast niet vergeten plezier te maken. Je bent een van de slimste personen die ik ken, met af en toe een hele domme actie waardoor ik me zo op mijn gemak voel bij je.

Katinka, bedankt voor je vriendschap, alle ongemakkelijke momenten en alle keren dat we hebben dubbel gelegen van het lachen. Jouw carrière gaat nu echt van start en ik wens je daar het allerbeste in. Je weet wat je kunt en wat je wilt dus je gaat het bereiken, daar ben ik zeker van.

Lars, wat hebben we veel fijne fietstochtjes gehad. Altijd even positief, zelfs als het weer eens stormde of regende. Je nuchterheid en je vrolijkheid maakten het elke dag weer een feestje om bij je in de buurt te zitten. Blijf alsjeblieft zoals je bent, want je bent een topper!

Furthermore, I would like to thank all the people that I've worked with in the Biomass

lab, Anne-Eva, Antonio, Beatriz, Caroline, Christopher, Egor, Erik, Fang, Homer, Ivan, Johan, Khaled, Kordula, Laurens, Luke, Maarten, Miguel, Pierre-François, Robert, Sandra, Wirawan, Yann and all other that I may have forgotten. Thank you for the nice working environment in the lab and for coping with me singing all day. Of course, I would also like to thank all other people from both ICC and OCC for all their help and gezelligheid.

Dan hebben we natuurlijk nog alle attente collega's, Anne-Eva, Jelle, Joris, Marjolein, Robin, Thomas, Tom, Ward en Wouter. Ik heb heel veel van jullie geleerd, voornamelijk dingen over zoals het locken van je computer, TEM-kunst, waterfall plots, hoe Illustrator te gebruiken, bowlen, poolen en cyclovoltammetrie (wat ik nooit langer dan een dag kan onthouden). Hartelijk bedankt voor alle leuke lunchloopjes, uitstapjes, hardlooprondjes en -evenementen en quarantaine skypemeetings!

Niet alleen de mensen op de vakgroep maar juist ook veel mensen daarbuiten hebben mij (wellicht onbewust) geholpen om dit tot een goed einde te brengen. Allereerst Sara en Eline, zonder danslessen om mijn hoofd weer leeg te maken had ik dit nooit kunnen volbrengen. Jullie vriendschap en alle gezellige evenementen met de rest van de UDA crew betekenen veel voor mij. Daarnaast heb ik erg genoten van de zondagochtend hardloop/bijkletssessies met jou Saar, moeten we snel weer oppakken.

En natuurlijk mijn beste vriendinnetje sinds groep 1, Moniek. Ik ben heel blij met een vriendin als jij. Tijdens onze lunches op de Uithof konden we heerlijk bijkletsen, waardoor de tijd altijd veel te snel ging. Ook al wonen we niet dicht meer bij elkaar ik weet dat ik altijd bij je terecht kan en dat is natuurlijk andersom ook het geval.

En dan is er natuurlijk nog de (schoon)familie. Lieve Kees en Jolanda bedankt voor jullie steun de afgelopen jaren en de interesse in wat ik aan het doen was. Bedankt dat jullie altijd voor ons klaarstaan.

Iësta, lieve zus, bedankt dat je hebt geprobeerd te begrijpen waar ik mee bezig was en voor het nalezen en corrigeren van mijn Nederlandse samenvatting. Ik heb genoten van al onze uitstapjes naar pretparken en cabaret en hoop dat we dat nog veel vaker gaan doen.

En pap en mam, bedankt voor jullie onvoorwaardelijke steun en het vertrouwen in mijn kunnen. Lieve mama, bedankt dat ik altijd bij je terecht kan en dat jij met je nuchtere blik alles kunt relativeren. Lieve paps, jij bent een van de sterkste en positiefste personen die ik ken. Hoewel het de afgelopen tijd niet altijd heeft meegezeten ben je altijd optimistisch gebleven. Ik ben er trots op dat ik jullie dochter mag zijn.

Wesley, wat ben ik blij dat ik jou naast me had tijdens deze hele reis. Allereerst bedankt voor het nalezen van mijn hele thesis en het spotten van lelijke losse regels of lettertypes die niet goed staan. Maar veel belangrijker nog, bedankt dat je om kunt gaan met mijn gestress en dan altijd probeert om mij te helpen en me op te vrolijken. We hebben samen zoveel plezier en met jou is alles gewoon net even wat leuker. Ik kijk heel erg uit naar wat we samen allemaal nog gaan beleven.

Heel veel liefs,
Carolien

Curriculum Vitea

Carolien Mariëlle Vis was born in Breukelen, the Netherlands, on October 12th 1991. After obtaining her high school diploma (VWO) from R.S.G. Broklede in 2010, she studied chemistry at the University of Amsterdam where she obtained her bachelor's degree in 2013 including an educational minor. She continued her education at the University of Amsterdam in the master program: *Chemistry, Science for Energy and Sustainability*. In 2015, she graduated with her master thesis entitled *Purification of Crude FDCA via Hydrogenation and Crystallization*, a research project that was performed during an internship at Avantium. After graduating from the University of Amsterdam she started her PhD research project, entitled *Pickering Emulsions as Compartmentalized Reaction Media for Catalysis* at Utrecht University under supervision of prof. dr. Pieter Bruijnincx. The results of this work are described in this PhD Thesis.